



**EVALUATION OF EFFECT OF TREE ROOTS ON
SHEAR STRENGTH OF SOIL DUE TO ROOT WATER
UPTAKE**

Amarasinghe Arachchige Supipi Kaushalya

(218075H)

Degree of Master of Science

Department of Civil Engineering

University of Moratuwa

Sri Lanka

April 2023

**EVALUATION OF EFFECT OF TREE ROOTS ON
SHEAR STRENGTH OF SOIL DUE TO ROOT WATER
UPTAKE**

Amarasinghe Arachchige Supipi Kaushalya

(218075H)

Thesis submitted in partial fulfillment of the requirements for the degree
Master of Science in Civil Engineering

Department of Civil Engineering

University of Moratuwa

Sri Lanka

April 2023

DECLARATION

“I declare that this is my own work and this thesis does not incorporate without acknowledgement any material previously submitted for a Degree or Diploma in any other University or institute of higher learning and to the best of my knowledge and belief it does not contain any material previously published or written by another person except where the acknowledgement is made in the text.

Also, I hereby grant to University of Moratuwa the non-exclusive right to reproduce and distribute my thesis/dissertation, in whole or in part in print, electronic or other medium. I retain the right to use this content in whole or part in future works (such as articles or books).

Signature:

Date: 27/06/2023

The supervisor/s should certify the thesis/dissertation with the following declaration.

The above candidate has carried out research for the Masters/MPhil/PhD thesis/Dissertation under my supervision.

Name of the supervisor: Dr. (Mrs.) M. A. Pallewatttha , Prof. U. P. Nawagamuwa

Signature of the supervisor:

Date: 27/06/2023

ABSTRACT

Tree roots play a major role in ground and slope stabilization by increasing the strength and stiffness of the soil positively. When evaluating how vegetation affects ground improvement, tree roots are the primary factor because that they improve the strength of the soil with the help of their mechanical properties and provide the additional soil suction by the root water uptake.

Previous studies, however, focused on the mechanical and hydraulic impacts of tree roots separately when evaluating the impact of vegetation, which failed to yield reliable results because suction influences on mechanical characteristics of tree roots. Recent laboratory research has shown that the mechanical interactions between roots and soil, such as root tensile strength and root cohesiveness, are suction-dependent.

There are still significant gaps in knowledge regarding the effects of suction and root concentrations on root reinforcement despite these extensive previous research. This study investigated the influence of matric suction on root reinforcement of the *Alstonia macrophylla* with Sri Lankan Silty Sand using large-scaled direct shear tests.

Cohesion due to root reinforcement of the *Alstonia macrophylla* should theoretically equal to the difference between the apparent cohesion of reinforced and unreinforced shear strength in saturated samples. This value was 2.99 kN/m² when RAR, dry biomass of roots per unit volume of soil, and total leaf area of the plant were 6.22 x 10⁻³ %, 0.575 kg/m³ and 1195 cm² respectively. However, the cohesion due to root reinforcement of the *Alstonia macrophylla* is slightly increased with the matric suction in the Sri Lankan Silty Sand as per the research outcomes.

ACKNOWLEDGMENTS

First and foremost, I would like to express my deepest appreciation to Dr. (Mrs.) M. A. Pallewatha, Senior Lecturer at Civil Engineering Department of University of Moratuwa, for her dedication and keen interest to make success and as well as for setting me the platform to proceed my career in Geotechnical Engineering. I would also like to express my sincere gratitude to my co supervisors Prof. U. P. Nawagamuwa, Professor at Civil Engineering Department of University of Moratuwa, for all the help he has provided during my Master. Sir, you are the best navigator of my academic life since my undergraduate research career.

I am thankful for the Senate Research Committee that provided financial support for my M.Sc. work. Moreover, I extend my sincere thanks to Department of Irrigation and National Building Research Organization (NBRO), Sri Lanka for supplying required testing instruments. Further, I would like to express my gratitude to Department of Material Science and Engineering and Department of Mechanical Engineering, University of Moratuwa for helps that gave to develop the large-scaled direct shear testing instrument. I also wish to acknowledge the contributions made by the technical officers and lab assistances during my laboratory experiments, especially Mr. L. H. K. Chandana, Mr. H. T. R. M. Thanthirige, Mr. U. K. Padmaperuma, Mr. M. A. Piyasiri, Mr. D. M. N. L. Dissanayake and Mr. P. P. R. Peiris. I extend my sincere thanks to all my friends at University of Moratuwa as well as undergraduate students of 18' and 20' Batch, Department of Civil Engineering, University of Moratuwa.

Last but not least, I would like to personally thank my superb husband Mr. W. T. L. Senevirathne Engineer, ICC (Pvt) Ltd and my parents A. A. U. Ranjith, D. M. D. L. D. Ranaweera who has given tremendous support not only for research matter but also my life.

Supipi Kaushalya

26th of March 2023

TABLE OF CONTENT

DECLARATION	i
ABSTRACT.....	ii
ACKNOWLEDGMENTS	iii
TABLE OF CONTENT	iv
LIST OF FIGURES	viii
LIST OF TABLES	xi
LIST OF SYMBOLS	xii
1 INTRODUCTION	1
1.1 General	1
1.2 Description of Problem	2
1.3 Objectives and Scope of the Study.....	3
1.4 Organization of the Thesis	4
2 LITERATURE REVIEW.....	6
2.1 General	6
2.2 Unsaturated Soils.....	7
2.2.1 Unsaturated Soil Mechanics.....	7
2.2.2 Need for Unsaturated Soil mechanics	8
2.2.3 Basic State variables of Unsaturated Soils.....	9
2.2.4 Measurement and Estimation of Basic State Variables of Unsaturated Soils.....	9
2.2.5 Unsaturated Soil Properties.....	12
2.3 Soil Water Characteristic Curve (SWCC).....	12
2.3.1 Developing SWCC using Experimental Procedures.....	14
2.3.2 Developing SWCC by using Prediction models	17

2.3.3	The available literature on the comparison of prediction models	20
2.4	Shear strength of unsaturated soil	20
2.4.1	Shear strength of saturated soil	20
2.5	Shear strength of the soil with tree roots	25
2.5.1	Root Reinforcement	26
2.6	Suction effect of the tree roots	32
2.7	Summary	35
3	BASIC SOIL STUDY AND PLANT SELECTION	36
3.1	Basic soil study.....	36
3.2	Plant selection.....	39
4	STUDYING MECHANICAL AND HYDROLOGICAL PROPERTIES OF <i>Alstonia macrophylla</i>	41
4.1	General	41
4.2	Evaluating the volume ratio between the soil and roots.....	41
4.3	Observing the suction variation of soil sample with and without a plant against the time	42
4.3.1	Variation of the matric suction in soil sample with time	42
4.3.2	Variation of the matric suction with respect to time in soil sample with plant.....	44
4.4	Developing an empirical correlation between the root water uptake and total area of leaves of the tree plant.....	45
4.5	Summary	47
5	OBJECTIVE 01 - STUDYING THE BEHAVIOR OF UNSATURATED SRI LANKAN SEMI-COSTAL SILTY SAND USING SWCC.....	48
5.1	General	48
5.2	Flow Chart for the Objective 1	48

5.3	Development of SWCC using experimental methods.....	49
5.3.1	Pressure plate	49
5.3.2	WP4C	50
5.3.3	Moisture and Suction Sensors.....	53
5.3.4	Curve fitting	55
5.4	Development of SWCC using prediction models	55
5.5	Results and Discussion	56
5.5.1	Development of SWCC using experimental methods	56
5.5.2	Development of SWCC using prediction models	57
5.6	Summary	60
6	OBJECTIVE 02 – INVESTIGATING THE INFLUENCE OF SUCTION ON ROOT REINFORCEMENT OF <i>Alstonia macrophylla</i> WITH THE SEMI-COASTAL SRI LANKAN SILTY SAND	62
6.1	General	62
6.2	Flow chart for the objective 1.....	64
6.3	Sample Preparation.....	64
6.4	Developing large-scaled direct shear testing setup	65
6.5	Conducting Direct shear tests.....	70
6.6	Results and Discussion	73
6.7	Summary	80
7	CONCLUSION AND RECOMMENDATION	82
7.1	General Summary.....	82
7.2	Specific Conclusion.....	83
7.2.1	Most reliable experimental and analytical procedures which can be used to SWCCs for Sri Lanka Silty Sand.....	83

7.2.2	Identified components of the increase in the shear strength of root permeated soil, during direct shear testing.....	83
7.3	Recommendations for future works	84
8	REFERENCES.....	86
	ANNEX 1 – BASIC SOIL STUDY.....	92
	ANNEX 2 – EMPIRICAL CORELATION BETWEEN THE ROOT WATER UPDATE AND TOTAL LEAF AREA	101
	ANNEX 3 – DEVELOPMENT OF SWCC.....	102
	ANNEX 4 – DEVELOPMENT OF LARGE-SCALE DIRECT SHEAR TESTING SETUP	103
	ANNEX 5 – SEM TEST RESULTS.....	104

LIST OF FIGURES

Figure 1.1: Hydro mechanical effects of vegetation on slope stabilization (modified after Mulyono et al., 2018).....	2
Figure 2.1: Unsaturated soil structure	7
Figure 2.2: Formation of the matric suction with capillary force	10
Figure 2.3: Determination of unsaturated soil property functions	12
Figure 2.4: Phases for the SWCC (after Fredlund and Rahardjo, 1993).....	13
Figure 2.5: Component of pressure plate apparatus.....	15
Figure 2.6: WP4C instrument	16
Figure 2.7: Shear failure envelop for saturated condition (after Fredlund and Rahardjo, 1993)	21
Figure 2.8: Shear failure envelop for unsaturated soil (after Fredlund and Rahardjo, 1993)	23
Figure 2.9: Mohr-coulomb envelopes in reinforced and unreinforced soils with circles describing failure by (a) slippage and, reinforcement rupture (after Hausmann, 1976)	27
Figure 2.10: Failure pattern of the roots (after Waldron, 1977)	27
Figure 2.11: Root Distribution (a) main roots system (b) fiber roots system	29
Figure 2.12: Various root systems	30
Figure 2.13: Root system of young barley plants with different bulk densities (Modified after Gilmen (1980))	30
Figure 2.14: Root growth pattern and shape of potato seedlings with the impact of the root zone temperature (modified after Sattelmacher et al. ,1990).....	31
Figure 2.15: Variation of rate of root water uptake as per volumetric water content (modified after Feddes et al., 1976)	34
Figure 3.1: Soil Barrow area	36

Figure 3.2: Particle size distribution	38
Figure 3.3: Standard proctor compaction curve	38
Figure 3.4: Initially selected tree plants	40
Figure 4.1: Observation for growing pattern and rate of <i>Alstonia macrophylla</i>	41
Figure 4.2: Variation of matric suction in soil sample within two weeks.....	43
Figure 4.3: Variation of environmental temperature within two weeks in above test	43
Figure 4.4: Variation of matric suction in soil sample with plant within two weeks	44
Figure 4.5: Variation of environmental temperature within two weeks in above test	44
Figure 4.6: Schematic diagram of potometer	46
Figure 4.7: Developed potometer.....	46
Figure 4.8: Method to obtained the total leaf area	46
Figure 4.9: Relationship between the root water uptake and total leaf area	47
Figure 5.1: Component of the pressure plate test.....	49
Figure 5.2: Testing procedure of EC test of the soil	51
Figure 5.3: Relationship between the average electrical conductivity of soil extract and moisture content	52
Figure 5.4: Calibration chart for moisture sensor 1	53
Figure 5.5: Calibration chart for moisture sensor 2	54
Figure 5.6: Calibration chart for moisture sensor 3	54
Figure 5.7: Installation moisture and suction to the soil sample and test procedure .	55
Figure 5.8: Experimental results and fitted curve for experimental results	57
Figure 5.9: Developed SWCCs according to the prediction models using modal parameters proposed by authors for granular soils	58
Figure 5.10: Developed SWCCs using prediction models using derived values of modal parameters	59

Figure 6.1: Sample preparation	65
Figure 6.2: Sample compaction procedure (a) wooden compactor, (b) collar, and (c) wooden box	65
Figure 6.3: Proposed large-scale mold.....	66
Figure 6.4: Large-scaled direct shear testing setup (a) proposed setup and.....	66
Figure 6.5: Developing stage of large-scale direct shear testing setup (a) test rig, (b) supporters, (c) mold, and (d) load plate	67
Figure 6.6: Calibration chart for horizontal settlement gauge	67
Figure 6.7: Calibration chart for vertical settlement gauge.....	68
Figure 6.8: Calibration chart for load cell	68
Figure 6.9: Developed Failure Envelops using standard direct shear testing apparatus	69
Figure 6.10: Developed Failure Envelops using large-scale direct shear testing setup	69
Figure 6.11: Trolley with a roller wheel tray	71
Figure 6.12: Sample installation (a) sensor installation, (b) sand pile installation	71
Figure 6.13: Conducting direct shear testing	72
Figure 6.14: Shear Stress vs. Shear Displacement for 0 kPa Matric Suction	73
Figure 6.15: Shear Stress vs. Shear Displacement for 10 kPa Matric Suction	73
Figure 6.16: Shear Stress vs. Shear Displacement for 20 kPa Matric Suction	74
Figure 6.17: Shear Stress vs. Shear Displacement for 150 kPa Matric Suction	74
Figure 6.18: Failure Envelops for 0 kPa matric Suction(Saturated condition)	76
Figure 6.19: Failure Envelops for 10 kPa Matric Suction	77
Figure 6.20: Failure Envelops for 20 kPa Matric Suction	77
Figure 6.21: Failure Envelops for 150 kPa Matric Suction	78

LIST OF TABLES

Table 2.1: Suction measurement devices	11
Table 3.1: Summary of the basic soil properties	37
Table 3.2: Summary of the soil classification	39
Table 4.1: Summary of observation for evaluating volume ratio between soil and tree roots.....	42
Table 5.1: Summary output obtained from pressure plate apparatus.....	50
Table 5.2: Summary of the results obtained using the WP4C instrument	52
Table 5.3: Test reading of the moisture and suction sensors	53
Table 5.4: Modal coefficient values recommended by the authors for granular soil. 56	
Table 5.5: SSR values for the models with modal parameters proposed by authors . 58	
Table 5.6: Derived values for modal parameters and SSR values	60
Table 6.1: Validation of large-scale direct shear testing setup	68
Table 6.2: Comparative study for the texture of the soil particles	70
Table 6.3: Summary of the test results.....	75
Table 6.4: c_r value calculated as the difference between the reinforced and unreinforced peak shear stresses under three vertical stresses for each matric suctions.....	76
Table 6.5: Failure envelopes for each case	78
Table 6.6: Calculated c_r values using failure envelopes	79
Table 6.7: Summary of the observed c_r values following both approaches	79

LIST OF SYMBOLS

A	Total area of soil
A_R	Root area
c'	Effective cohesion
C_p	Specific heat capacity of air at constant pressure
D_a	Vapor pressure deficit of air
e	Void ratio
EC	Electrical conductivity of the saturated extract
$f(\beta)$	Root density function
f_i	Fractional of each leaf expressed in terms of the total leaf area of the canopy
g	Gravity on earth
h	Matric water suction
h_c	Elevation
h_{co}	Equivalent capillary rise
h_p	Water potential of roots
h_s	Water potential of soil
k	Fitting parameter
k	Unsaturated hydraulic conductivity
$L(z)$	Length of root per unit soil volume
m	Pore size distribution parameter of the model
$r_{a,i}$	Boundary layer resistance of each leaf
$R_{n,i}$	Net radiation flux density absorbed by each leaf
$r_{s,i}$	Stomatal resistance of each leaf
r_i	Mean pore radius

R_s	Radius of the curvature
S	Slope of saturation vapour pressure curve at the ambient air temperature
$Sa *$	Degree of saturation
Sc	Degree of saturation associated with capillary forces
T	Transpiration rate per unit of the soil surface area
T_s	Surface tension of the soil
$u_a - u_w$	Matric suction
u_w	Pore water pressure
Vvi	Pore volume of each fraction
W_i	Solid mass per unit sample mass in the i^{th} particle-size range
z	Depth below the soil
$zmax$	Maximum depth of the root zone
α	Scale parameter inversely proportional to mean pore diameter
$\beta(x, y, z)$	Root density as the length of root per unit of soil volume
γ	Psychometric constant
δ	Water potential of roots
θ	Volumetric water content
Θ	Normalized water content
θ	Angle of shear distortion in the shear zone
θ_r	Soil residual moisture content
θ_s	Saturated volumetric water content
θ_{vi}	Accumulated volumetric water content
ρ_a	Air density
ρ_{dry}	Dry density of the soil
ρ_p	Particle density

ρ_w	Density of water
$\sigma_n - u_a$	Net normal stress
σ_t	Mobilized tensile stress of root fibers developed at the shear plane
τ'	Shear strength of unsaturated soil
τ_{ff}	Shear stress plane at failure
ϕ'	Effective angle of internal friction
ϕ^b	Rate of shear strength growth in relation to a change in matric suction
χ	Parameter proportional to degree of saturation
Ψ_o	Osmatic suction
Ψ_{os}	Osmatic suction of saturated soil sample
Ψ_0	Suction at complete dryness
Ψ_n	Normalization parameter
Ψ_r	Residual suction

Chapter 1

1 INTRODUCTION

1.1 General

Bioengineering solutions are usually recommended as a complementary technique combined with geosynthetic reinforced soil retaining walls, gabions, concrete crib walling, timber crib, retention and drainage (Barker, 2001; Martin, 2001; Martin et al., 2001). Engineers typically anticipate that it takes 5–10 years before the roots of plants produced using bioengineering procedures have improved the strength of the soil sufficiently in heavily populated urban regions where rapid ground improvement techniques are necessary. Nonetheless, bioengineering methods have benefits for Australia, Southeast Asia, and other tropical areas where deforested highland sites with significant landslide risk and soft soil formation are extremely sensitive to precipitation. If the tree can be introduced in these areas, it can reduce the moisture content of soil and increase the soil suction. The bioengineering technique of using vegetation to stabilize the ground is typically more cost-effective than using other traditional techniques. A cost comparison between geo-structure (vegetation) and traditional civil structure elements has been made by Noraini & Ghani (2001). They concluded that bioengineering slope stabilization methods are at least 80% cheaper than conventional methods of slope stabilization like rock gabions.

The purpose of vegetation is to stabilize slopes by mechanically strengthening soils through root systems and hydrologically reducing soil water content through transpiration and precipitation interception (Ziemer, 1981; Greenway, 1987; Mulyono et al., 2018). Figure 1.1 illustrates the hydrological and mechanical components of the vegetative contribution.

According to the above summarization, tree roots play a major role in ground and slope stabilization by increasing the strength and stiffness of the soil positively. When evaluating how vegetation affects ground improvement, tree roots are the primary factor because they: (a) strengthen the soil through their mechanical properties; (b)

dissipate excess pore water through the shorter paths.; and (c) increase suction by the root water uptake.

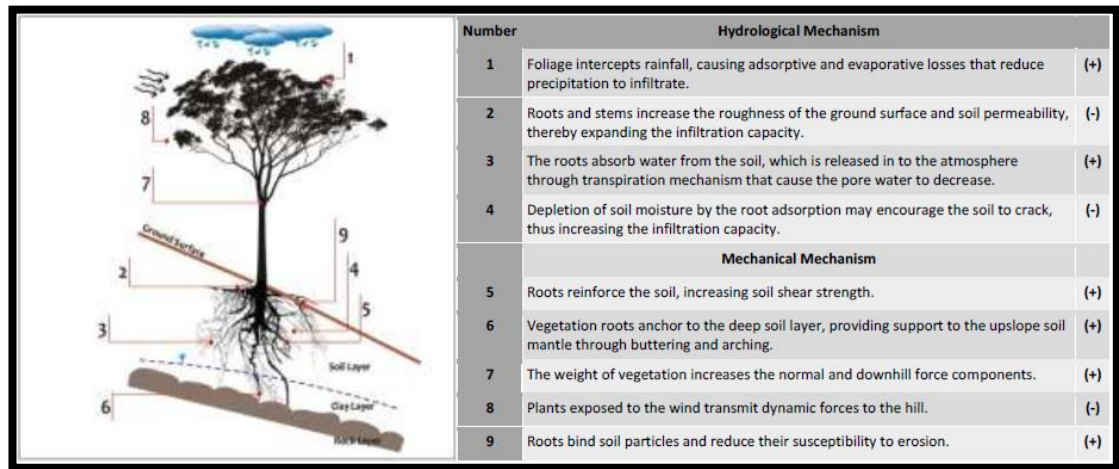


Figure 1.1: Hydro mechanical effects of vegetation on slope stabilization (modified after Mulyono et al., 2018)

1.2 Description of Problem

Influences of tree roots on bioengineering solutions such as slope stabilization involve mechanical (root reinforcement) and hydrological (evapotranspiration) effects (Greenway, 1987; Pollen-Bankhead & Simon, 2010). Previous studies, however, considered the mechanical and hydraulic behavior of tree roots separately when evaluating the impact of vegetation, which failed to yield reliable results because mechanical properties of tree roots depend on suction. Most of centrifuge modeling studies (e.g., Eab et al., 2015; Ng et al., 2014) simulated the roots using artificial materials such as cellulose acetate, polyester fibers, or fishing line. The results of those tests might not accurately reflect how real plant roots behave on slopes as these synthetic materials are less sensitive to moisture than actual plant roots.

However, the coupled behavior of root reinforcement and root water uptake has been tried to model by previous researchers, but these models are very complicated. Therefore, the investigation was carried out to recognize the effect of the soil suction on the root reinforcement in this study.

1.3 Objectives and Scope of the Study

This empirical model can be easily used by Sri Lankan practicing engineers. Therefore, this will greatly impact ground improvement and slope stabilization works in Sri Lanka. Moreover, the above-mentioned deliverables in this research can be developed for the different soil and ground conditions with different tree species.

This study mainly consists of laboratory and field experiments to achieve the following main two objectives.

- Objective 01 - Studying behavior of unsaturated Sri Lankan Semi-Coastal Sandy soil using Soil Water Characteristic Curves (SWCCs)
- Objective 02 - Investigating the influence of suction on root reinforcement of the *Alstonia macrophylla* with Sri Lankan Silty Sand

The specific deliverables which are used to achieve objective 01 as follows,

- ✓ Developing Soil Water Characteristic Curves (SWCCs) for the selected soil by using a few instrumentations
- ✓ Developing SWCCs for the selected soil according to prediction models
- ✓ Evaluating the reliability of the prediction models for selected soil comparing the experimental model
- ✓ Recalculating the values of modal parameters for the most reliable prediction models

The specific deliverables which are used to achieve objective 02 as follows,

- ✓ Preparation of test specimens
- ✓ Developing large-scale direct shear testing setup
- ✓ Conducting direct shear tests for soil samples with and without tree roots for different levels of the matric suction
- ✓ Analyzing the test results to investigate the influence of the soil suction on the root reinforcement of the plant.

The studies of the selected soil type and tree plant were initially conducted as per the standard. The mechanical and hydrological behavior of the selected plant were measured by fulfilling the below sub deliverables,

- ✓ Plant selection
- ✓ Evaluating volume ratio between volumes of the soil and roots
- ✓ Observing the suction variation of the soil sample with and without a plant against the time
- ✓ Developing an empirical correlation between the root water uptake and total area of leaves of the tree plant
- ✓ Quantifying the root volume

1.4 Organization of the Thesis

Chapter 1 is the introduction

Chapter 2 is a literature review. The basic idea and the application of unsaturated soil mechanics are initially discussed. After that, the introduction of the Soil Water Characteristic Curve is discussed under the indirect measurement of unsaturated soil. Furthermore, the development of the SWCC is discussed with experimental and analytical procedures. For the second part of Chapter 2, the broad introduction to employing tree roots for ground improvement is discussed with cohesion due suction and root reinforcement. After that, the proposed model for ground improvement with vegetation are presented in Chapter 2. Furthermore, the basic introduction of the root system and root water uptake are discussed.

Chapter 3 includes the experimental methodology used to determine the basic soil properties of the selected soil type including specific gravity test, liquid and plastic limit test, particle size distribution, and organic content test. The soil classification conducted according to the Unified Soil Classification System is discussed in the latter part of the chapter.

Chapter 4 explains the study of the mechanical and hydrological behaviors of the selected plant. The reasons which caused to the selection of plant are initially discussed. After that, evaluating the volume ratio between volumes of the soil and selected roots is discussed to understand the growth pattern and rate of the roots.

Furthermore, the suction variation of the soil with and without tree roots against the time is discussed. The empirical correlation between the root water uptake and total leaf area is also discussed in this chapter.

Chapter 5 mainly describes the developing methods of SWCC using experimental and analytical procedures. Then, this chapter presents the SWCC for the selected soil type which is developed according to the experimental (pressure plate apparatus, moisture, and suction sensors, and WP4C) and analytical (prediction models of Arya & Paris, 1981; Aubertin et al., 2003; Wang et al., 2017) procedures. Further, the reliability of the prediction models is discussed in this chapter comparing the experimental results.

Chapter 6 explains the influence of matric suction on root reinforcement. This chapter initially described the sample preparation for the shear tests, developing a large-scale direct shear testing setup. The latter part of the chapter presents the test results and observations of the 24 large-scale direct shear tests which can be used to confirm the statement that “The mechanical interactions between roots and soil, such as root tensile strength and root cohesiveness, are suction-dependent” proposed by previous researchers.

Chapter 7 concludes the conclusions and recommendations for future works.

Chapter 2

2 LITERATURE REVIEW

2.1 General

The basic soil mechanics are mostly encountered with saturated soil, including saturated sand, silts, and clays. However, various soil materials in engineering practice are encountered whose behavior needs to be inconsistent with the theories of traditional, saturated soil mechanics. Most soils that do not behave according to traditional saturated soil mechanics are unsaturated soils (i.e., water and air in the voids). It is necessary for the excavation, remolding, and compacting processes. Within the parameters of traditional soil mechanics, it has been hard to anticipate the behavior of unsaturated soils. Therefore, an overview of unsaturated soils is presented in the first half of this chapter with a discussion of the main aspects of unsaturated soils named, an introduction to unsaturated soil mechanics, needs for unsaturated soil mechanics, basic state variables for unsaturated soils, measurement and estimation of basic state variables of unsaturated soils, and unsaturated soil properties.

There are mainly two ways to quantify the unsaturated soil properties, including direct and indirect measurements. The challenging issue is to develop accurate prediction models for the behavior of the unsaturated soil using direct measurements to reflect the actual unsaturated soil properties. Therefore, a brief introduction about the Soil Water Characteristic Curve is made in this chapter as an indirect measurement that can describe the behavior of the unsaturated soil. Furthermore, the experimental and analytical methods are discussed that are used to develop the SWCC.

The strength of the subsurface soil influences the stability of many engineering designs. Many geotechnical applications, such as lateral earth pressures, bearing capacity, slope stability, etc., rely on the shear strength of the soil. Many engineered designs are built on unsaturated soil. Because of that, quantifying the shear strength of the unsaturated soil is a main aspect of the site investigation. Therefore, this chapter also has been included with the theoretical models that can be used to quantify the shear strength of unsaturated soil.

As the bioengineering solutions, the tree roots improve the shear strength of unsaturated soil, including (a) the mechanical strengthening provided by root reinforcement with main root, and (b) hydrological strengthening with the matric suction of soil generated by the root water uptake. In the latter part of this chapter, the above processes are reviewed which promote the shear strength of the unsaturated soil with vegetation.

2.2 Unsaturated Soils

2.2.1 Unsaturated Soil Mechanics

Soils are naturally formed with solids and voids and the void spaces may be filled with water, air, and both. As per the filling material, the soil can be divided into two categories: saturated soils, where all voids are filled with water; and unsaturated soils, where the voids are partially filled with water. The foundation of classical soil mechanics was laid in saturated soils with water and solid in two phases.

An unsaturated soil has three phases and they are (1) solids, (2) water, and (3) air as per the Figure 2.1. However, the specialty of the unsaturated soil is the existence of a fourth phase and that is named as air-water interface or the contractile skin (D. G. Fredlund & Morgenstern, 1977). The contractile skin creates a permanent barrier between the water and air phases by acting like a thin membrane interwoven throughout the voids of the soil. The water content, volume, and shear strength of the unsaturated soil can alter as a result of modifications to the contractile skin.

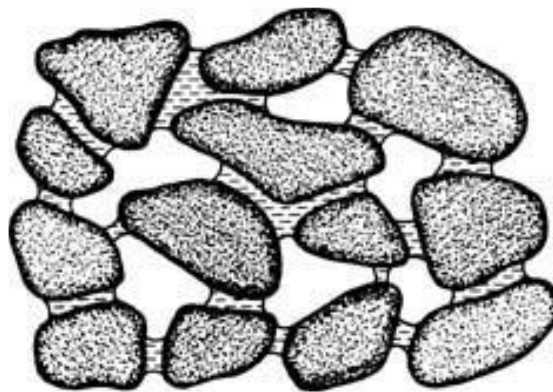


Figure 2.1: Unsaturated soil structure

2.2.2 Need for Unsaturated Soil mechanics

“Why has not a useful science developed and thrived for unsaturated soils” is a valid question. A superficial study might make one believe that such a science is unnecessary. However, this becomes a real case when the problems are caused by expansive soil. According to Jones & Holtz (1973), swelling and shrinking soils alone cause at least \$2.3 billion in damages to homes, roads, buildings, and pipelines per year in the United States, which is more than twice as much damage as is caused by floods, hurricanes, tornadoes, and earthquakes combined. The expansive soil is a hidden disaster. Sometimes, a practical science has not been well developed for unsaturated soils due to two reasons (D. G. Fredlund, Ranhardjo, et al., 2012b). First, there did not appear to be an adequate science with a theoretical basis, and second, it would not seem to have been a procedure for recovering money for the engineer's services. Certainly, studying the unsaturated soil behavior should develop as a suitable technique. Such a system must be (1) applicable, (2) affordable to implement, (3) theoretically sound, and (4) conceptually similar to traditional saturated soil mechanics.

Several applications in the construction sector heavily rely on unsaturated soil behavior. The expansive clays are used as a filling material in earth dam construction. When soil is unsaturated, engineers should give more attention to the behavior of the unsaturated soil. In addition, a key aspect of the design of an earth dam, slope stability, is evaluated as a safety factor. A change in the safety factor may be related to a change in the shear strength. The unsaturated condition of filling soil is a good indicator of the increment of the shear strength of the soil.

Natural slopes always affect by changing environment. Undisturbed soil samples are taken from potential failure surfaces that are above the groundwater table while investigating the stability of a natural slope. The potential failure surface can pass through the unsaturated soils as per the above. This makes it essential to understand unsaturated soil mechanics when analyzing the natural slope stabilization.

Vertical excavations are often used to install a foundation or a pipeline. The soil type, the depth of the excavation, the amount of precipitation, the depth of tension cracks,

etc., can cause the failure of these excavations. The excavations should be done above the groundwater table with negative pore-water pressures. The pore water pressure temporally decreases with the excavation of the soil for the trench; due to that, the shear strength of the soil is increased. The pore water pressures in the back slope may gradually rise with time and lose the shear strength.

Furthermore, the unsaturated soil mechanics should be applied to analyze the shallow foundation's bearing capacity, ground movements involving expansive soils, soil cover systems, capillary breaks, etc.

2.2.3 Basic State variables of Unsaturated Soils

The state of stress in the soil can be used to characterize the mechanical behavior of the soil. Certain combinations of stress variables of the soil can be referred to as stress state variables. Net normal stress ($\sigma - u_a$), matric suction ($u_a - u_w$), and pore-air pressure (u_a) are the independent normal stresses of the equilibrium for the soil structure. The matric suction and net normal stress are the two independent stress variables for unsaturated soil.

2.2.4 Measurement and Estimation of Basic State Variables of Unsaturated Soils

Soil suction is the state variable with the greatest influence on unsaturated soil mechanics. It is the general term that can be used to describe total suction, matric suction, and osmotic suction. Another primary state variable of unsaturated soil is the volumetric or gravimetric water content. A combination of these two variables can be referred to as SWCC, a function used to evaluate the characteristics of unsaturated soil. A detailed introduction of the SWCC is discussed under upcoming titles.

Soil suction can be measured using relative humidity immediately adjacent to the water surface and is called “total suction”. The summation of the matric and osmotic suction is the total suction. The definitions of the above three suction are as follow,

2.2.4.1 Matric Suction

Surface tension leads to the formation of a meniscus at the soil-air interface, which decreases the water vapor pressure. Because when vapor pressure falls and turns more negative, there is an indirect relationship between the radius of the meniscus curvature and the matric suction. The magnitude of the radius of curvature and, consequently, the matric suction pressure is determined by the size of the soil pores and the size of the soil particle. When the degree of saturation decreases, correspondingly decreases the vapor pressure.

Equation [2.1] uses capillary forces to describe the matric suction. The capillary rise is caused by the attractive forces and surface tension between the water molecules and soil ions in the absorbed water as shown in Figure 2.2.

$$u_a - u_w = \rho_w g h_c = \frac{2T_s}{R_s} \quad [2.1]$$

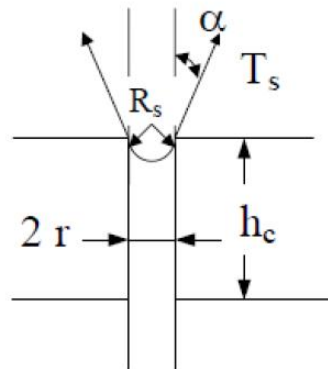


Figure 2.2: Formation of the matric suction with capillary force

2.2.4.2 Osmotic Suction

Osmotic suction is a considerable component of the total soil suction which develops when dissolved ions in water cause a reduction in soil vapor pressure and humidity.

The theoretical relationship between the matric and osmotic suction can be expressed as following Equation [2.2] (D. G. Fredlund, Ranhardjo, et al., 2012a),

$$\psi = (u_a - u_w) + \pi \quad [2.2]$$

Where,

$u_a - u_w$ = Matric Suction in kPa

u_a = Pore air pressure in kPa

u_w = Pore water pressure in kPa and

π = Osmotic suction in kPa

And, few instruments which can be used to measure the above three components are included in Table 2.1 (Fredlund, Ranhardjo, et al., 2012).

Table 2.1: Suction measurement devices

Name of Device	Suction Component Measured	Range, kPa	Comments
Psychrometers (Peltier type)	Total	100 to 8000	Constant-temperature environment required
Filter paper	Total	Entire range	May measure matric suction when in good contact with moist soil
Tensiometers	Negative pore-water pressure or matric suction when pore-air pressure is atmospheric	0-90	Difficulties with cavitation and air diffusion through ceramic cup
Null-type pressure plate (axis translation)	Matric	0-1500	Range of measurement is a function of the air-entry value of ceramic plate
Thermal conductivity sensors	Matric	10-1500	Indirect measurement using variable-pore-size ceramic sensors
Pore fluid squeezer	Osmotic	Entire range	Used in conjunction with psychrometer or electrical conductivity measurements

2.2.5 Unsaturated Soil Properties

The execution of unsaturated soil mechanics has been expedited by estimating unsaturated soil property functions, which introduces a novel philosophical framework (or paradigm). Determining prediction models for characterizing unsaturated soil properties that accurately reflect the actual unsaturated soil properties is a difficult task. Figure 2.3 illustrates how many general approaches can be used to determine the property functions of unsaturated soil.

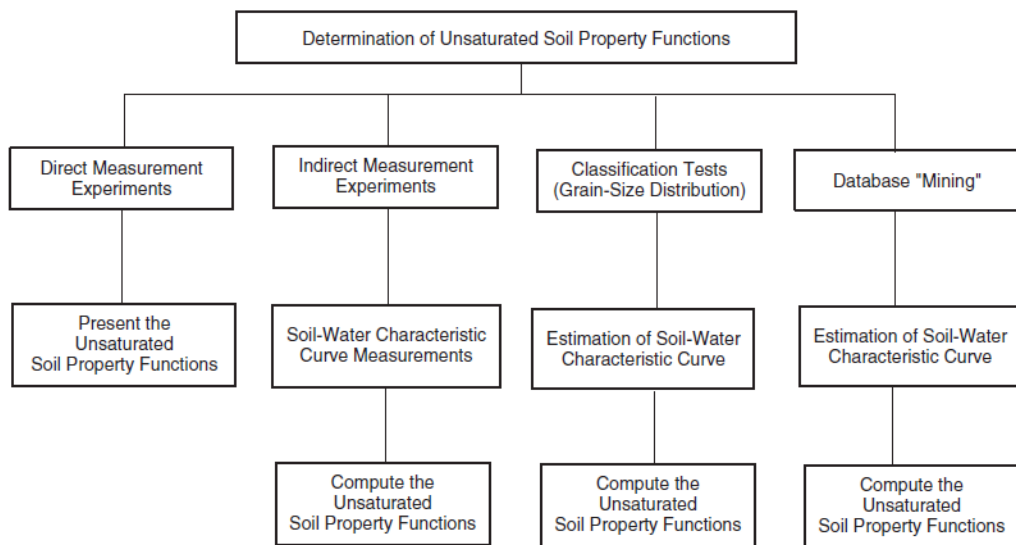


Figure 2.3: Determination of unsaturated soil property functions

The direct measurements of the unsaturated soil testing in the laboratory becomes very cost and labour consuming task in many engineering projects (D. G. Fredlund, Ranhardjo, et al., 2012b). Other approaches for implementing unsaturated soil theories in practice have been suggested wherein, the SWCC is used along with saturated soil parameters to estimate unsaturated soil properties (D. G. Fredlund, 1996).

2.3 Soil Water Characteristic Curve (SWCC)

The mechanical and hydraulic properties of unsaturated soils are predicted using the Soil Water Characteristic Curve (SWCC) initially developed in agriculture science to represent the water storage capacity of a specific material (D. G. Fredlund & Ranhardjo, 1993). SWCC represents the relationship between degree of saturation and matric suction. The degree of saturation can be replaced by gravimetric or volumetric

water content. SWCC depends on the soil mineralogy, grain, pore-size distribution, porosity, surface tension, texture, fabric, particle shape, wetting-drying cycles, contact angle, and entrapped air (Alves et al., 2020).

The SWCC has three phases, namely, 1) the capillary saturation zone (boundary effect zone), 2) the desaturation zone (transition zone), and 3) the residual saturation zone (residual zone), as shown in Figure 2.4 (D. G. Fredlund & Ranhardjo, 1993). The soil remains saturated even when the pore water is in tension due to capillary forces in the capillary saturation zone. This zone ends at the air entry value of the soil; which air starts to enter the soil. In the desaturation zone, the water is displaced by air within the pores, and the zone ends with residual water content where a larger suction is required to remove the additional water. In the residual saturation zone, the water is strongly adsorbed onto the soil particles and flows as vapor.

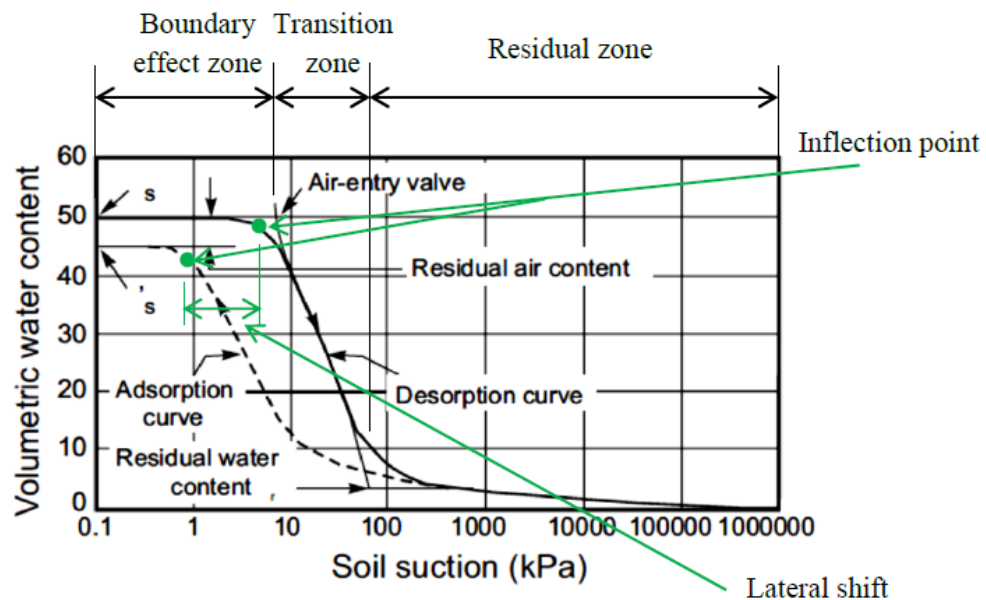


Figure 2.4: Phases for the SWCC (after Fredlund and Rahardjo, 1993)

The SWCC can be developed by conducting experimental procedures with pressure plate apparatus, tensiometers, filter paper, moisture, suction sensors, etc. Mahannopkul & Jotisankasa (2019) experimentally developed the SWCC for clayey sand in Southern Thailand using three types of equipment varying according to the matric suction value. Isopiestic Humidity Control has been used for matric suction values ranging from 10^3 to 10^5 kPa, whereas tensiometer ranges from 10^{-1} to 10^2 . The Pressure Plate has

covered the range in between. Croney & Coleman (1954) observed the behavior of incompressible and compressible soils by developing SWCCs using the pressure plate. Developing SWCC using the apparatus mentioned above are time and labor-consuming task. Gee et al., (1992) introduced the chilled mirror or dew-point method to measure the total suction in the medium to high suction range using the water activity meter.

Moreover, this device was further developed as WP4C- Dew Point Potential Meter (ASTM D6836-02(2008)E2), which measures water suction quickly, precisely, and consistently. Hence, WP4C can be used to develop the SWCC. Although WP4C is convenient equipment, the development of SWCC utilizing this instrument is rare in the literature. Thus, verifying the results obtained from WP4C using other apparatus will increase the reliability of the output.

Furthermore, prediction models have been developed to estimate the SWCC by using basic soil properties such as grain size distribution, void ratio, and densities due to the complex retention behavior of soils. Arya & Paris, (1981), Haverkamp & Parlange, (1986), Arya & Dierolf, (1989), Fredlund M.D. (2000), Aubertin et al., (2003), and Wang et al., (2017) developed different models to predict the SWCC. However, the models are based on different theories and fundamentals. As a result, they have some restrictions and may yield inconsistent findings. Alves et al. (2020) focused on evaluating the performance of prediction models using 19 particle size distribution curves (PSD) using Arya & Paris, (1981b), Arya & Dierolf, (1989), Aubertin et al., (2003) and Wang et al., (2017).

2.3.1 Developing SWCC using Experimental Procedures

This section describes the details of the pressure plate apparatus, WP4C, and moisture and suction sensors.

2.3.1.1 Pressure Plate Apparatus

The pressure plate apparatus manufactured by SoilMoisture Equipment Cooperation can be used to develop the SWCC of soil by following the pressure plate test (ASTM D2325). The main elements of the pressure plate apparatus are the high-air-entry

ceramic disk and pressure chamber as shown in Figure 2.5. The ceramic plate should always be in contact with water in a compartment below the disk and maintained in a saturated condition. This apparatus can be used with a high matric suction range (i.e., up to 1500 kPa). Soil specimens are placed on the ceramic plate and pressurized with the desired matric suction such that it does not exceed the air entry value of the ceramic plate. The water starts draining through the disk due to the applied pressure, and at the equilibrium stage, the soil specimen has reached the desired matric suction. The corresponding volumetric water content can be obtained at this stage by measuring the weight of the specimen. The SWCCs have been developed using pressure plate apparatus in many countries (D. G. Fredlund & Ranhardjo, 1993).

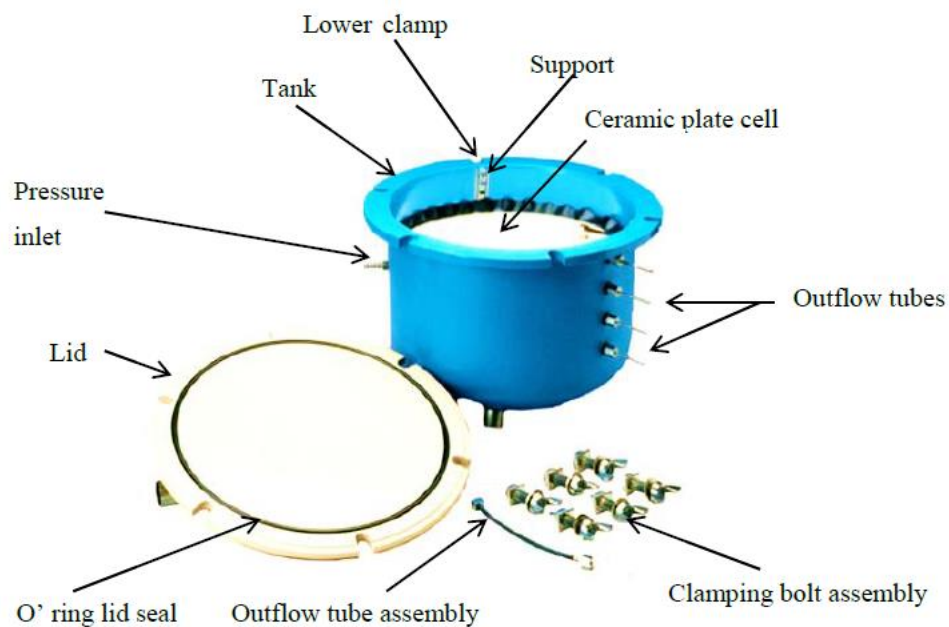


Figure 2.5: Component of pressure plate apparatus

2.3.1.2 WP4C

WP4C can be used to determine the SWCC in an extensive range. It uses the dew point chilled mirror technique to measure the soil suction and consists of a sealed chamber with a fan, a photoelectric cell, a mirror, and an infrared thermometer, as shown in Figure 2.6.

The soil specimen can be prepared in plastic container or stainless steel ensuring the soil does not spill and contaminate the sample chamber. The specimen is then put

inside the chamber, where it is thermodynamically adapted to the surroundings. A Peltier cooling device can be used to bring a mirror's surface temperature down to the dew-point temperature while the fan speeds up the equilibration process. The first indication of condensation on the mirror is discovered by a photoelectric cell. The dew point temperature is determined by using a thermocouple, and it is the temperature at which condensation forms on the mirror. The chamber temperature considered the same as the temperature of the soil specimen at equilibrium, is measured using an infrared thermometer. The above mentioned two temperatures are used to calculate the vapor pressure above the soil specimen in the chamber and the saturated vapor pressure at the same temperature. Finally, the total suction of the specimen is calculated using Kelvin's equation.

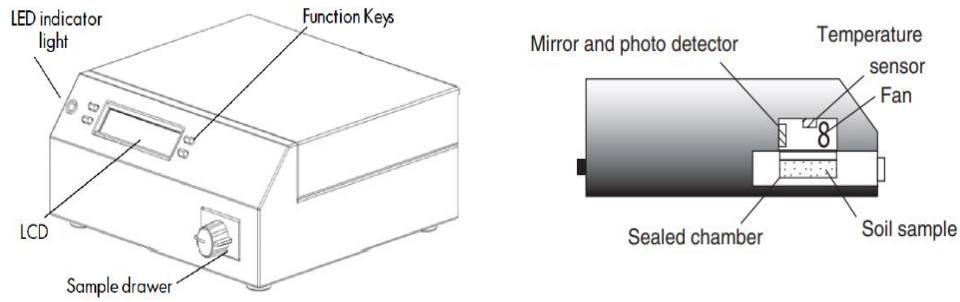


Figure 2.6: WP4C instrument

The total suction of a sample is the sum of matric and osmotic suction. The osmotic suction can be approximately determined by measuring the electrical conductivity (EC) of the saturation extract of the soil. The osmotic suction of the saturation extract is computed using Equation 2.3, and the osmotic component of the water suction is calculated using Equation 2.4.

$$\Psi_{os}(MPa) = -0.036EC(ds/m) \quad [2.3]$$

$$\Psi_o = \Psi_{os} \left(\frac{\theta_s}{\theta} \right) \quad [2.4]$$

2.3.1.3 Moisture and Suction Sensors

Volumetric moisture content is measured as a voltage reading in moisture sensors, and the voltage reading depends on the soil. Therefore, calibration should be conducted for

the soil to develop the relationship between the moisture content and voltage reading for each sensor. The continuous field measurements of matric suction can be measured using TEROS 21 suction sensor, a maintenance-free matric suction sensor designed for the long term.

2.3.1.4 Van Genuchten's model

The SWCCs developed using experimental procedures can be fitted according to Van Genuchten's (VG) model using Equation [2.5] (van Genuchten, 1980).

$$\theta = \theta_r + \frac{\theta_s - \theta_r}{[1 + (\alpha|h|)^n]^m} \quad [2.5]$$

Where,

θ = volumetric moisture content,

h = matric water suction (kPa),

θ_s = soil saturated moisture content,

θ_r = soil residual moisture content,

α = scale parameter inversely proportional to mean pore diameter (cm^{-1}), and

n and m = shape parameters of soil water characteristics, $m = \frac{n-1}{n}$, $0 < m < 1$.

2.3.2 Developing SWCC by using Prediction models

2.3.2.1 Arya and Paris model (1981)

Arya and Paris model generate the SWCC curve using the soil's particle size distribution (PSD) (Arya & Paris, 1981a). The particle density and the bulk density are also used as inputs in the model. The cumulative PSD is divided into n fractions, and each segment's pore size is determined. The pore volume of each fraction (V_{vi}) is calculated according to Equation [2.6].

$$V_{vi} = \frac{W_i}{\rho_p} e \quad (i = 1, 2, 3, \dots, n) \quad [2.6]$$

The accumulated volumetric water content (θ_{vi}) stored up to the fraction i is given by Equation [2.7],

$$\theta_{vi} = \sum_{i=1}^n \frac{V_{vi}}{V} = \sum_{i=1}^n V_{vi} \rho_{dry} \quad [2.7]$$

Where,

W_i = solid mass per unit sample mass in the i^{th} particle-size range,

ρ_p = particle density,

e = void ratio, and

ρ_{dry} = dry density.

A mean volumetric water content corresponding to its midpoint for a given particle size range, can be calculated by using Equation [2.8],

$$\theta_{vi}^* = \frac{\theta_{vi} + \theta_{vi+1}}{2} \quad [2.8]$$

The matric suction ($u_a - u_w$) is estimated as Equation [2.9],

$$(u_a - u_w) = \frac{2T_s}{r_i} \quad [2.9]$$

T_s = surface tension

r_i = mean pore radius

r_i is related to the mean particle radius (R_i) by Equation [2.10].

$$(u_a - u_w) = \frac{2T_s}{r_i} \quad [2.10]$$

Where n_i is the number of particles, to account for the non-spherical nature of the particles, an empirical parameter α has been introduced. The authors suggest a value between 1.35-1.40 for α . Change in α produces a translation of the entire SWCC along the matric suction axis. α can be obtained by an iterative method such that the value of $|\ln(u_a - u_w)_{\text{measured}} - \ln(u_a - u_w)_{\text{calculated}}|$ becomes minimum.

2.3.2.2 Aubertin et al. (2003)

The primary soil properties of soil are used to predict SWCC in this method (Aubertin et al., 2003). The degree of saturation (S_r) is computed as the Equation [2.11],

$$S_r = \frac{\theta}{n} = S_c + S_a^* (1 - S_c) \quad [2.11]$$

Where,

θ = matric suction

S_c = degree of saturation associated with capillary forces

S_a^* = degree of saturation caused by the adhesion and S_a^* is computed as the Equation [2.12], Equation [2.13], Equation [2.14] and Equation [2.15],

$$\text{if, } S_a < 1 \quad S_a^* = S_a \quad \text{else, } S_a = 1 \quad [2.12]$$

$$S_a = a_c C_\Psi \frac{\left(\frac{h_{co}}{\Psi_n}\right)^{2/3}}{e^{1/3} \left(\frac{\Psi}{\Psi_n}\right)^{1/6}} \quad [2.13]$$

$$C_\Psi = 1 - \frac{\ln\left(1 + \left(\frac{\Psi}{\Psi_r}\right)\right)}{\ln\left(1 + \left(\frac{\Psi_0}{\Psi_r}\right)\right)} \quad [2.14]$$

$$S_c = 1 - \left[\left(\frac{h_{co}}{\Psi}\right)^2 + 1\right]^m * \exp\left[-m \left(\frac{h_{co}}{\Psi}\right)^2\right] \quad [2.15]$$

Where h_{co} is the equivalent capillary rise, m : pore size distribution parameter of the model, a_c is the adhesion coefficient; Ψ_n is a normalization parameter. Ψ_0 is suction at complete dryness and Ψ_r is residual suction. For granular materials, a_c is proposed as 0.01 by the authors and $m = 1/C_u$. Different equations are presented for h_{co} depending upon the coarse and clayey nature of the soil. h_{co} for granular material is determined by parameters C_u , e , D_{10} .

2.3.2.3 Wang et al. (2017)

SWCC is developed based on Van Genuchten's water retention model and basic soil properties (Wang et al., 2017). The degree of saturation is measured using Equation [2.16] in this method. α is a parameter related to air entry value, and n is a parameter

associated with the slope of the water retention curve where n , α is dependent on C_u and D_{60} . Also, two different constants C_1 , C_2 are introduced, which depend on the soil material. The authors have proposed 1.07 & 12.07 for C_1 , C_2 , respectively.

$$S = [1 + (\frac{u_a - u_w}{\alpha})^n]^{1/n - 1} \quad [2.16]$$

2.3.3 The available literature on the comparison of prediction models

Different research has focused on comparing the available prediction models with experimental data to evaluate the reliability of the prediction models. Alves et al. (2020) focused on evaluating the performance of prediction models for the coefficient values proposed by the authors (Arya & Paris, (1981b), Arya & Dierolf, (1989), Aubertin et al., (2003) and Wang et al., (2017)) using 19 glass beads varying in particle size distribution, density and porosity. The goodness of fit of the models was evaluated using regression analysis and it was found that Wang et al., (2017) predictions were more accurate as it was originally been developed for sands. Further, Arya & Paris, (1981b), and Arya & Dierolf, (1989) predictions overestimated the matric suction.

2.4 Shear strength of unsaturated soil

The strength of the underlying soil affects the safety of many engineering designs. Many geotechnical applications depend on the shear strength of the soil including bearing capacity, lateral earth pressures, slope stability, etc. Many engineered designs are built on unsaturated soil. Because of that, it is important to quantify the shear strength of the unsaturated soil and the changes in shear strength that might occur due to water infiltration into the soil. Theories for the shear strength of unsaturated soil are also based on the basics of saturated soil. The net normal stress ($\sigma - u_a$) and the matric suction ($u_a - u_w$) can be used to characterize the stress state in the case of unsaturated soil.

2.4.1 Shear strength of saturated soil

The Mohr-Coulomb failure criterion and the effective stress variable can be used to describe the shear strength of a saturated soil (Terzaghi, 1936) as the Equation [2.17],

$$\tau_{ff} = c' + (\sigma_f - u_w)_f \tan \phi' \quad [2.17]$$

Where:

τ_{ff} is the shear stress plane at failure, c' is the effective cohesion, which is the shear strength intercept when effective normal stress is equal to zero, $(\sigma_f - u_w)_f$ is the effective normal stress at failure, σ_{ff} is the total normal stress at failure, u_{wf} is the pore-water pressure at failure, and ϕ' is the effective angle of internal friction.

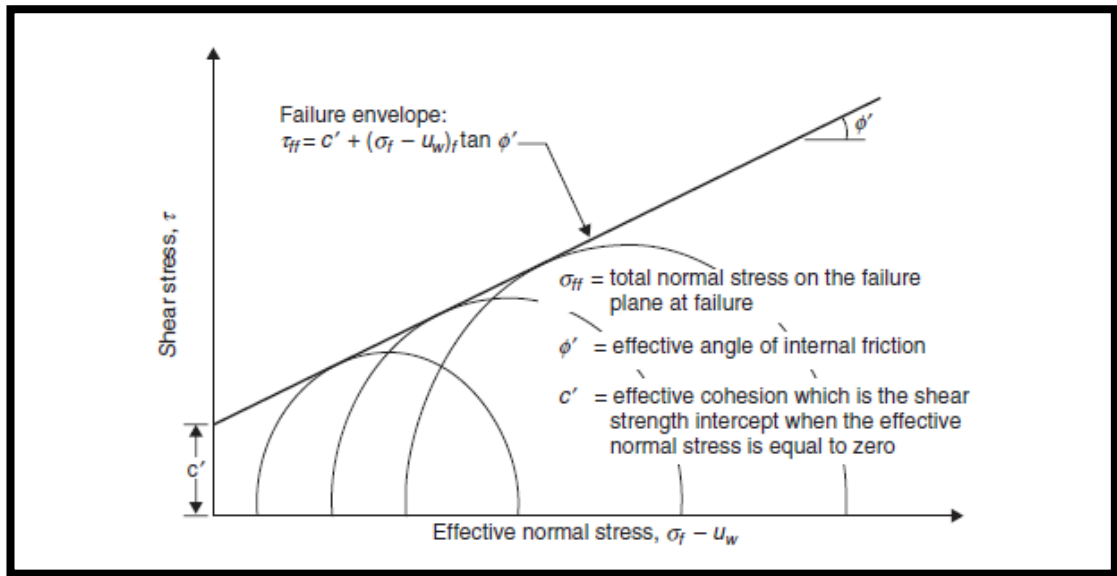


Figure 2.7: Shear failure envelop for saturated condition (after Fredlund and Rahardjo, 1993)

As shown in Figure 2.7, Equation [2.17] defines a linear relationship between shear strength and effective stresses. The line tangent to the Mohr circles is commonly defined as a failure envelope because it represents possible combinations of shear stress and effective normal stress on the failure plane at the failure. The slope of the failure envelope refers to the effective angle of internal friction, and the intercept of the line is called the effective cohesion, c' .

As per the above, Extensions to the concepts and mathematical equations used for shear strength theories for saturated soils have been proposed for theories of shear strength for unsaturated soil. Bishop (1959) has extended Terzaghi's principle of

effective stress for saturated soil to provide an equation for the shear strength of the unsaturated soil, as shown in Equation [2.18].

$$\tau' = c' + (\sigma_n - u_a)\tan\phi' + (u_a - u_w)\chi\tan\phi' \quad [2.18]$$

Where τ' is the shear strength of unsaturated soil, $\sigma_n - u_a$ is the net normal stress, $u_a - u_w$ is the matric suction, and χ is a parameter proportional to degree of saturation.

The value of χ has been varied from 1 to 0 to reflect the transformation from a fully saturation to a totally dryness. Furthermore, there is a number of researchers found theoretical and experimental limitations for quantifying the parameter χ . The effective friction angle and cohesion of the unsaturated soil are similar to the values of the saturated soils.

Mohr-Coulomb failure equation for the saturated soils was extended for the unsaturated soils by Fredlund et al. (1978) as the Equation [2.19].

$$\tau' = c' + (\sigma_n - u_a)\tan\phi' + (u_a - u_w)f_1 \quad [2.19]$$

Where σ_n is the total normal stress on the failure plane at failure, and f_1 is the soil property function defining the relationship between shear strength and soil suction, the derivative of which gives the instantaneous rate of change in shear strength with respect to soil suction. Other variables have same meaning as the above.

Depending on the outcomes of the experiments, the form of Equation [2.19] enables the shear strength envelope for matric suction to be either linear or curved. Measured share strength envelopes are frequently curved over a broad range of matric suction values. The f_1 tends to a value equal to the tangent of the effective friction angle of the saturated soil (i.e. $\tan\phi'$) under low matric suction values less than the air-entry value of the soil. Then, the shear strength envelops gradually curved up to residual suction condition. At high suction values greater than the residual soil suction, f_1 has become zero for several soils with varying silt and clay content (Nishimura & Fredlund, 2001)

A linear equation of the shear strength for an unsaturated soil can be formulated as the equation [2.20] (Fredlund et al., 1978).

$$\tau' = c' + (\sigma_n - u_a)\tan\phi' + (u_a - u_w)\tan\phi^b \quad [2.20]$$

Where,

c' = effective cohesion

$(\sigma_n - u_a)$ = net normal stress state on the failure plane at failure,

u_a = pore-air pressure on the failure plane at failure,

ϕ' = angle of internal friction,

$(u_a - u_w)$ = matric suction on the failure plane at failure, and

ϕ^b = showing the rate of shear strength growth in relation to a change in matric suction

Figure 2.8 shows that Mohr circles corresponding to failure conditions can be plotted in three dimensions for an unsaturated soil using two stress state variables $(\sigma_n - u_a)$ and $(u_a - u_w)$ as abscissas. The envelope slopes at angles of ϕ' and ϕ^b , respectively.

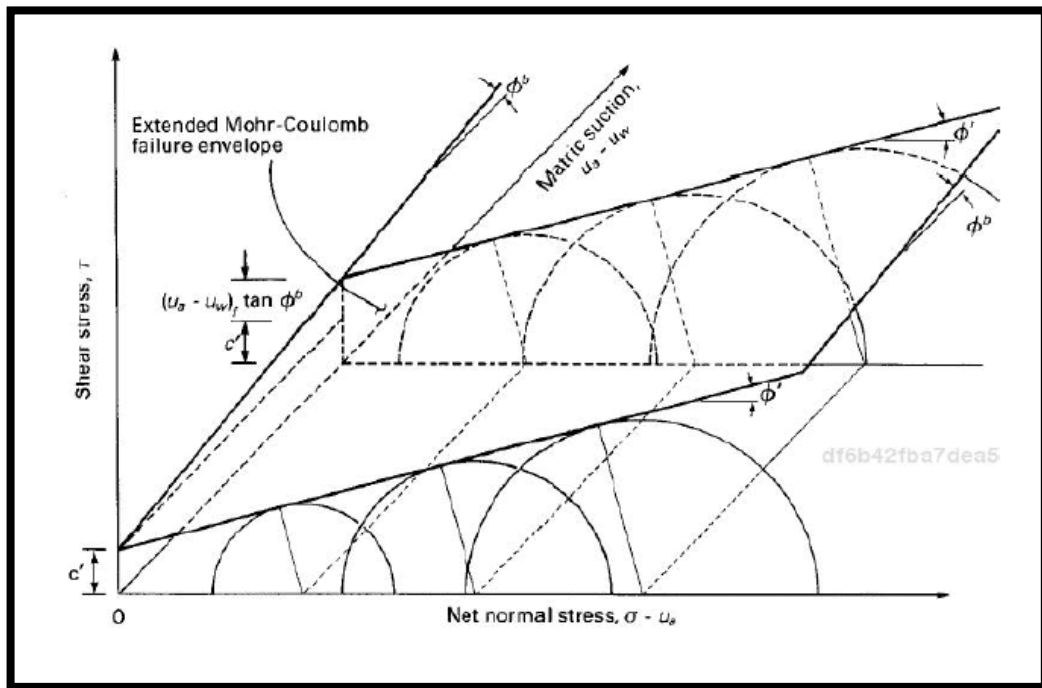


Figure 2.8: Shear failure envelop for unsaturated soil (after Fredlund and Rahardjo, 1993)

Many researchers concluded that the shear strength of the unsaturated soil and matric suction has a linear relationship, whereas (Gan & Fredlund, 1988) and (Escario & Juca, 1989) found that the above relationship is non-linear. However, Equation () can be used for both cases.

The changing shear strength of an unsaturated soil depend on the moisture content of the soil sample. It reflects the relation between the SWCC and shear strength. Using this conclusion, a general non-linear function predicted by S. K. Vanapali et al. (1996) and Fredlund et al. (1996) is given in Equation [2.21]

$$\tau' = [c' + (\sigma_n - u_a)\tan\phi'] + [(u_a - u_w)\Theta^k \tan\phi^b] \quad [2.21]$$

Where,

k = fitting parameter, and

$$\Theta = \text{normalized water content} = \frac{\theta_w}{\theta_s}$$

Fredlund & Xing, (1994) have proposed Equation [2.22] that can be used to obtain the best fit SWCC in terms of a , n , m parameters.

$$\theta_w(\psi) = \theta_s \left[1 - \frac{\ln\left(1 + \frac{\psi}{h_r}\right)}{\ln\left(1 + \frac{10^6}{h_r}\right)} \right] \left[\frac{1}{\ln\left\{\exp(1) + \left(\frac{\psi}{a}\right)^n\right\}^m} \right] \quad [2.22]$$

Where, ψ is the soil suction, θ_w is the volumetric water content, θ_s is the saturated volumetric water content, a is the suction related to the inflection point on the curve, n , m , and h_r are the soil parameters related to the slope at the curve, residual water content, and volumetric water content respectively.

Vanapali et al., (1996) proposed another equation to estimate the shear strength of the unsaturated soil as shown Equation [2.23].

$$\tau' = c' + (\sigma_n - u_a)\tan\phi' + (u_a - u_w) \left[\frac{\theta_w - \theta_r}{\theta_s - \theta_r} \right] \tan\phi' \quad [2.23]$$

Where θ_w is the volumetric water content, θ_r is the saturated volumetric water content, and θ_s is the residual volumetric water content.

Equation [2.21], Equation [2.23], and the other two proposed models were tested by Vanapali & Fredlund (2000) on three distinct soils, and they discovered that they can be applied to all types of soil with a suction range of 0–15000 kPa.

2.5 Shear strength of the soil with tree roots

Some attempts have been made over the past few decades to extend the theories about the bioengineering aspects of vegetation with geotechnical engineering, which affect to the increment of soil stiffness, stabilize slopes, and limit erosion. While earlier research studies mainly concentrated on quantifying the impact that vegetation has on soil shear strength, none adequately described and quantified factors that might be used in the design. The absence of proper information regarding the quantification and design approaches has also been the biggest obstacle to the more widespread application of this technology in practice.

As the bioengineering solutions, the tree roots improve the shear strength of unsaturated soil, including (a) the mechanical strengthening provided by root reinforcement with main root, and (b) hydrological strengthening with the matric suction of soil generated by the root water uptake. The majority of previous studies that measure the mechanical improvement impact of tree roots are mostly based on empirical equations, and frequently these equations only concentrate on specific tree species or conditions (Docker & Hubble, 2008). The experimental interpretation of these equations restricts the applicability of early study findings in this area. It is also challenging to adapt these equations to represent other settings. Furthermore, most of these research studies conducted to quantify the effect of root reinforcement in slope stabilization have been mainly focused on saturated conditions (Docker & Hubble, 2001, 2008). Moreover, many studies only considered the mechanical behavior of tree roots, ignoring the implications of transpiration on the pore water pressure. Indraratna et al. (2006) introduced most of these missing theories by estimating the matric suction caused by root water uptake. However, the coupled effect of root reinforcement, and

root water uptake has been tried to model by previous researchers and these models are very complicated (Pallewaththa, 2019).

2.5.1 Root Reinforcement

Tree roots can increase the shear strength as the apparent cohesion develops due to root reinforcement. Dobson & Moffat (1995) and Docker & Hubble (2001) said that the shear strength is increased due to the apparent cohesion provided by smaller roots less than 20mm diameter while larger and stiffer roots increase the shear strength using the ability of anchoring. According to test results of experiments conducted by Operstein & Frydman (2000) and Docker & Hubble (2001), the influence in soil friction angle caused by tree roots is negligible when the presence of active roots or the drainage condition of the soil has not been considered. Wu et al. (1979), Waldron & Dakessian (1981) and Docker & Hubble (2009) have described the mechanical strengthening generated by root reinforcement (ΔS) in saturated conditions. A root model was developed to theoretically explain the behavior of roots under a shearing action by Warden 1979 and Wu et al. 1981. However, Docker & Hubble (2001) said that there was a 50% difference between the results from using this model and actual data because of oversimplification of the root system.

As per the Waldron (1981), since the friction angle remains unchanged, S can be applied directly to the coulomb equation, as illustrated in Equation [2.24].

$$\tau = c + \Delta s + \sigma_N \tan \phi \quad [2.24]$$

Figure 2.9 represent the behavior of Mohr-coulomb envelopes in reinforced and unreinforced soils

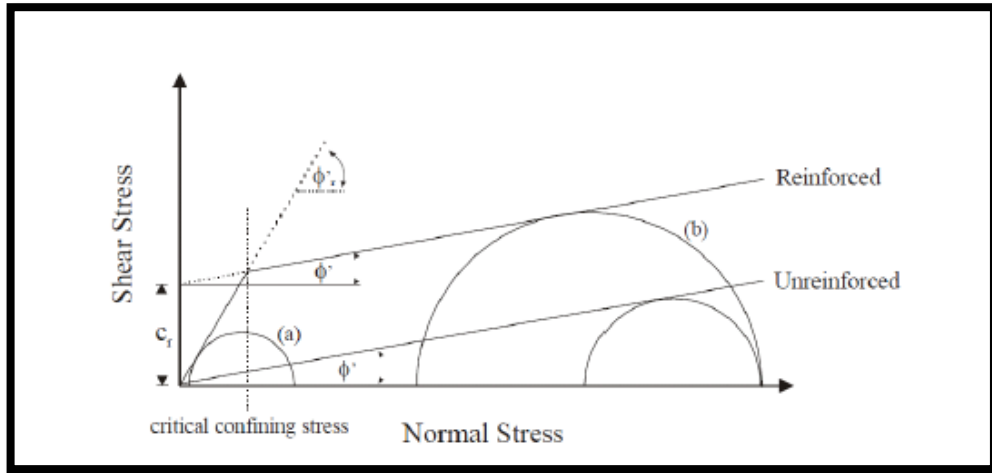


Figure 2.9: Mohr-coulomb envelopes in reinforced and unreinforced soils with circles describing failure by (a) slippage and, reinforcement rupture (after Hausmann, 1976)

Wu et al. (1979) initially developed a simplified model for cohesion due to roots, which is as Equation [2.25].

$$\Delta s = \sigma_t \left(\frac{A_R}{A} \right) (\sin \theta + \cos \theta \tan \phi) \quad [2.25]$$

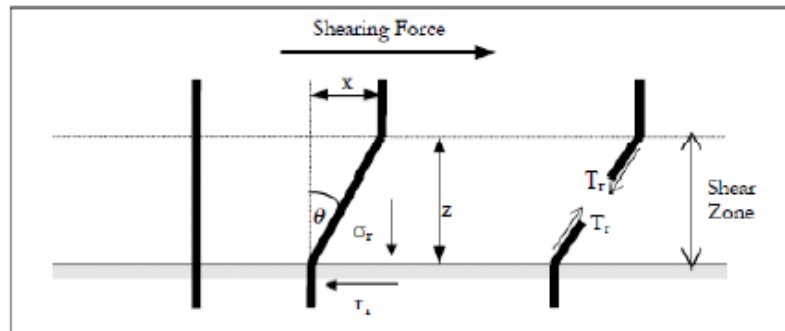


Figure 2.10: Failure pattern of the roots (after Waldron, 1977)

Where,

ϕ = the angle of friction of the soil

θ = the angle of shear distortion in the shear zone

σ_t = the mobilized tensile stress of root fibers developed at the shear plane

$\left(\frac{A_R}{A} \right)$ = the root area ratio

A_R = the root area, and

A = total area of soil

This model merely assumes that the tensile strength of roots is completely mobilized during failure because it does not consider slipped or pulled out roots from the soil prior to failure.

The roots with different diameters and properties tend to gradually fail at different strains and stresses according to the fiber bundle model developed by Schwarz et al. (2010). Therefore, the average ratio between the mobilized tensile stress of roots and the tensile strength of root (T_R) in this study was about 0.4 varied according to plant species and moisture condition.

Furthermore, Docker & Hubble (2001) conducted in situ field shear tests for *Casuarina galuca*, *Eucalyptus amplifolia*, *Eucalyptus elata* and *Acacia floribunda* to capture the relationship between the Δs and RAR and reported the following Equation [2.26], [2.27], [2.28], and [2.29].

$$S_r = 60.61RAR - 1.78 \quad [2.26]$$

$$S_r = 38.12RAR - 0.85 \quad [2.27]$$

$$S_r = 47.44RAR - 0.07 \quad [2.28]$$

$$S_r = 116.43RAR - 8.25 \quad [2.29]$$

Nevertheless, these empirical relationships are limited because RAR is the only variable. These do not consider the effect of suction generated through the root water uptake. As per the above empirical and theoretical relationships, measuring the quantity of the roots is very important to capture the reinforced effect of the roots.

2.5.1.1 Spatial distribution of roots

The root water uptake and suction are significantly influenced by the spatial distribution of roots. When assessing the vegetation's contribution to soil stabilization, many scholars claimed that the distribution of roots has a substantial bearing.

Moreover, the mechanical failure is influenced by the size and shape of the root system.

2.5.1.2 Root systems

Roots serve various purposes, such as anchoring plants, absorbing water, minerals, and nutrients, synthesizing numerous vital substances, including growth regulators, and storing food in root crops (Kramer, 1995). The various tree species have various root systems that have affected the properties of the soil. There are two root systems, as shown in Figure 2.11, which are categorized according to distribution pattern of the root system.

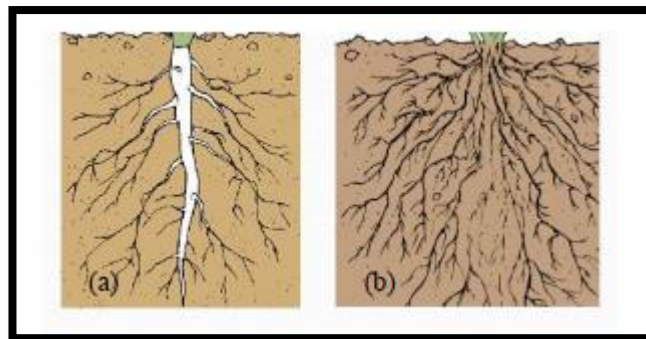


Figure 2.11: Root Distribution (a) main roots system (b) fiber roots system

According to Lynch (1995), Ghestem et al. (2011) and Leung et al. (2015), there are various root architectures as per the Figure 2.12 which are useful for geotechnical concepts of the vegetated environment.

According to Kramer (1995), environmental factors that influence the growth of tree roots include,

- ✓ Water content in the soil
- ✓ soil texture and structure
- ✓ aeration, moisture, pH, temperature, and salinity of the soil.
- ✓ presence of hazardous substances like lead, copper, and aluminum.
- ✓ competition with other plants; and
- ✓ presence of fungi, bacteria, and animals that inhabit the soil.

The impact of various soil compaction levels on the spiral distribution of soil is depicted in Figure 2.13.

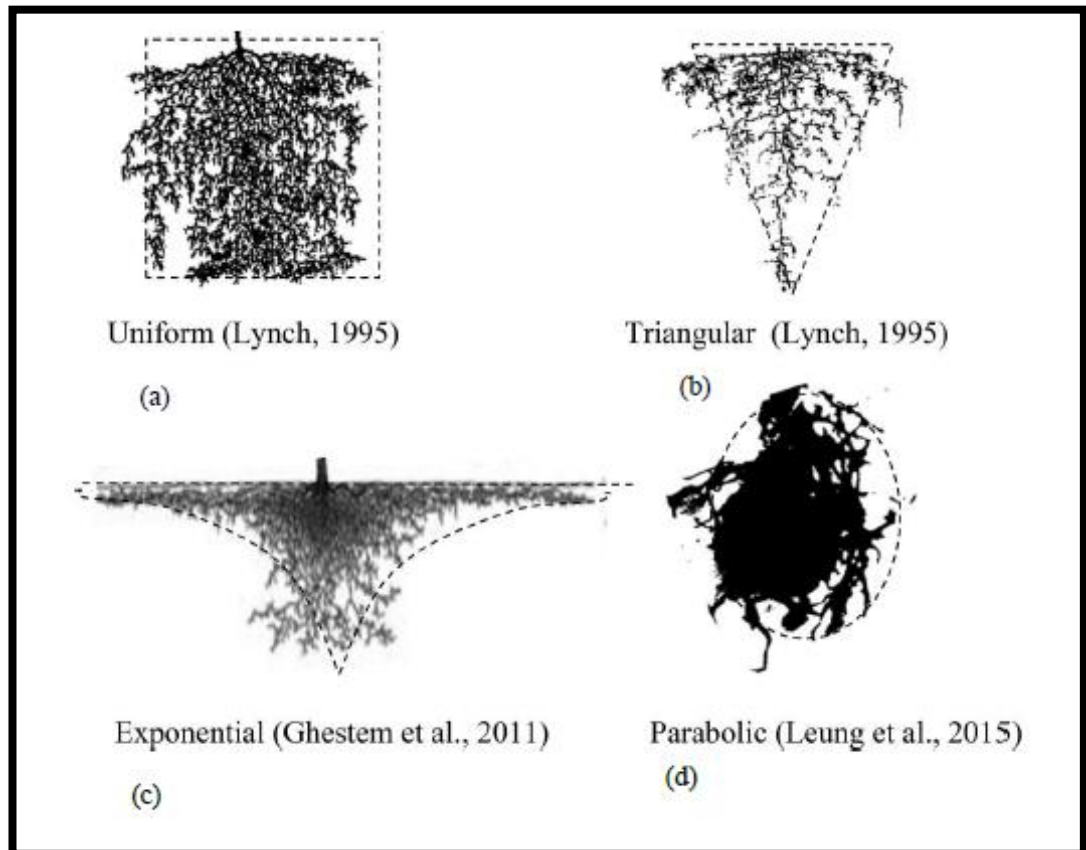


Figure 2.12: Various root systems

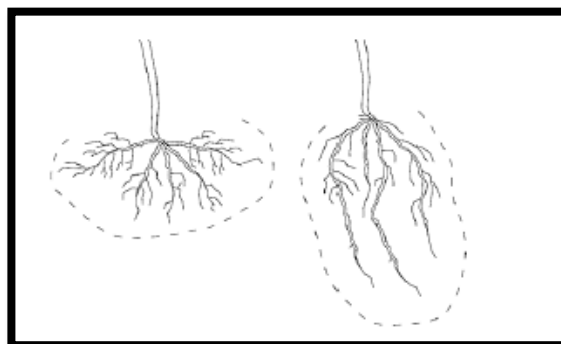


Figure 2.13: Root system of young barley plants with different bulk densities
(Modified after Gilmen (1980))

A normal spiral distribution of the root system requires a healthy gas exchange in the soil, but this gas exchange is impacted by poor structure. According to Kramer (1995),

low oxygen levels would lead to poor root type, and low nitrogen levels would restrict legumes' ability to fix nitrogen in their roots. The optimum temperature must be maintained for the greatest possible spatial distribution of trees. Figure 2.14 demonstrates the impact of temperature on the structure of the root system.

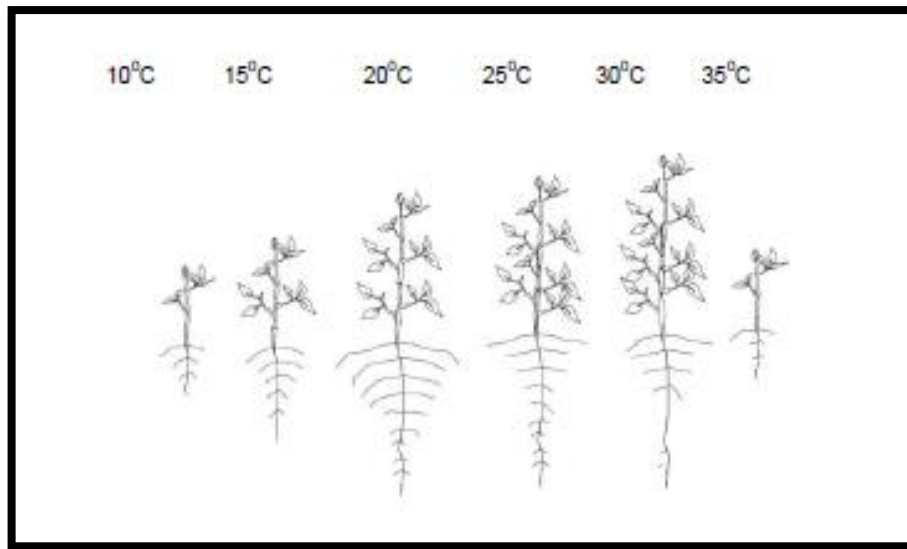


Figure 2.14: Root growth pattern and shape of potato seedlings with the impact of the root zone temperature (modified after Sattelmacher et al. ,1990)

2.5.1.3 Quantification of the root system

Measuring the root system is very important to identify the quantity and structure of the root system. The root systems can be quantified by using excavation, auger, glass wall, profile wall, and monolith. These techniques require a lot of time and labor compared to the utilization of radioactive traces (Böhm, 1980).

2.5.1.4 Root Area Ratio

The percentage of a total cross-sectional soil area taken up by roots is known as the "root area ratio." When directly compared to the cross sectional area in the shear plane, the root area ratio plays a significant part in the root fibers' contribution to the shear strength. The root area ratio, which fluctuates with depth, is difficult to quantify on a plane perpendicular to the direction of root growth. When measured in a parallel plane, it is easy to observe and represents an average of the root fiber contribution in the soil.

2.5.1.5 Dry biomass of the roots per unit volume

Apiniti (2017) has directly measured the root contents in terms of “root biomass per soil volume”. The specimen was disassembled once the saturated permeability test was finished and the final soil moisture content was found. The remaining soil with roots was washed and passed through sieve #18 to find the roots. Then, the exposed root was dried in an oven at 105⁰C recommended by Böhm (1980), to determine the dry biomass of roots. Using this mass, the dry biomass per unit soil volume was measured.

2.6 Suction effect of the tree roots

The soil suction can be rapidly increased with moisture reduction of the soil due to the root water uptake. Most mature trees may create soil suction up to 30 MPA, and Pinus radiata can absorb from the ground a water content equivalent to its weight in one day (Fahati et al., 2007). Rate of transpiration of the tree is the primary factor that affects the root water uptake. It depends on the physiology of the tree and environmental parameters. Most previous research only studied and observed the root water uptake behavior.

The temperature, humidity, wind speed and moisture condition of the soil are the environmental parameters that affect the transpiration rate. There are several equations to calculate the transpiration rate using various correlations with the factors affecting transpiration.

Green (1992) introduced the equation for the rate of transpiration as shown in Equation [2.30],

$$T_p = \sum_i f_i \left[\frac{sR_{n,i} + \frac{0.93\rho_a C_p D_a}{r_{a,i}}}{S + 0.93\gamma \left(2 + \frac{r_{s,i}}{r_{a,i}} \right)} \right] \quad [2.30]$$

Where,

f_i = fractional of each leaf expressed in terms of the total leaf area of the canopy,

$R_{n,i}$ = net radiation flux density absorbed by each leaf,

D_a = vapour pressure deficit of air,

$r_{a,i}$ = boundary layer resistance of each leaf,

$r_{s,i}$ = stomatal resistance of each leaf,

S = slope of saturation vapour pressure curve at the ambient air temperature

γ = psychometric constant,

ρ_a = air density, and

C_p = specific heat capacity of air at constant pressure.

Iskandar (1978) introduced an equation for the root water uptake by considering the rate of transpiration as shown in Equation [2.31],

$$S = \frac{T \cdot L(z) \cdot k}{\int_0^{zmax} L(z) \cdot k \cdot dz} \quad [2.31]$$

Where,

T = transpiration rate per unit of the soil surface area,

$L(z)$ = length of root per unit soil volume,

$zmax$ = maximum depth of the root zone, and

z = depth below the soil.

Indraratna et al. (2006) developed a relationship for root water uptake based on the potential transpiration of a tree and the reduction factors due to soil suction as shown in Equation [2.32].

$$S(x, y, z, t) = f(\psi)G(\beta)F(T_p) \quad [2.32]$$

Where,

$f(\psi)$ computed using Feddes et al. (1974) and $F(T_p)$ = factor related to the potential transpiration by referring to the relationship developed by Nimah & Hanks (1973).

Further, the rate of root water uptake is affected by the condition of the surrounding soil (moisture content of the soil). Feddes et al. (1976) suggested the model for root water uptake subject to soil moisture content as the following figure 2.15.

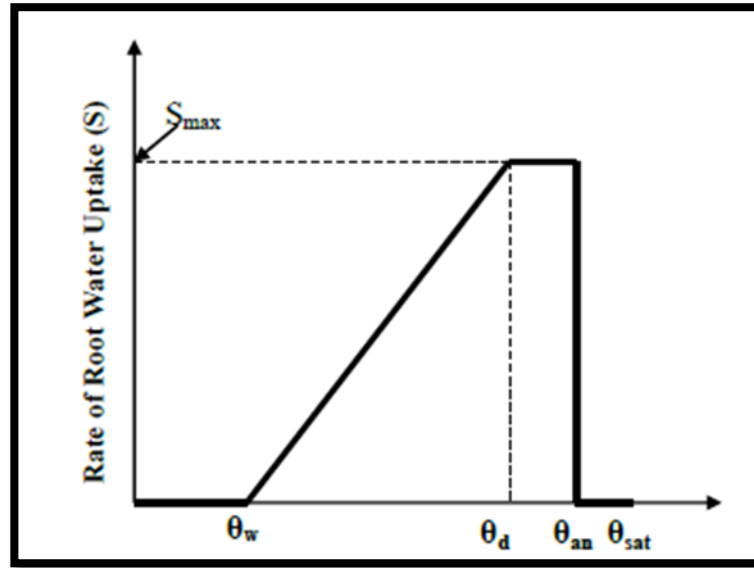


Figure 2.15: Variation of rate of root water uptake as per volumetric water content
(modified after Feddes et al., 1976)

Moreover, hydraulic conductivity of the soil and water potential difference between the roots and the soil affected the root water uptake.

Gardner (1960) carried out a quantitative study on root water uptake and developed the following Equation [2.33] to quantify the root water uptake,

$$S(x, y, z) = b \cdot (\delta - \psi - z) \cdot k \cdot \beta(x, y, z) \quad [2.33]$$

Where,

$S(x, y, z)$ = rate of root water uptake,

b = a constant,

δ = water potential of roots,

ψ = soil suction,

z = depth below soil surface,

k = unsaturated hydraulic conductivity, and

$\beta(x, y, z)$ = root density as the length of root per unit of soil volume.

Whisler et al. (1968) suggested a linear relationship for $S(x,y,z)$ with Equation [2.34].

$$S(z) = f(\beta) \cdot k \cdot (h_p - h_s) \quad [2.34]$$

Where,

$f(\beta)$ is root density function,

h_p is water potential of roots, and

h_s is water potential of soil

Hillel et al. (1976) proposed a relationship to predict the root water uptake as the following Equation [2.35],

$$S = \frac{(\theta_{soil} - \theta_{plant})}{(R_{soil} - R_{plant})} \quad [2.35]$$

Where θ_{soil} , θ_{plant} are the hydraulic heads of the plant, and R_{soil} , R_{plant} are resistance to the water flow in soil related to hydraulic conductivity

According to the above findings, root system, spatial distribution of roots, and soil suction also, affect to the root water uptake as well as the mechanical properties of the soil.

2.7 Summary

Vegetation (i.e., tree roots) is the best way to improve the shear strength of unsaturated soils. Tree roots can increase the shear strength of the soil as the mechanical strength provided by root reinforcement and suction provided by root water uptake. Several theoretical and empirical models have been captured the root reinforcement effect and suction effect separately. Most attempts to calculate root reinforcement's impact have been performed under saturated conditions. Furthermore, the increment of soil suction due to the vegetation, has been proven in many studies, and this impact has been well captured in theoretical models. However, the coupling effect of the mechanical and hydrological features of the tree roots should be captured to identify the accurate behavior of the tree roots on the improvement of the soil strength.

Chapter 3

3 BASIC SOIL STUDY AND PLANT SELECTION

3.1 Basic soil study

In this chapter, the basic properties of selected soil type are presented. Furthermore, the soil classification of the soil according to the Unified Soil Classification System (USCS) is included in this chapter. Moreover, the test results of proctor compaction test and in-situ density test are presented in this chapter. This soil sample was collected from Katunayaka area in Sri Lanka. The soil barrow area is shown in Figure 3.1.

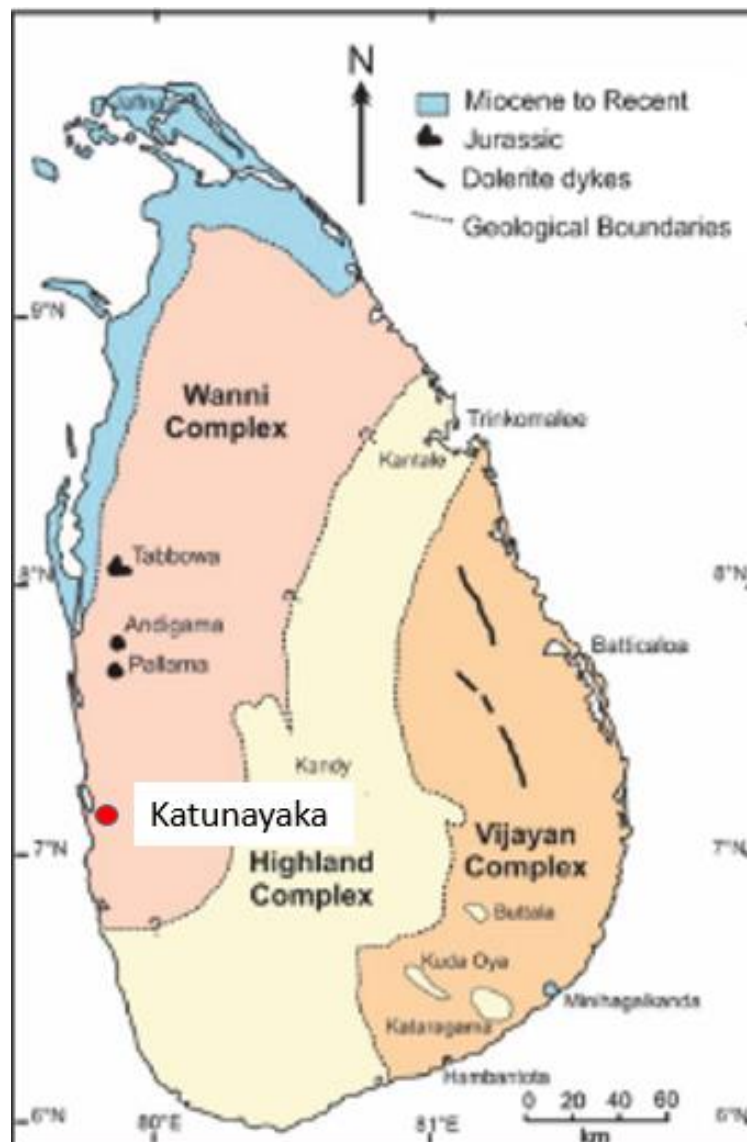


Figure 3.1: Soil Barrow area

Table 3.1 summarizes the results of basic soil testing conducted according to ASTM standards, and the PSD curve of the soil is shown in Figure 3.2. The sample dry density was considered 1500 kg/m^3 (i.e., 80% of maximum dry density) for experimental procedures. Furthermore, the proctor compaction curve is illustrated in Figure 3.3. Detailed study of the selected soil is included in Annex 1.

Table 3.1: Summary of the basic soil properties

Parameter	Results	Test Conducted
Percentage of gravel	0.3%	ASTM D422-63
Percentage of sand	87.8%	
Percentage of fines	11.9%	
Coefficient of uniformity (C_u)	6	
Coefficient of curvature (C_c)	1.36	
Liquid Limit	17.5%	ASTM D4318-83
Plasticity Index	Nearly zero	ASTM D4318-83
Specific gravity	2.67	ASTM D854-83
Organic content	1.28%	ASTM D2974 - 71
*Average in-situ density (kg/m^3)	1520	ASTM D1556
Maximum dry density (kg/m^3)	1919	ASTM D698
Optimum moisture content	6.8%	

*The Average in-situ density was measured at the barrow site

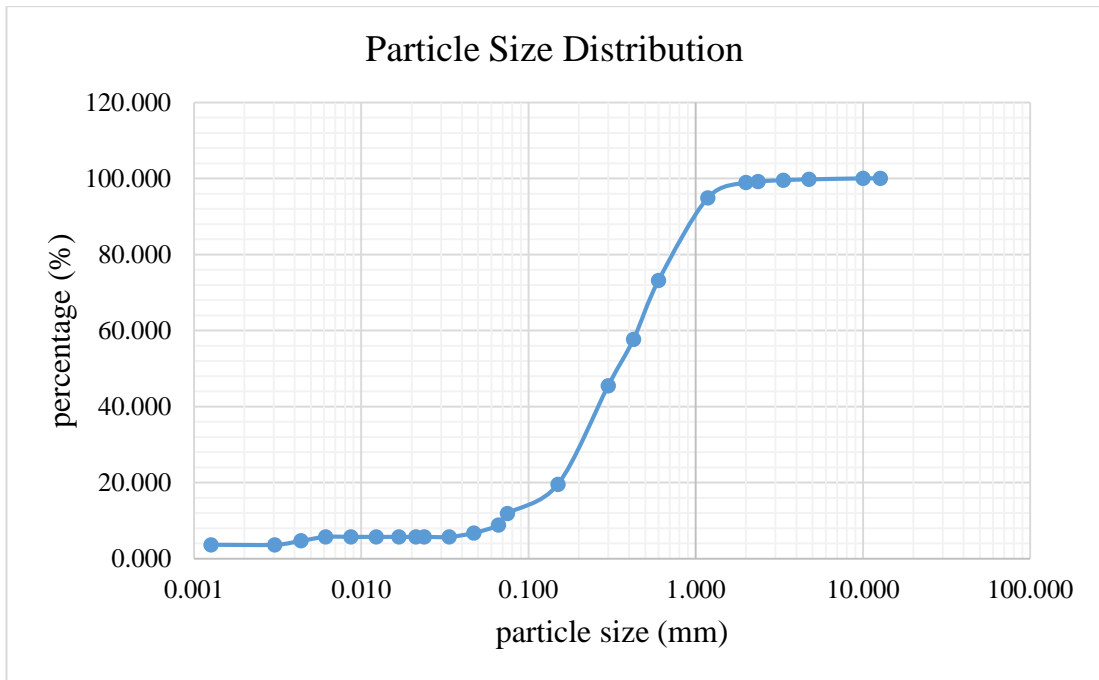


Figure 3.2: Particle size distribution

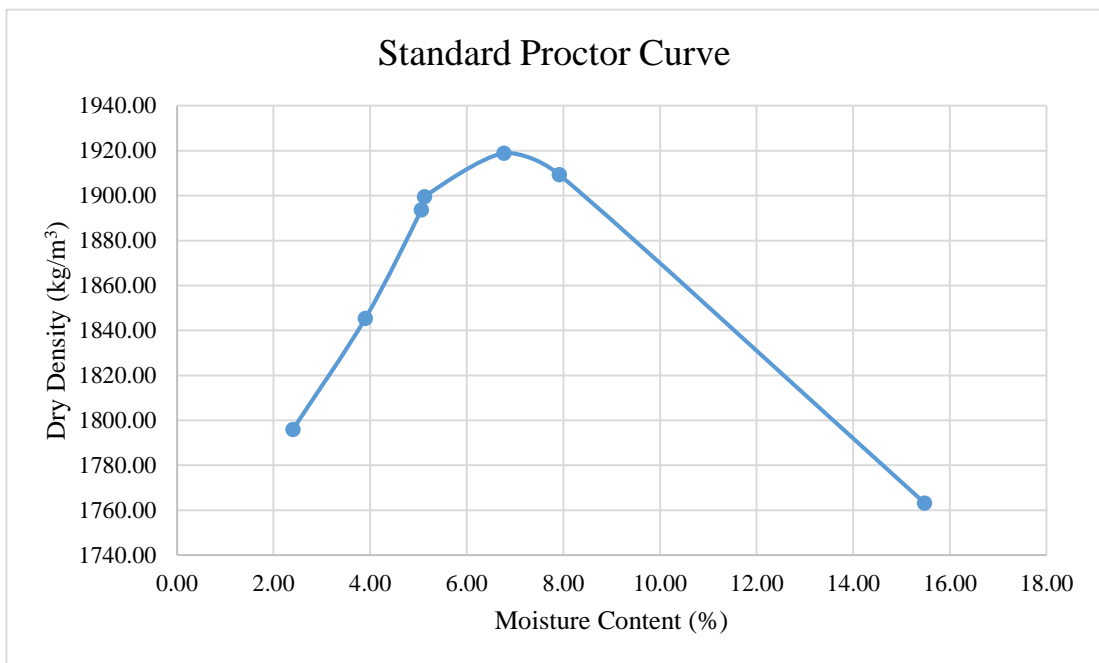


Figure 3.3: Standard proctor compaction curve

Soil classification was conducted according to “Unified Soil Classification System”. Therefore, the soil was classified as **SW-SM (well graded sand with inorganic silt)** and the summary of the calculation are presented in the Table 3.4. Furthermore, the selected soil can be named as Sri Lankan semi-costal silty sand.

Table 3.2: Summary of the soil classification

Step No.	Description	Calculations	Remarks
1	Percentage of coarse grained particles	88.1%	Coarse Grained Soil
	Percentage of fine grained particles	11.9%	
2	Percentage of gravel particles	0.3%	Sandy Soil (First letter – S)
	Percentage of sand particles	87.8%	
3	Percentage of fine grained particles	11.9%	5-12% Fines, Therefore, dual symbol was used
4	Coefficient of uniformity	$C_u = \frac{D_{60}}{D_{10}} = \frac{0.42}{0.07} = 6$	Cu=6 and 1<Cc<3, Therefore, well graded soil(SW)
	Coefficient of curvature	$C_c = \frac{D_{30}^2}{D_{60} \times D_{10}} = \frac{0.2^2}{0.42 \times 0.07} = 1.36$	
5	LL and PI	LL=17.5% and PI nearly zero (it did not show the plastic region)	Inorganic silt (SM)

3.2 Plant selection

The main objective of this research is to identify the influence of the matric suction on the root reinforcement in the vegetated soil. Therefore, a root system should be introduced in the above-selected soil type classified as well graded Silty Sand to

arrange the main direct shear testing procedure. The main factors were considered for the plant selection as follows,

- ✓ Familiarity with the selected soil type
- ✓ Survivability in any environmental conditions
- ✓ Root system
- ✓ Growing pattern and rate of the roots
- ✓ Hydrological behavior of the tree root in the selected soil type with respect to the time
- ✓ Mechanical properties of the roots

According to the familiarity with the selected soil type, five tree plant species were collected from the soil barrow area, including *Swietenia mahogany* (Mahogany Tree), *Adenanthera pavonina* (Madatiya Tree), *Alstonia macrophylla* (Attonia Tree), *Terminalia catappa* (Kottamba Tree), and *Artocarpus heterophyllus* (Jackfruit Tree) as shown in Figure 3.4.

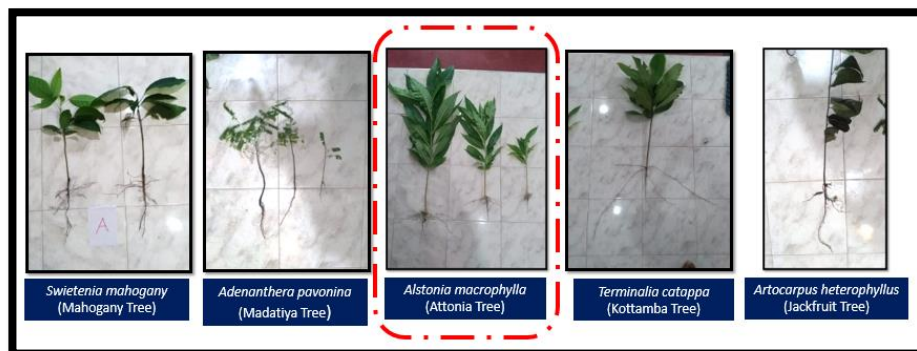


Figure 3.4: Initially selected tree plants

From above, *Alstonia macrophylla* is a very **survivable tree** in any environment and widespread tree species in Sri Lanka. Because of that, this tree species is used to arrange the research methodology. After that, other selected tree species recommended for slope stabilization according to National Building Research Organization can be tested according to the proposed methodology.

Chapter 4

4 STUDYING MECHANICAL AND HYDROLOGICAL PROPERTIES OF *Alstonia macrophylla*

4.1 General

This chapter describes the growing pattern and rate of the *Alstonia macrophylla*. Then, the hydrological behavior of the tree was studied by observing the suction variation of the soil with and without roots. Furthermore, the mechanical properties and quantification of the tree roots are discussed. The empirical correlation between the root water uptake and total leaf area of the tree was also captured under this title.

4.2 Evaluating the volume ratio between the soil and roots

This study was carried out to identify the **growing pattern** and **rate** of *Alstonia macrophylla* in the above selected soil condition. Sample bags were filled with the same quantity of soil with maintaining a similar density. Then, collected *Alstonia macrophylla* plants with the same growing condition were grown in the prepared soil sample and maintained with the same moisture and environmental conditions. Once 30 days, the roots were extracted from a selected sample and the volume of the roots was measured using the water displacement method. The summary of the test results is presented in Table 4.1 and the growing pattern and rate of the tree plant can be observed with the time in Figure 4.1.



Figure 4.1: Observation for growing pattern and rate of *Alstonia macrophylla*

Table 4.1: Summary of observation for evaluating volume ratio between soil and tree roots

Feature	Dimensions / Number of		
	23/01/2022	23/02/2022	23/03/2022
Total height of plant (with root) (cm)	65	82	90
Height of plant (cm)	32	46	49
Length of main root (cm)	14	-	-
Number of leaves	15	17	19
Volume of the soil (cm ³)	36192	36191.15	36191.15
Volume of the roots (ml/cm ³)	24	29	30
Volume ratio (%)	0.066	0.080	0.082

The required duration of the growing plant in the main testing procedure was decided according to the above observations.

4.3 Observing the suction variation of soil sample with and without a plant against the time

4.3.1 Variation of the matric suction in soil sample with time

The soil was initially compacted to replicate the field dry density of 1500 kg/m³ and made fully saturated condition. After that, the matric suction sensor installed to the sample. The matric suction was monitored within two weeks as per Figure 4.2. As per the observations, the maximum suction was 57.88 kPa achieved in the soil sample within the above duration. The experiment was conducted at a controlled temperature (26-32⁰C) according to Figure 4.3 and humidity level (70-72%) in order to minimize the impact of environmental fluctuations on the suction measurements.

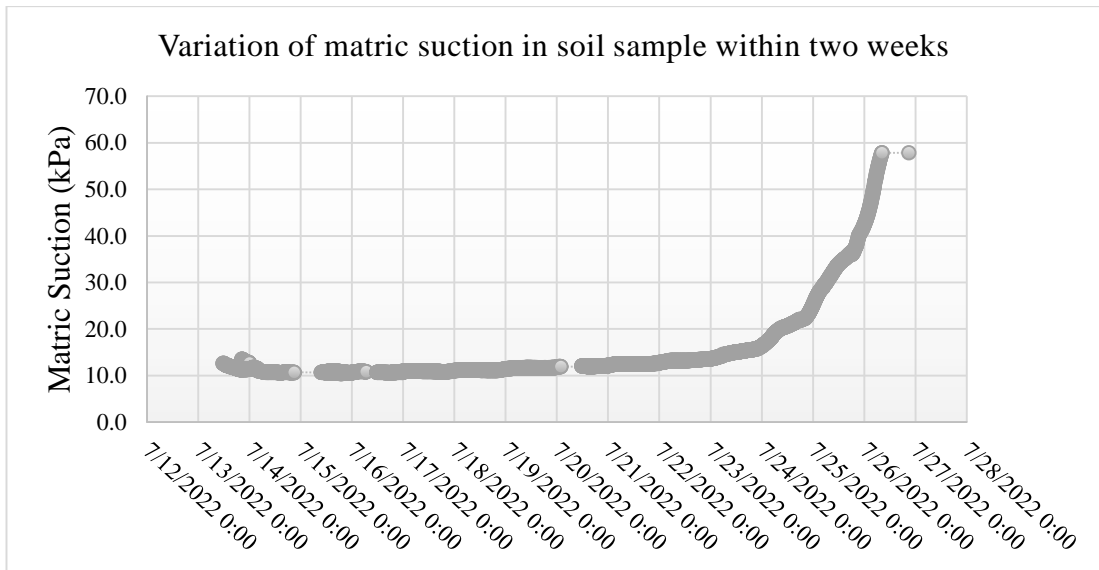


Figure 4.2: Variation of matric suction in soil sample within two weeks

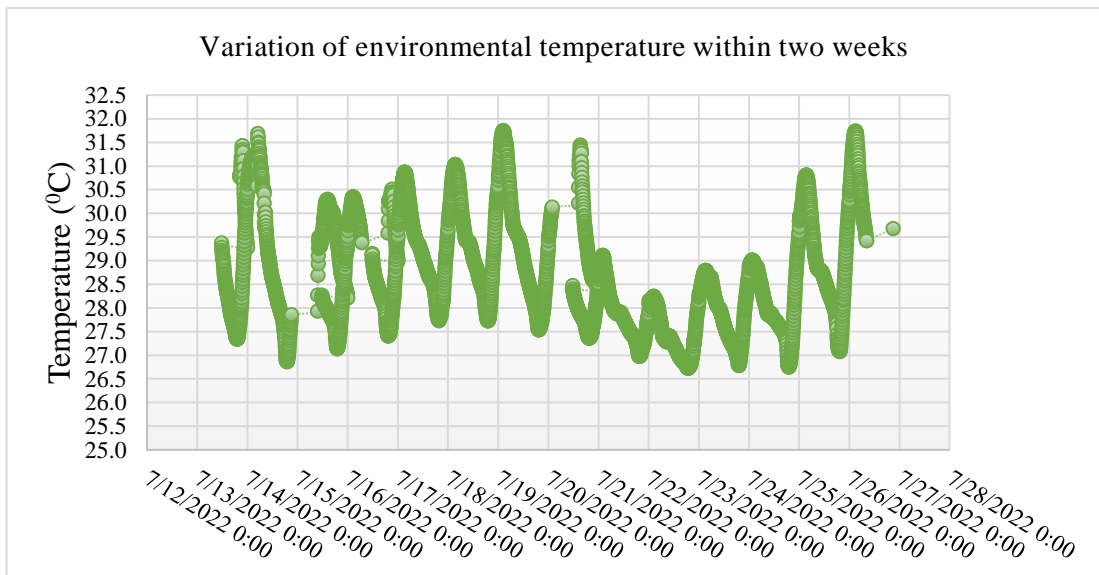


Figure 4.3: Variation of environmental temperature within two weeks in above test

	Timestamp	Matric Suction (kPa)	Environmental Temperature (°C)
Maximum matric suction	7/26/2022 20:55	57.88	29.7

4.3.2 Variation of the matric suction with respect to time in soil sample with plant

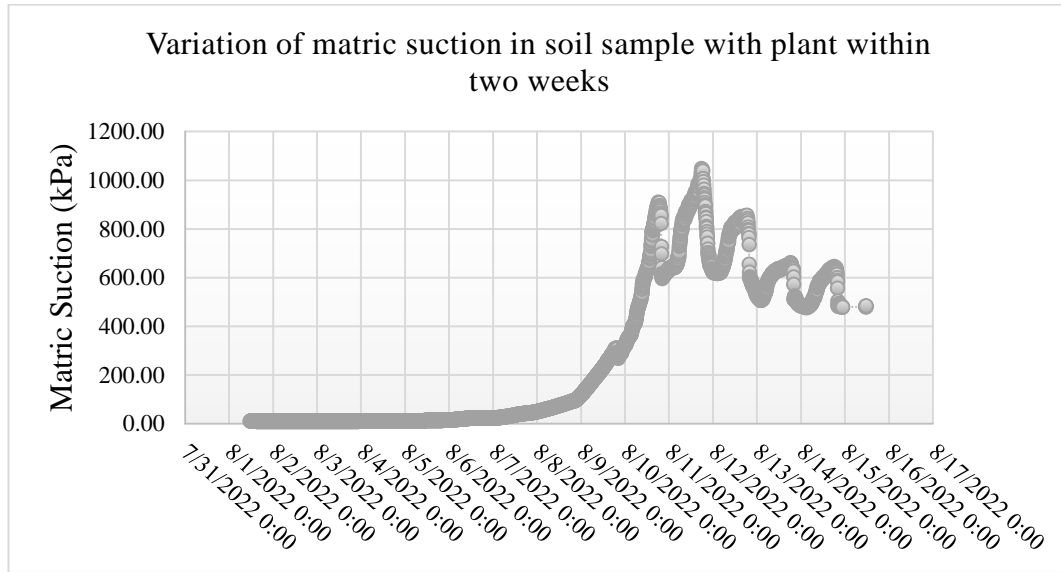


Figure 4.4: Variation of matric suction in soil sample with plant within two weeks

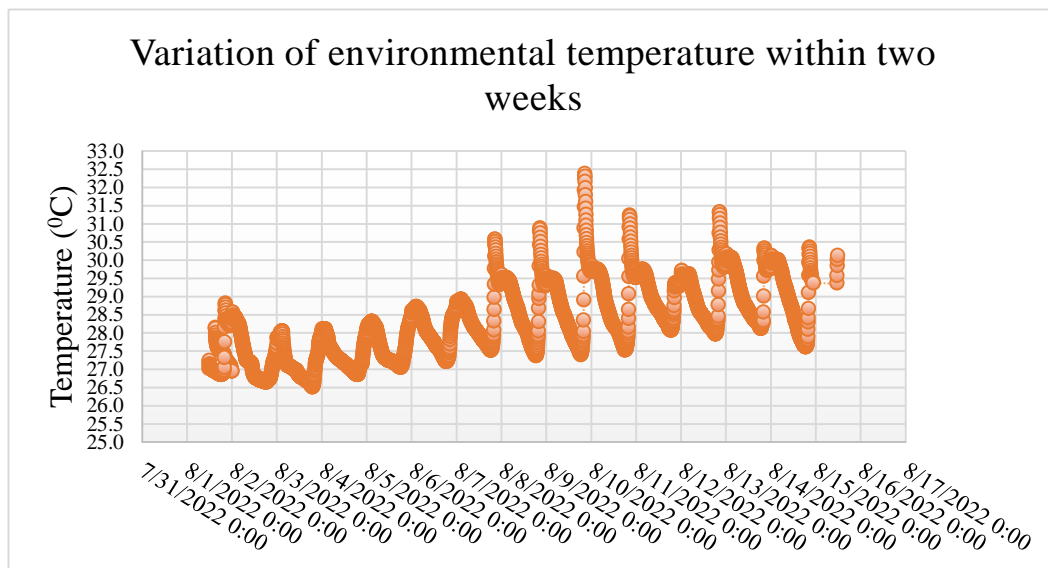


Figure 4.5: Variation of environmental temperature within two weeks in above test

	Date	Timestamp	Matric Suction (kPa)	Environmental Temperature (°C)
maximum	8/11/2022	17:45:00	1048.57	28.11

After four months from preparing soil sample with a tree plant, the matric suction sensor installed to the sample. The matric suction was monitored within two weeks as per Figure 4.4. As per the observations, the maximum suction was 1048.57 kPa achieved in the soil sample within the above duration. According to Figure 4.5, the experiment was conducted at a controlled temperature (26-32⁰C) and humidity level (70-72%) in order to minimize the impact of environmental fluctuations on the suction measurements as the above mentioned test.

The suitability of *Alstonia macrophylla* for the main test procedure can be recognized according to the outcomes of the above two tests because it improved the matric suction of the soil sample by a significant value within a short time period.

4.4 Developing an empirical correlation between the root water uptake and total area of leaves of the tree plant

As per Section 2.6, the root water uptake of the tree depends on the physiology of the tree and environmental parameters. The root water uptake (S_p) and total leaf area (TLA) of the tree plant were measured for the several tree plants in the same environmental condition to capture a relationship between the parameter as mentioned earlier when other parameters are constant which influence the root water uptake.

Biddle (1998) concluded although photosynthesis process uses water, less than 1% of the water required by a plant is incorporated into sugar or forms part of the cell content. Reminder of more than 99% is lost via transpiration from the leaves. Therefore, it is assumed that the amount of water lost by transpiration is the same as the amount of root water uptake at a given time. Because of that, the rate of root water uptake can be measured approximately by rate of transpiration. A Potometer as shown in Figure 4.6 was used to measure the rate of transpiration instead the root water uptake of the tree. Therefore, a photometer was developed to measure the root water uptake per Figure 4.7.

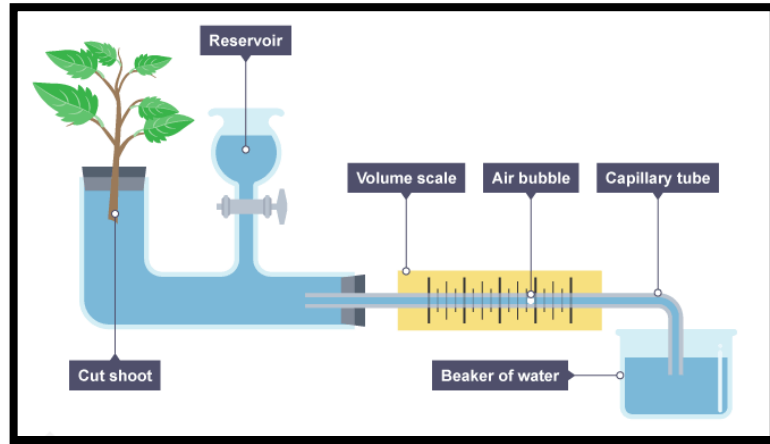


Figure 4.6: Schematic diagram of potometer



Figure 4.7: Developed potometer

The total leaf area was measured by mapping each leaf on the graph sheets as presented in Figure 4.8.

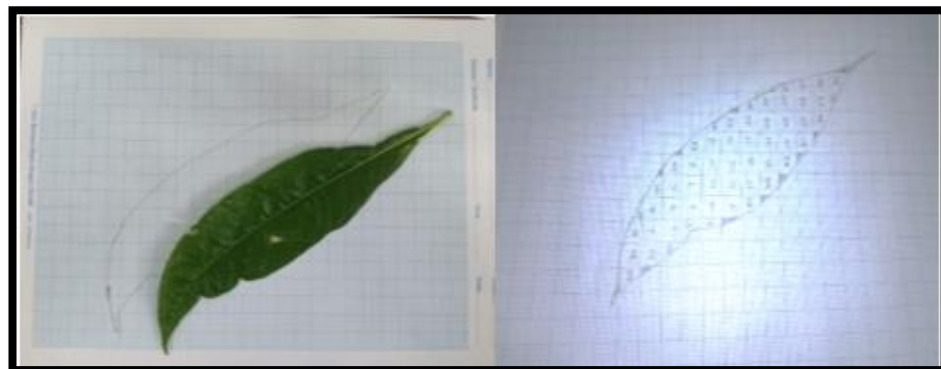


Figure 4.8: Method to obtained the total leaf area

The test was conducted in controlled environment with 75-85% humidity and 26-32⁰C environmental temperature. The summary of the test results is shown in Table 1 of Annex 2 and the empirical correlation between the two parameters then can be obtained as the figure 4.9.

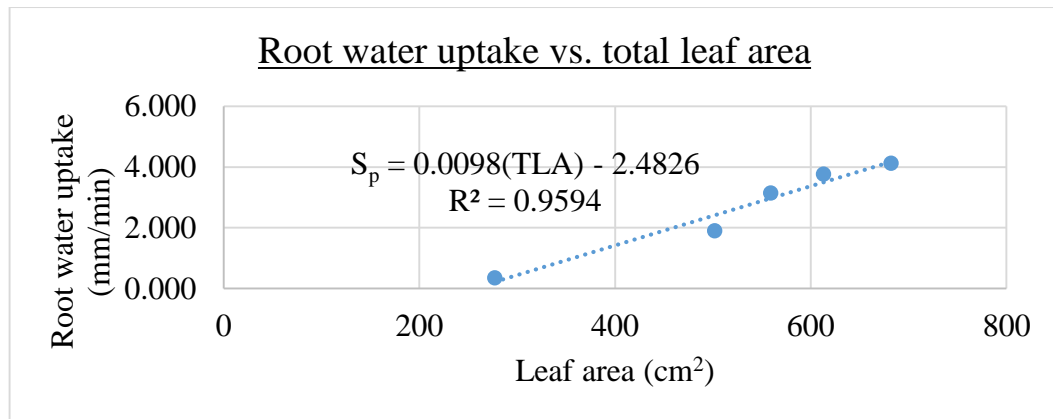


Figure 4.9: Relationship between the root water uptake and total leaf area

This relationship was also used to determine the root water uptake of the plants which were used in main direct shear tests. Furthermore, The R square value was obtained 0.9594.

4.5 Summary

Alstonia macrophylla is a very **survivable tree** in any environment and widespread tree species in Sri Lanka. Because of that, this tree species is used to arrange the research methodology. It is evaluating the volume ratio between the soil and roots that study was carried out to identify the **growing pattern** and **rate** of *Alstonia macrophylla* in above selected soil condition. The suitability of the selected plant for the main test procedure could be identified according to the observation of the suction variation because it improved the matric suction of the soil sample from a significant value within short time period. The empirical relationship between the root water uptake and total leaf area of *Alstonia macrophylla* plant as following Equation [4.1] and it can be also used to determine the root water uptake of the plants which were used in main direct shear tests.

$$S_p = 0.0098(TLA) - 2.4826 \quad [2.33]$$

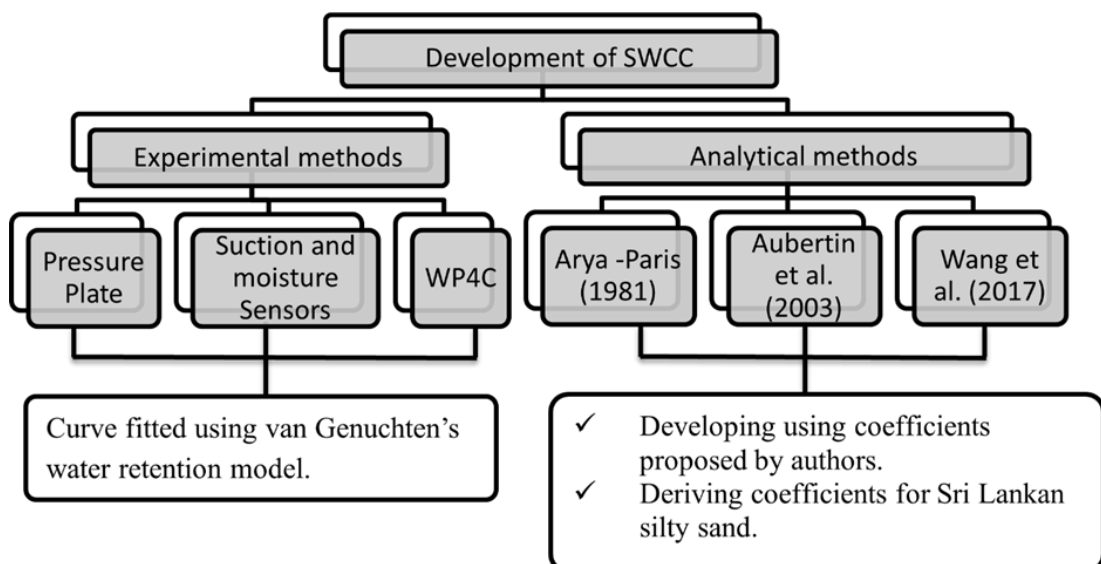
Chapter 5

5 OBJECTIVE 01 - STUDYING THE BEHAVIOR OF UNSATURATED SRI LANKAN SEMI-COSTAL SILTY SAND USING SWCC

5.1 General

Soil Water Characteristic Curve (SWCC) is one of the indirect methods to study the behavior of unsaturated soil. This study presents the SWCC for Sri Lankan semi-coastal silty sand developed using chilled mirror dew-point technique, WP4C and compared the performance of a few prediction models. The SWCC was also developed experimentally using the pressure plate and suction-moisture sensors, to verify the results obtained using the WP4C. The fitted curve was developed using Van Genuchten's (VG) model. The prediction models of Arya and Paris (1981), Aubertin et.al (2003), and Wang et al. (2017) were used to compare the performance with the model parameters suggested by the authors. Further, suitable values for the model parameters are proposed for reasonably accurate models by using the least square method.

5.2 Flow Chart for the Objective 1



5.3 Development of SWCC using experimental methods

The experimental procedure that was followed to develop the SWCC using the pressure plate, suction-moisture sensors, and WP4C is discussed in this section. All experiments were conducted in the drying path and the sample dry density was considered as 1500 kg/m^3 .

5.3.1 Pressure plate

Twelve samples were prepared in the retaining rings (refer to Figure 5.1) with an internal diameter of 47mm and a height of 10 mm. The sample was compacted to desired dry density using the proposed compactor and the collar (Figure 5.1). The air pressure (u_a) was applied to the apparatus from 100 kPa to 300kPa, and water pressure (u_w) was maintained at 100 kPa. Therefore, the specimens were brought to equilibrium under matric suction values from 0 to 200 kPa. The detailed experimental procedure is described in section 2.3.1.1

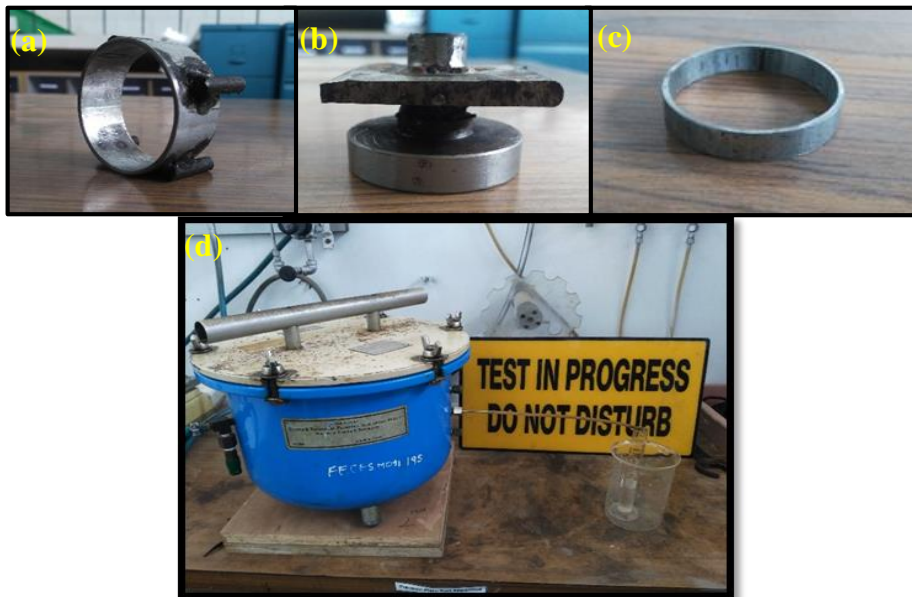


Figure 5.1: Component of the pressure plate test

The values of matric suction and calculated volumetric moisture content for each trails using pressure plate are shown in table 5.1.

Table 5.1: Summary output obtained from pressure plate apparatus

Test No.	Pore air pressure u_a (kPa)	Pore water pressure u_w (kPa)	Matric suction ($u_a - u_w$)	Gravimetric MC Calculation				Volumetric MC (%)
				Weight of Can (g)	Weight of Can+Wet soil (g)	Weight of Can+Dry soil (g)	MC (%)	
1	100	100	0	21.22	48.08	47.09	3.827	5.740
2	110	100	10	21.19	46.83	46	3.345	5.018
3	120	100	20	18.67	45.52	44.59	3.588	5.382
4	140	100	40	21.21	47.37	46.49	3.481	5.222
5	160	100	60	19.3	45.24	44.37	3.470	5.205
6	180	100	80	21.19	44.78	44.05	3.193	4.790
7	200	100	100	20.17	45.27	44.46	3.335	5.002
8	220	100	120	18.65	42.2	41.5	3.063	4.595
9	240	100	140	18.66	43.43	42.69	3.079	4.619
10	260	100	160	19.31	44.08	43.37	2.951	4.426
11	280	100	180	19.3	40.03	39.48	2.725	4.088
12	290	100	190	13.21	30.72	30.22	2.939	4.409

5.3.2 WP4C

The samples were prepared in stainless steel sample cups to ensure quick equilibrium at sample temperature and kept at half the height of the sampler to reduce the possibility of spilling sample material and contaminating the sample chamber. The WP4C was allowed to warm up for a 15 to 30 min period to achieve reliable readings. The instrument was calibrated using the 0.50 mol/kg KCl salt standard before the experiment. Furthermore, the sample and block temperature ($T_s - T_b$) difference was maintained between -0.5 and 0. The detailed experimental procedure is described in section 2.1.2. and Figure 5.2 shows a few steps of the test procedure. The results shown in Table 1 of Annex 3 were obtained in the range of 0 to 300 MPa for the total suction.

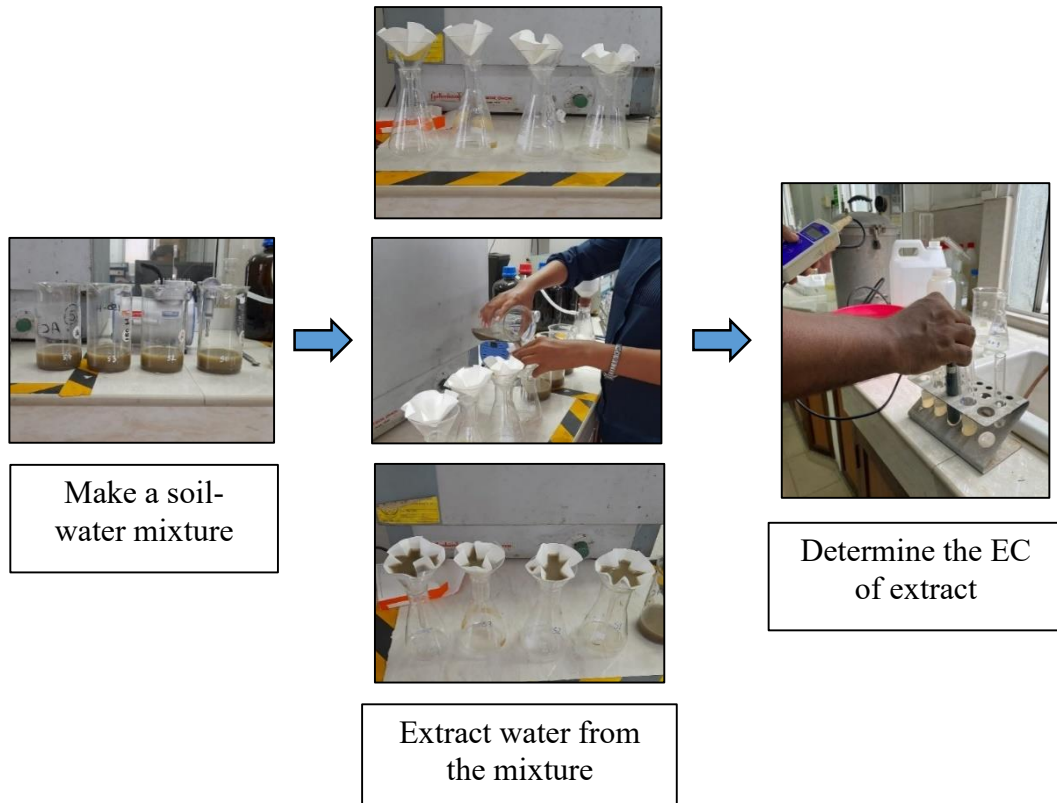


Figure 5.2: Testing procedure of EC test of the soil

The osmotic suction of saturated soil extract should be calculated to obtain the osmotic suction for each trail as per the section 2.3.1.2. Saturated moisture content for selected soil type was calculated using Equation 5.1 as 29.2%,

$$w = \frac{S \left(\frac{G_s \gamma_w}{\gamma_d} - 1 \right)}{G_s} \quad [5.1]$$

However, extracting water from the saturated soil sample was not an easy task. Therefore, a relationship was developed between the electrical conductivity (EC_{soil}) of soil extract and gravimetric moisture content (GMC) as per Figure 5.3 to estimate the EC of the saturation extract of the selected soil. The developed relationship is shown in Equation [5.2] with 94.1% of accuracy.

$$EC_{soil} = -0.0826(GMC) + 150.94 \quad [5.2]$$

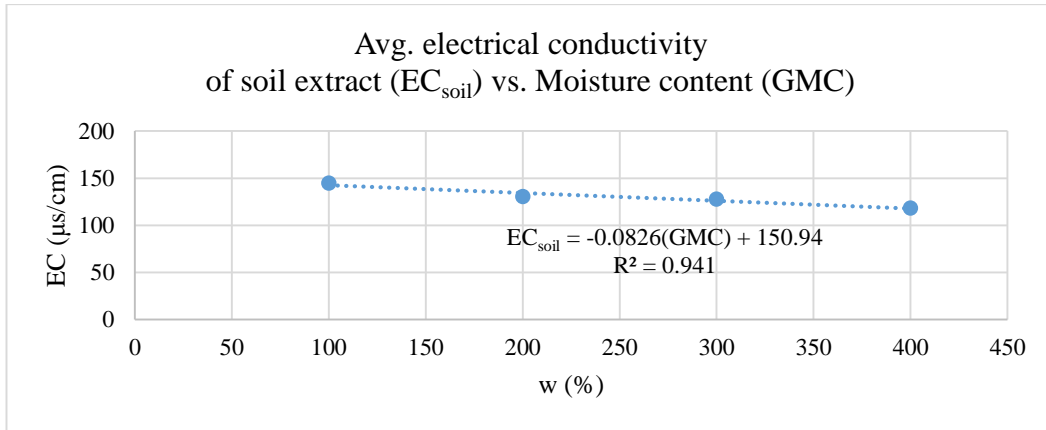


Figure 5.3: Relationship between the average electrical conductivity of soil extract and moisture content

From above relationship,

Electrical conductivity of saturated soil extract (GMC=29.2%) = 148.53 $\mu\text{s}/\text{cm}$

$$\Psi_{Os}(MPa) = -0.036EC(ds/m) = -0.036 \times 148.53 \times 10^{-3} = -0.00535 MPa$$

Specimen calculation for osmotic suction for given conditions.

$$\Psi = \Psi_{Os} \left(\frac{\theta_s}{\theta} \right) = -0.00535 \times \left(\frac{0.438}{0.128} \right) = -0.0183 MPa$$

Summary of the results obtained using the WP4C instruments is shown in Table 5.2.

Table 5.2: Summary of the results obtained using the WP4C instrument

Volumetric moisture content (%)	Total Suction (kPa)	Osmotic Suction (kPa)	Matric Suction (kPa)
24.606	5	4.44	0.56
19.488	10	7.88	2.12
12.402	20	12.02	7.98
8.465	140	27.68	112.32
5.709	270	41.05	228.95
4.921	370	47.62	322.38
4.331	1240	54.11	1185.89
2.165	5510	108.22	5401.783
1.772	8850	132.27	8717.734

5.3.3 Moisture and Suction Sensors

The matric suction of the soil sample was measured using TEROS 21 suction sensor. The three moisture sensors were initially calibrated by observing the voltage readings of three moisture sensors and volumetric moisture content for each trail as the Table 5.3. The proctor mold was used to prepare the compacted soil samples. The calibration graphs for all three moisture sensors with calibration equation are shown in Figure 5.4, 5.5 and 5.6.

Table 5.3: Test reading of the moisture and suction sensors

Volumetric Moisture content (VMC) (%)	Voltage reading (V)		
	Moisture Sensor 1	Moisture Sensor 2	Moisture Sensor 3
7.0635	2.4457	2.4283	2.3464
10.5042	2.1320	2.0190	2.0977
15.0595	1.8082	1.8306	1.7683
19.7558	1.5733	1.5331	1.4468
26.1884	1.2077	1.2425	1.1734
31.2614	1.0381	1.0884	1.0314
19.6156	1.7195	1.7461	1.5607

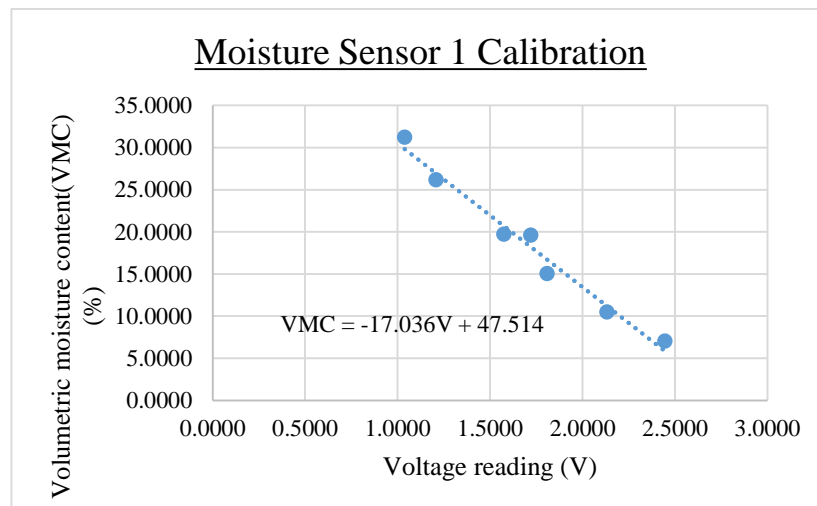


Figure 5.4: Calibration chart for moisture sensor 1

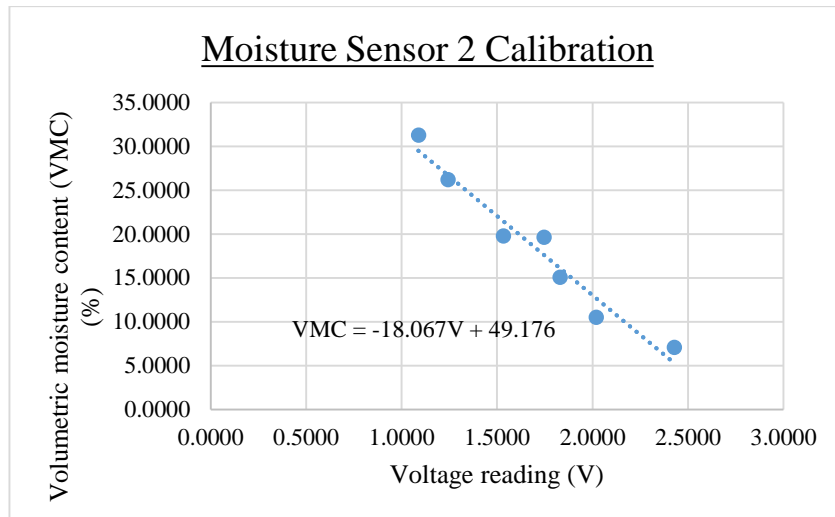


Figure 5.5: Calibration chart for moisture sensor 2

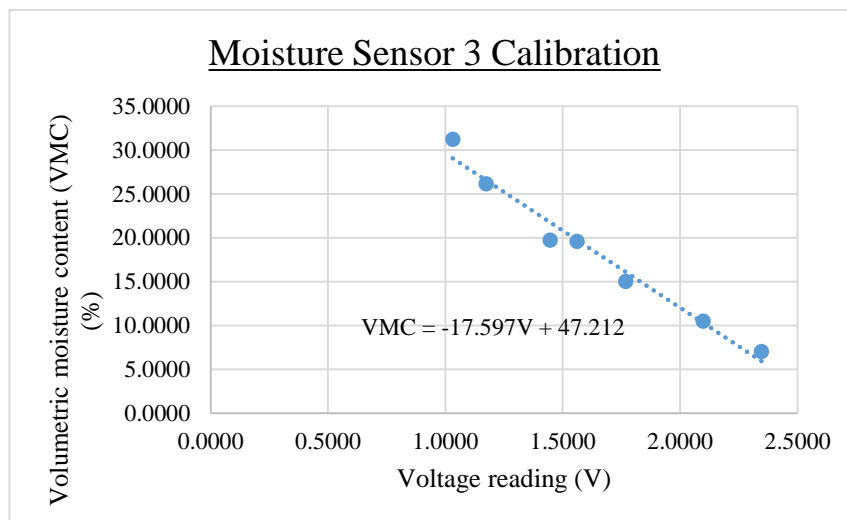


Figure 5.6: Calibration chart for moisture sensor 3

The soil setup was prepared in a wooden box with internal dimensions of 300 mm (W) × 300 mm (L) × 300 mm (H). Then, the suction-moisture sensors were installed at a depth of 150mm as shown in Figure 5.7 and continuous data were obtained for four months using the sensors.

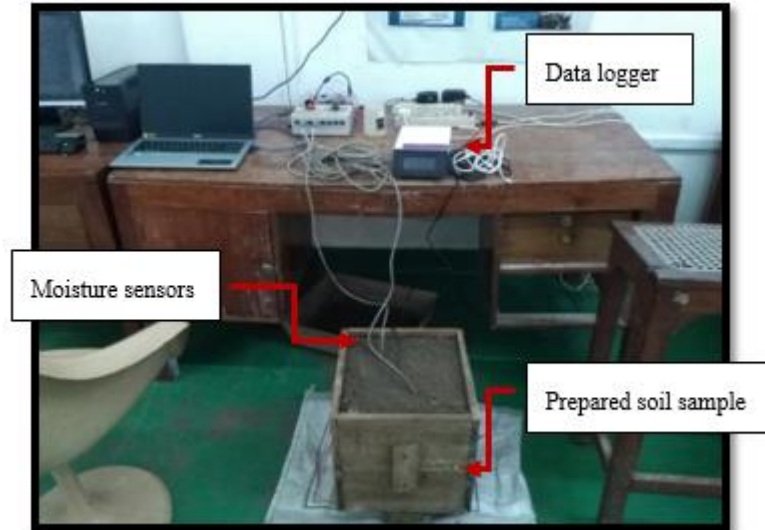


Figure 5.7: Installation moisture and suction to the soil sample and test procedure

5.3.4 Curve fitting

The data obtained from the above instruments were utilized to develop the SWCC curve using the VG model. The values of θ_s , θ_r were calculated as 0.438 and 0.025, respectively in this study. The values of α , n parameters of the VG model were estimated by using the least square method. Moreover, the range of the above parameters was considered according to the studies of Parker et al., (1985) and Shao & Horton, (1998), where α was set within $0-1 \text{ cm}^{-1}$ and n was between 1 and 10.

5.4 Development of SWCC using prediction models

SWCC was developed using the models suggested by Arya & Paris, (1981); Aubertin et al., (2003); Wang et al., (2017). First, the curves were developed using the values of modal parameters which was recommended by the authors for granular soil. Table 5.4 indicates the values proposed by the authors for the modal parameters of three different models.

According to the studies discussed in section 2.3.2, it can be observed that the main reason for the deviations is that the values of modal parameters proposed by the authors which rely on the soil type. Hence, the values of model parameters were recalculated for the selected soil by reducing the deviation between the experimental and analytical results. The recalculation was carried out according to the least square method.

Table 5.4: Modal coefficient values recommended by the authors for granular soil

Model	Parameter	Recommended values
Arya-Paris (1981)	α	1.38
Aubertin et.al (2003)	a_c	0.01
Wang et al. (2017)	C_1	1.07
	C_2	12.07

5.5 Results and Discussion

5.5.1 Development of SWCC using experimental methods

The experimental results were obtained using chilled mirror dew-point technique, WP4C in the range of 0 to 10^4 kPa and these results were verified using the pressure plate and suction-moisture sensors. The 5-bar pressure plate produced results for matric suction in the range of 0 to 200kPa whereas moisture-suction sensors covered the 7 to 365kPa within 4 months. It was observed that results obtained using WP4C have a slight deviation compared to the results of the pressure plate and suction-moisture sensors. This could be due to the minor variation in the dry density of soil samples used in the testing with the WP4C. However, maintaining the dry density of the prepared soil samples at 1500 kg/m^3 was a difficult task due to the height of the prepared samples was low. Accordingly, the experimental results obtained from all three instruments was used to develop SWCC of the selected soil as the Figure 5.8. Then the fitted SWCC was developed using the VG model and that also shown in Figure 5.8. The curve equation of the VG model is represented in Equation [5.2].

$$\theta = 0.025 + 0.375 \left[\frac{1}{1 + (0.0845|h|)^{1.561}} \right]^{0.3592} \quad [5.2]$$

Where h is the suction matric head in cm. This soil type's corresponding α and n values were derived as 0.0845 and 1.561, respectively.

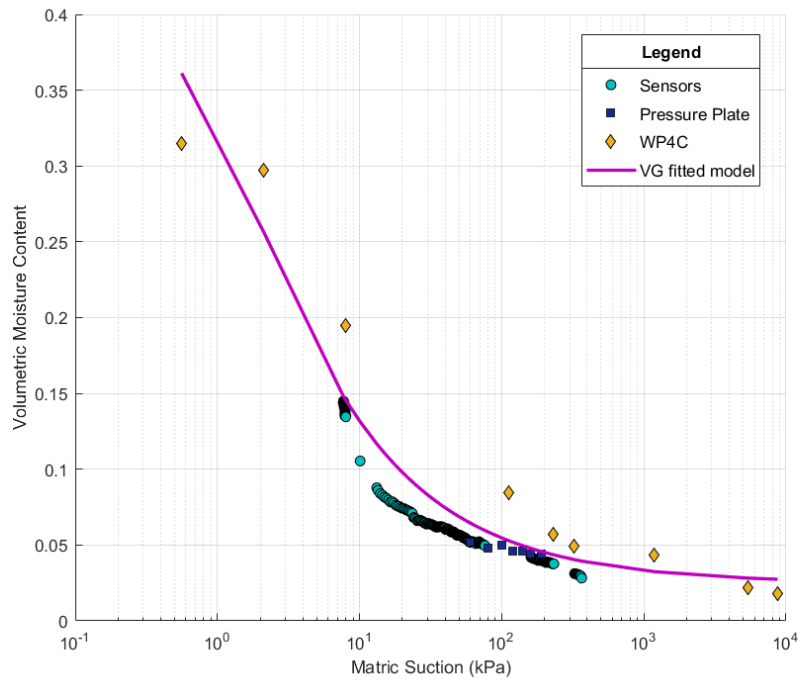


Figure 5.8: Experimental results and fitted curve for experimental results

5.5.2 Development of SWCC using prediction models

Figure 5.9 represents the SWCCs developed using the model parameters mentioned in Table 5.5. It was observed that the curve developed using the Arya-Paris model (1981) has significantly differ from the experimental fitted curve. This could be because the Arya-Paris (1981) model is directly related to the particle size distribution; therefore, it follows the shape of the particle size distribution. Further, the matric suction and the volumetric water content are calculated separately using the PSD. The number of data points of the curve relies on the sieve sizes used in the experiment. Therefore, the calculated matric suction values ranged from 0 to 5000 kPa, and most of the data points were less than 100kPa for this soil. Moreover, the VG-fitted model lies between the matric suction values of 0.6 to 8700 kPa. Therefore, only a limited set of data can be used for the comparison yielding unreliable predictions. On the other hand, the models developed by Aubertin et.al (2003) and Wang et al. (2017) can be used for a wider range of matric suction, allowing for a comparison that produces accurate predictions. The deviations obtained from prediction models are listed in Table 5.5.

Table 5.5: SSR values for the models with modal parameters proposed by authors

Model	Values proposed by Authors		
	Parameter	Parametric value	SSR
Arya-Paris (1981)	α	1.38	Incomputable
Aubertin et.al (2003)	a_c	0.01	0.1605
Wang et al. (2017)	C_1	1.07	0.0513
	C_2	12.07	

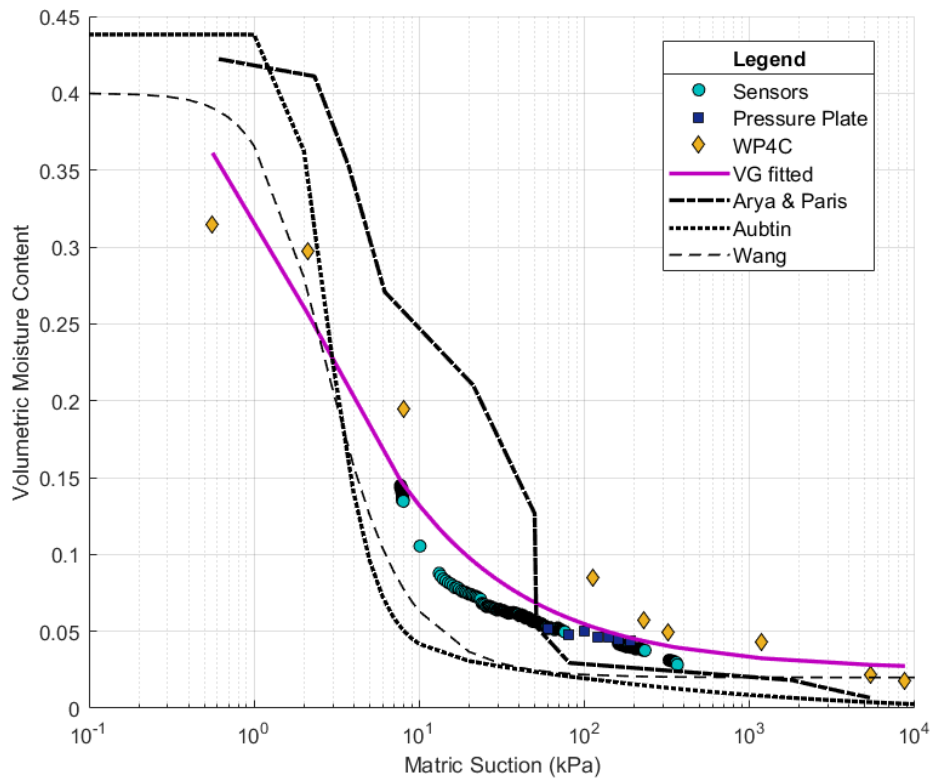


Figure 5.9: Developed SWCCs according to the prediction models using modal parameters proposed by authors for granular soils

This study was further extended by recalculating the values of model parameters for Aubertin et.al (2003) and Wang et al. (2017) models such that the SSR among the VG-fitted curve and the models became the least. As per the above-mentioned reasons, Arya-Paris (1981) model was excluded from this study.

Predictions of Aubertin et al. deviated from the experimental results for matric suction values less than 3 kPa. The parametric values obtained for this soil type are listed in Table 5.6 with the deviations, and Figure 5.10 shows the SWCC developed for the proposed values of model parameters.

Aubertin et.al (2003) and Wang et al. (2017) models produced SWCC of reasonable accuracy even with the coefficients proposed by the authors. Further, the coefficients presented in Table 5.6 can be used for this soil type to obtain the SWCC of higher accuracy. Moreover, Wang et al. produced the best prediction model for the Sri Lankan silty sand.

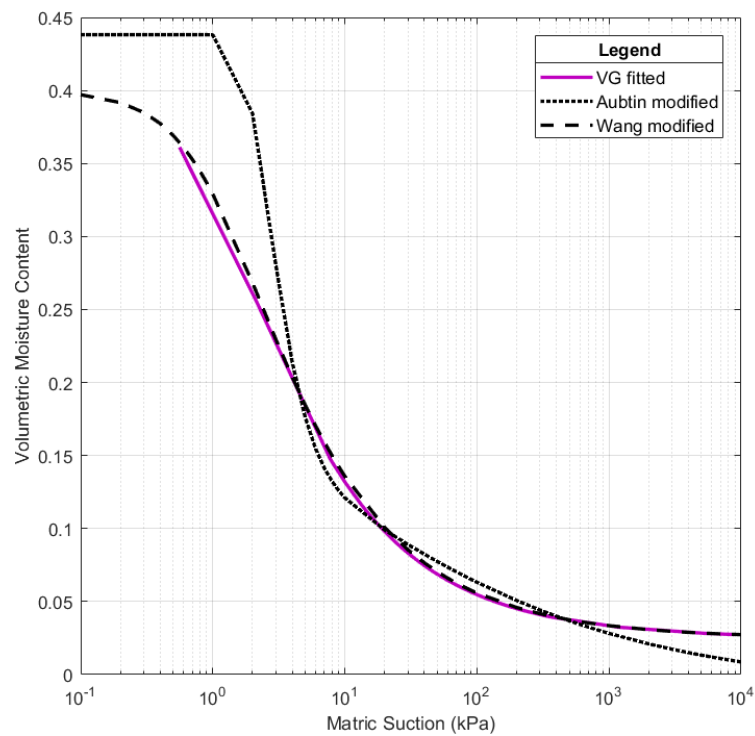


Figure 5.10: Developed SWCCs using prediction models using derived values of modal parameters

Table 5.6: Derived values for modal parameters and SSR values

Model	Derived values for this soil type		
	Parameter	Parametric value	SSR
Aubertin et al (2003)	a_c	0.0327	0.08
Wang et al. (2017)	C_1	0.44	4.17 E ⁻¹²
	C_2	6.77	

5.6 Summary

This study presented the SWCC for Sri Lankan coastal silty sand developed using chilled mirror dew-point technique, WP4C and compared the performance of a few prediction models. The SWCC was also developed experimentally using pressure plate and suction-moisture sensors to validate the findings from the chilled mirror dew-point technique, WP4C. The performance of the prediction models by Arya and Paris (1981), Aubertin et al. (2003), and Wang et al. (2017) was evaluated.

According to the verification obtained using the pressure plate and suction-moisture sensor, WP4C (chilled mirror dew-point meter) can produce results quickly, precisely, and consistently in a wider range of total suction. Therefore, the chilled mirror dew-point technique with WP4C instrument can be recommended as a convenient experimental method to develop the SWCC for Sri Lankan silty sand. However, samples need to be handled carefully to preserve the basic soil properties (i.e., dry density) as the original soil due to the challenges involved in collecting/preparing soil samples. The experimentally fitted curve was developed using Van Genuchten's (VG) model and the corresponding α and n values were derived as 0.0845 and 1.561, respectively for the selected soil.

Prediction models were firstly developed using the values of model parameters proposed by the authors for granular soils. Aubertin et al. (2003) and Wang et al. (2017) predictions were more accurate than Arya and Paris (1981) model as the comparison between the experimental results. In addition, the values of model parameters of Aubertin et al. (2003) and Wang et al. (2017) were recalculated specially for the Sri Lankan silty sand such that the deviation between experimental and analytical SWCC became the minimum. Accordingly, the a_c value of the Aubertin et al. (2003) model was evaluated as 0.0327 and the C_1 , and C_2 values of the Wang et al.

(2017) model was determined as 0.44,6.77 respectively for this soil type. The above deviation of Wang et al. (2017) model with the experimentally fitted curve was 4.17×10^{-12} for the proposed model parameters.

As the sum up, the chilled mirror dew-point technique, WP4C can be utilized to produce SWCC experimentally, however, the Wang et al. (2017) model is more suited to analytically generate SWCC for the Sri Lanka silty sand with values of the model parameters suggested above. Nevertheless, the values of model parameters of Wang et al. (2017) model proposed by the authors also produce the SWCC with reasonable accuracy for the selected soil.

Chapter 6

6 OBJECTIVE 02 – INVESTIGATING THE INFLUENCE OF SUCTION ON ROOT REINFORCEMENT OF *Alstonia macrophylla* WITH THE SEMI-COASTAL SRI LANKAN SILTY SAND

6.1 General

Influences of tree roots on bioengineering solutions such as slope stabilization involve mechanical (root reinforcement) and hydrological (evapotranspiration) effects (Greenway, 1987; Pollen-Bankhead & Simon, 2010).

As stated in section 2.5 , the shear strength of unsaturated root-reinforced soil (τ_f) can be expressed as the following Equation 6.1.

$$\tau_f = c' + c_r + c_s + (\sigma_n - u_a) \tan \phi' \quad [6.1]$$

Where,

c' =effective cohesion intercept of saturated non-reinforced soil

ϕ' =effective angle of friction of saturated non-reinforced soil

σ_n =normal stress

u_a =pore air pressure which is normally zero for the case of root-soil composite

c_r =cohesion due to root reinforcement

c_s =cohesion due to suction

The unsaturated soil mechanics concept can be used to calculate the cohesion due to suction (c_s) as the following Equation 6.2 (Bishop, 1959; D. G. Fredlund & Ranhardjo, 1993; Lu & Likos, 2006).

$$c_s = (u_a - u_w)\chi \tan \phi' = (u_a - u_w) \tan \phi^b = (u_a - u_w) \left[\frac{\theta_w - \theta_r}{\theta_s - \theta_r} \right] \tan \phi' \quad [6.2]$$

Wu et al. (1979) initially developed a simplified model for cohesion due to roots, which is as Equation 6.3.

$$c_r = t_r(\sin \theta + \cos \theta \tan \phi) \quad [6.3]$$

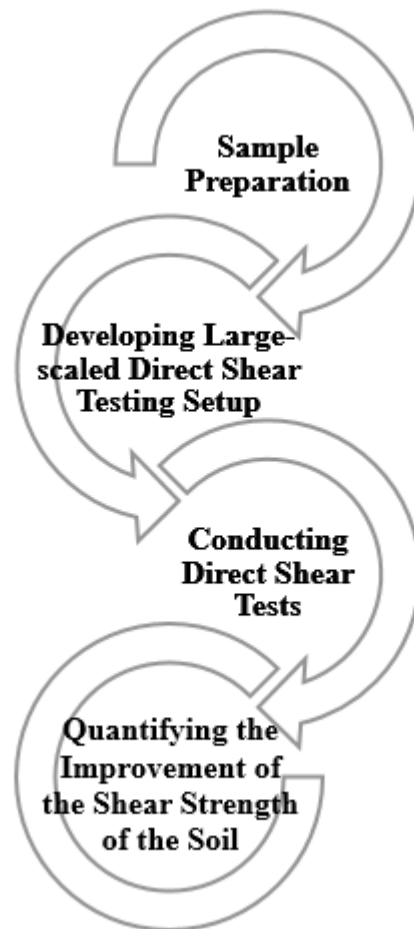
All parameters have the same meaning described previous sections. If the soil becomes saturated, the c_s will be cancelled, and c_r will become an important component.

Previous studies to quantify the increase in shear strength were conducted in saturated conditions only considering the mechanical effect of root reinforcement (Wu et al., 1979; Waldron & Dakessian, 1981; Docker & Hubble, 2009). Further, for instance, most of the previous researchers (such as Jotisankasa et al., 2014; Rahardjo et al., 2014) considered that the tensile strength of the roots and any additional shear strength produced by the root cohesion were independent of suction and would remain constant over time. Most of centrifuge modeling studies (e.g., Ng et al., 2014; Eab et al., 2015) simulated the roots using artificial materials such polyester fibers, cellulose acetate, or fishing line. The results of those tests might not accurately reflect how real plant roots behave on slopes as these synthetic materials are less sensitive to moisture than actual plant roots.

Moreover, other previous studies carried out in the field to capture the vegetated-induced suction effect of the tree roots on the strength of the soil (e.g. Fatahi et al., 2009; Leung & Ng, 2013; Ng et al., 2013). Even through the above, these studies did not explicitly quantify how suction affected mechanical root reinforcement. Recent laboratory research has shown that the mechanical interactions between roots and soil, such as root tensile strength and root cohesiveness, are suction-dependent (Jotisankasa & Taworn, 2016; Gonzalez-Ollauri & Mickovski, 2017).

There are still significant research gap regarding the effects of suction on root reinforcement despite these extensive previous research. This study investigated the influence of soil suction on root reinforcement of the *Alstonia macrophylla* with the selected soil using large-scaled direct shear tests. This chapter initially described the sample preparation for the shear tests, developing a large-scale direct shear testing setup. The latter part of the chapter presented the test results and observations of the 24 large-scale direct shear tests.

6.2 Flow chart for the objective 1



6.3 Sample Preparation

15 specimens were prepared only with soil, and another 15 specimens were prepared with soil and plant, as shown in Figure 6.1. The wooden boxes (figure 6.2) with internal dimensions 300mm (W) x 300mm (L) x 300mm (H) were used for specimen preparation. Sample size was selected as per the investigation of the rate of root growing. The heavy wooden rammer and collar which are shown in Figure 6.2, were used to compact the soil in the wooden boxes as the two layers. The soil dry density was maintained as 1500 kgm^{-3} which was comparable to the typical in-situ dry density of the barrow region. Every sample was prepared using equivalent compaction with 13% of initial gravimetric moisture content.



Figure 6.1: Sample preparation

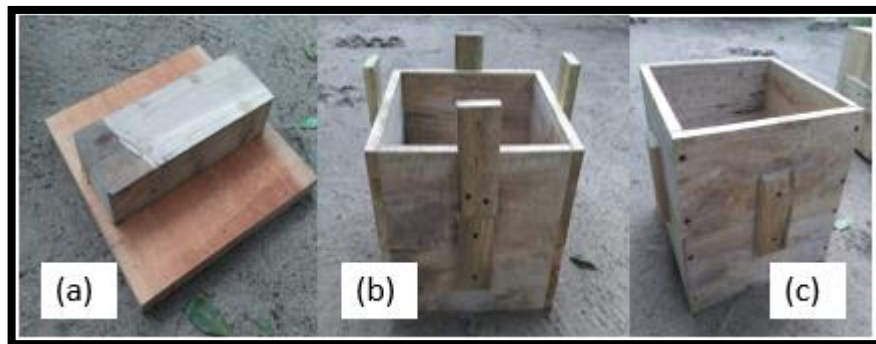


Figure 6.2: Sample compaction procedure (a) wooden compactor, (b) collar, and (c) wooden box

6.4 Developing large-scaled direct shear testing setup

A large-scaled direct shear testing setup was proposed and developed to conduct the shear testing. The main concerns of the design, were the mold size (Figure 6.3), and varied normal loads. The 3D and 2D presentations of the developed testing setup is shown in Figure 6.4. The relative drawing is in Annex 4 for further reference.

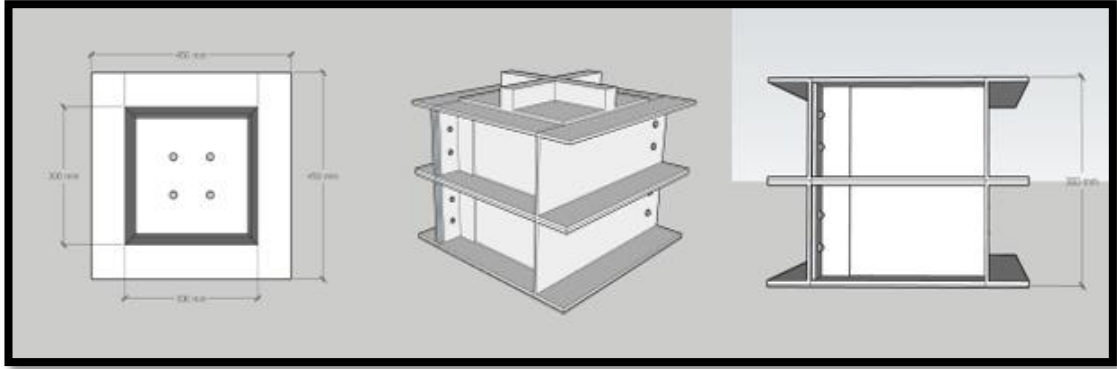


Figure 6.3: Proposed large-scale mold



Figure 6.4: Large-scaled direct shear testing setup (a) proposed setup and (b) developed setup

This setup was designed and developed by following mechanism and technique of the standard direct shear testing apparatus to measure the reaction of the applied horizontal force as the shear force. The steel mold was prepared as L angles for easy handling. Furthermore, the steel balls were used to reduce the contact area between the lower and upper half of the mold. As Figure 6.4, the roller wheels were introduced to make smooth shear displacement with minimal friction force. Figure 6.5 presents the proposed and developed main component of the direct shear testing setup.

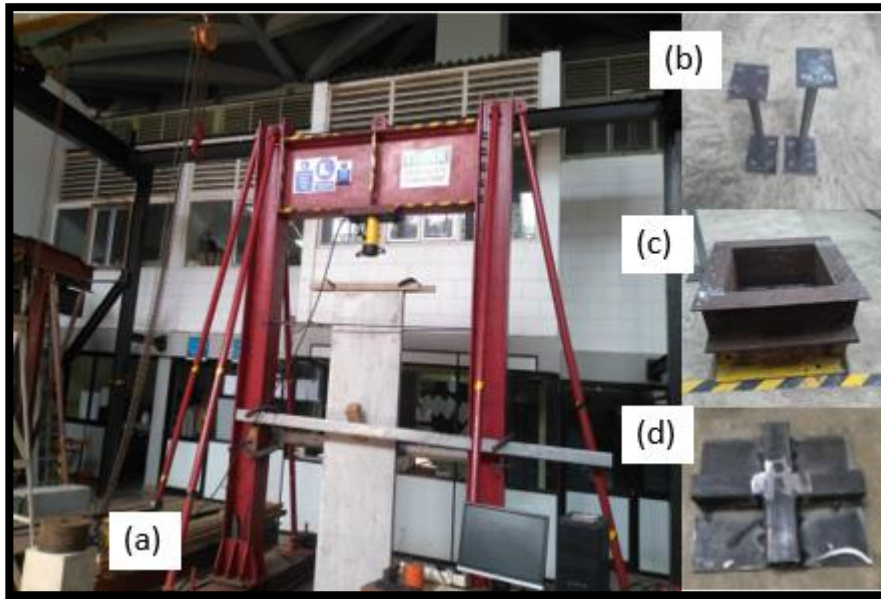


Figure 6.5: Developing stage of large-scale direct shear testing setup (a) test rig, (b) supporters, (c) mold, and (d) load plate

The vertical and horizontal forces were applied to the sample with the support of a hydraulic jack and manual jack, respectively. The applied load was measured using load cells. Further, horizontal and vertical settlements were captured and stored using the settlement gauges with the data logger. All these settlement gauges and load cells were calibrated prior to the direct shear testing as the following Figure 6.6, 6.7, and 6.8.

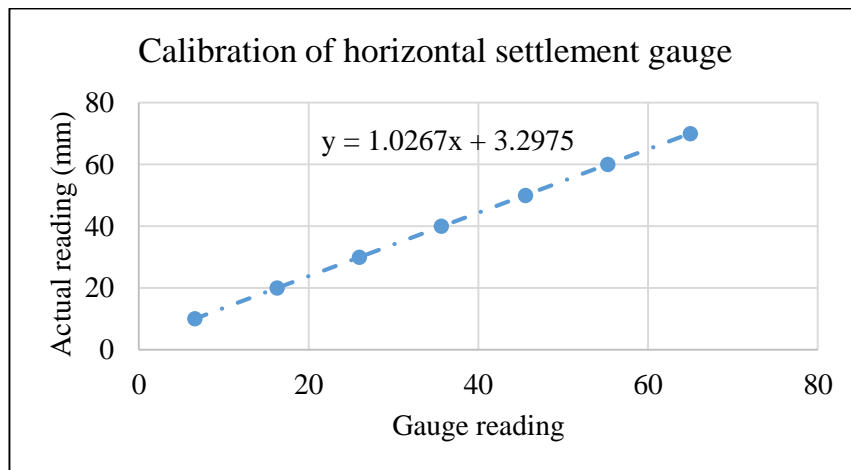


Figure 6.6: Calibration chart for horizontal settlement gauge

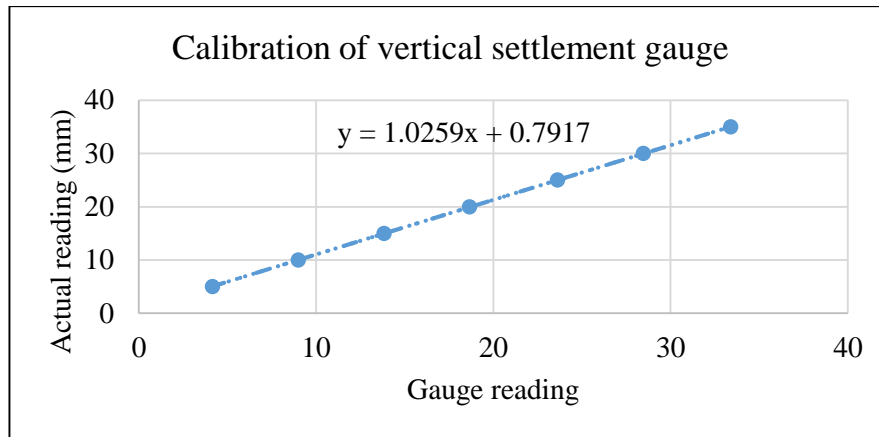


Figure 6.7: Calibration chart for vertical settlement gauge

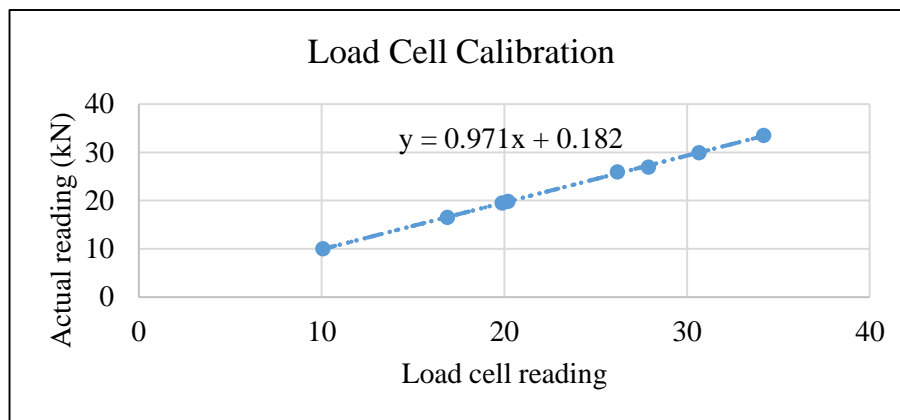


Figure 6.8: Calibration chart for load cell

The shear strength parameters obtained for dry and fully saturated soil samples by using developed setup were validated with the results obtained from standard direct shear testing apparatus. The summary of the test results was included in Table 6.1 and failure envelopes for both instruments were present in Figures 6.9 and 6.10.

Table 6.1: Validation of large-scale direct shear testing setup

Testing apparatus/ setup	Shear strength parameters for dry soil with 1500 kgm^{-3} density		Shear strength parameters for fully saturated soil (V. Mc.=0.44) with 1500 kgm^{-3} density	
	Friction Angle ($^{\circ}$)	Cohesion (kN/m^2)	Friction Angle ($^{\circ}$)	Cohesion (kN/m^2)
Standard direct shear testing apparatus	43	3.51	42	0.89
Developed large scaled direct shear testing setup	41	5.64	41	2.21

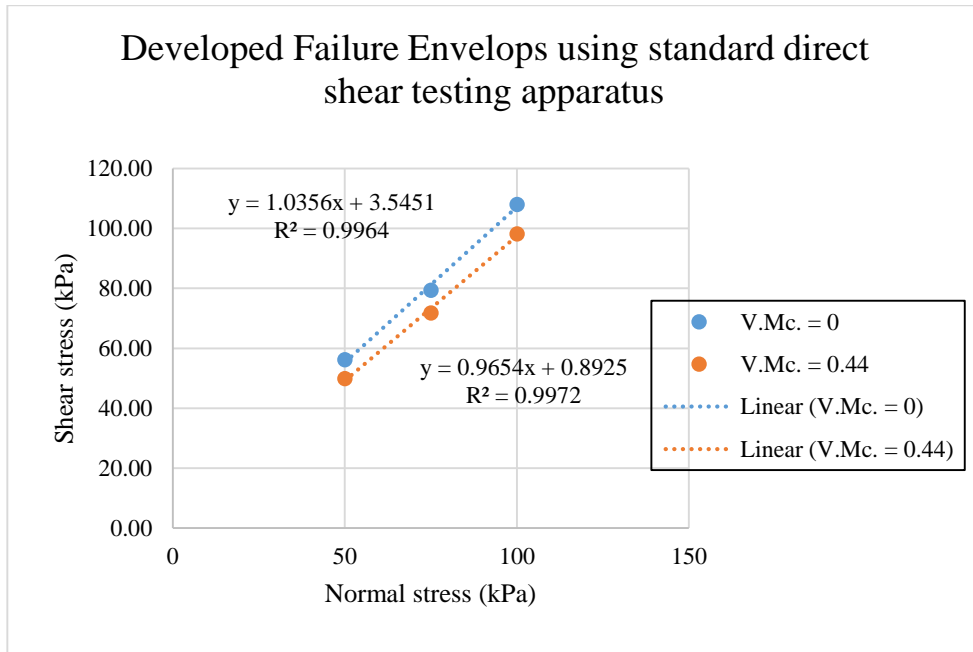


Figure 6.9: Developed Failure Envelops using standard direct shear testing apparatus

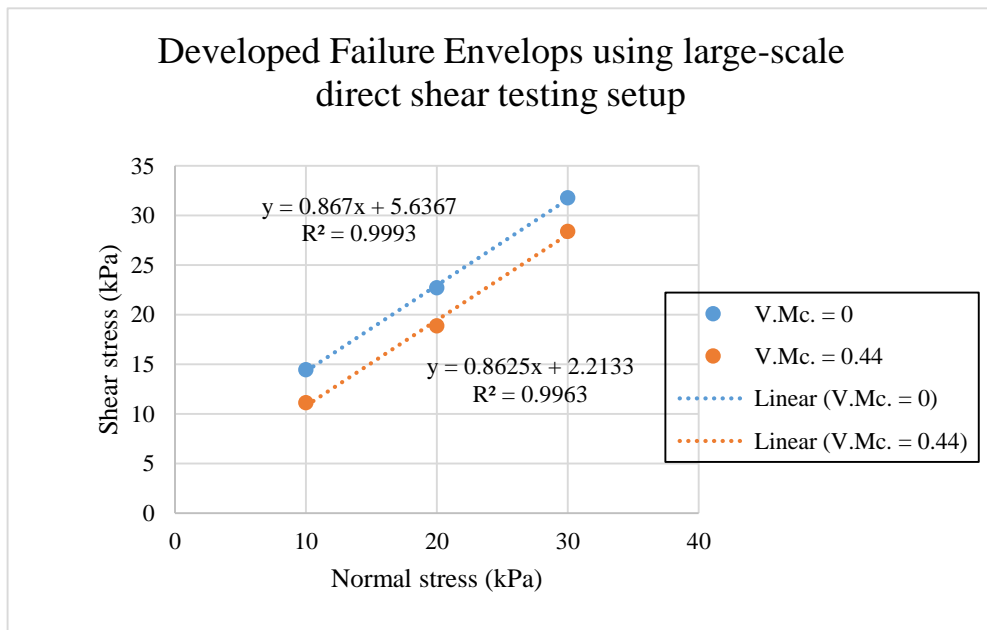
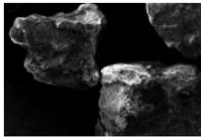
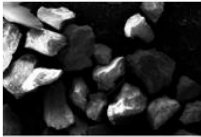

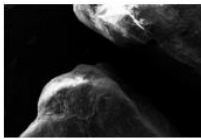


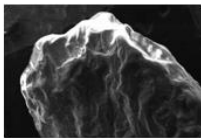
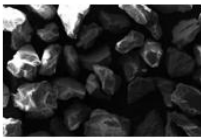
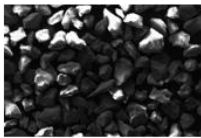


Figure 6.10: Developed Failure Envelops using large-scale direct shear testing setup

According to the above results, the selected soil type had a relatively higher value of effective friction angle. A SEM test was conducted to capture texture of soil particles. Moreover, a comparative study was carried out for the selected soil with quarry dust

and river sand to find the reason behind the relatively high friction angle. The summary of the output of SEM test were presented in Table 6.2 (more clear images were added in Annex 5). According to that, relatively high angularity of the particles was observed as per the particles of quarry dusk and river sand. That would be a reason for the above mentioned behavior of the semi-coastal silty sand.

Table 6.2: Comparative study for the texture of the soil particles

Soil type	Particle size (mm)		
	4.75 – 1.18	1.18 – 0.425	0.425 – 0.075
Quarry dusk			
Selected Soil type (SW-SM)			
River sand			

6.5 Conducting Direct shear tests

12 soil samples with plants with the same growing qualities were selected for direct shear testing, after the same environmental condition was maintained on 30 samples during the four months. A root-reinforced soil specimen was tested under 4 different suction values which was selected as 0kPa, 10kPa, 20kPa and 150kPa and three tests were carried out for each suction value considering 10kPa, 20kPa, and 30kPa vertical/normal stresses. Moreover, 12 additional tests on unreinforced direct shear specimens were performed for comparison.

Above mentioned developed large 300 mm x 300mm x300mm the shear box was used to carry out the test. The soil specimen with tree roots was transferred to shear box from the wooden box with minimal disturbance to the specimen. After that, the mold was easily installed to the direct shear testing setup with the helps of the trolley contained the roller wheel tray, as shown in Figure 6.11. Furthermore, the easy

removal method of the side board of the wooden boxes convened to sample installation.



Figure 6.11: Trolley with a roller wheel tray

Then, the suction sensor was installed to the soil specimen with a depth which can reach the shear plane, as shown in Figure 6.12a. The specimens were allowed several days to achieve the required level of suction. As illustrated in Figure 6.12b, a vertical sand pile with a 15 mm diameter was installed inside the shear box to measure the width of the shear zone.



Figure 6.12: Sample installation (a) sensor installation, (b) sand pile installation

The direct shear tests were then conducted at each suction level at three different normal stress values (10kPa, 20kPa, and 150kPa) as per Figure 6.13; 2.5 mm per minute was used to shred the specimen. All tests relevant to each suction level and

normal stress were repeated on the specimens without tree roots in order to quantify the shear improvement of the soil brought by those roots.



Figure 6.13: Conducting direct shear testing

After the test, the following factors were also measured those are important parameters to evaluate the effect of root reinforcement in geotechnical applications because they have been considered most of the models and concepts that previous researchers proposed.

- ✓ The amount root present in the shear plane measured as RAR-Root Area Ratio
- ✓ The amount of root present in the shear box as dry bio mass of root per unit volume the soil
- ✓ The failure pattern of a root
- ✓ Height of the shear zone
- ✓ Total Leaf Area and height of the plant

6.6 Results and Discussion

The shear stress vs. shear displacements test result for four different matric suctions with three different normal stresses in case with root and without roots are graphically represented in Figure 6.14, 6.15, 6.16, and 6.17.

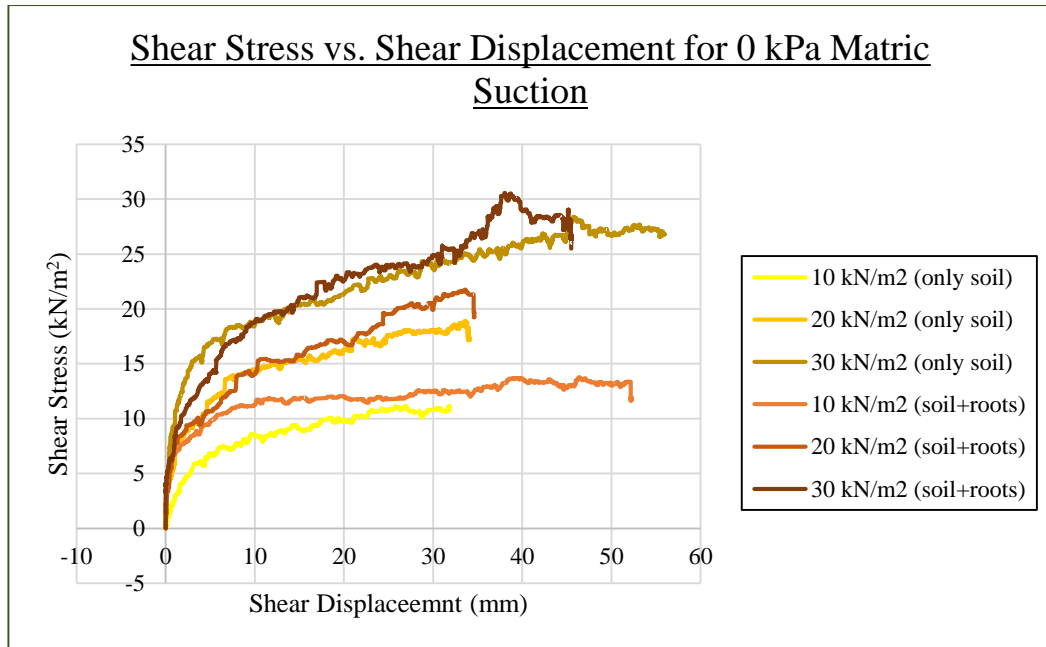


Figure 6.14: Shear Stress vs. Shear Displacement for 0 kPa Matric Suction

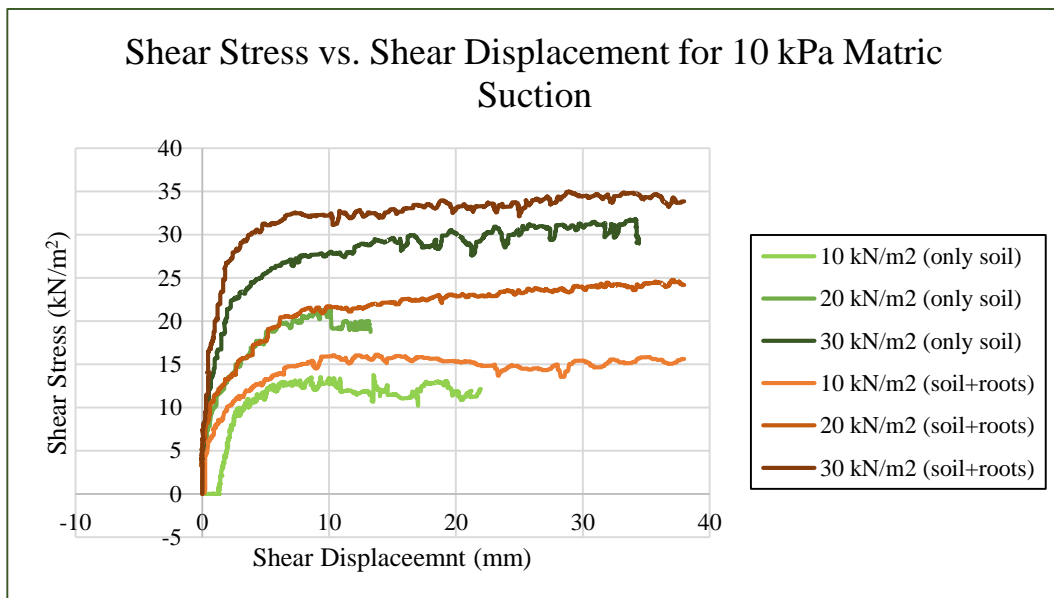


Figure 6.15: Shear Stress vs. Shear Displacement for 10 kPa Matric Suction

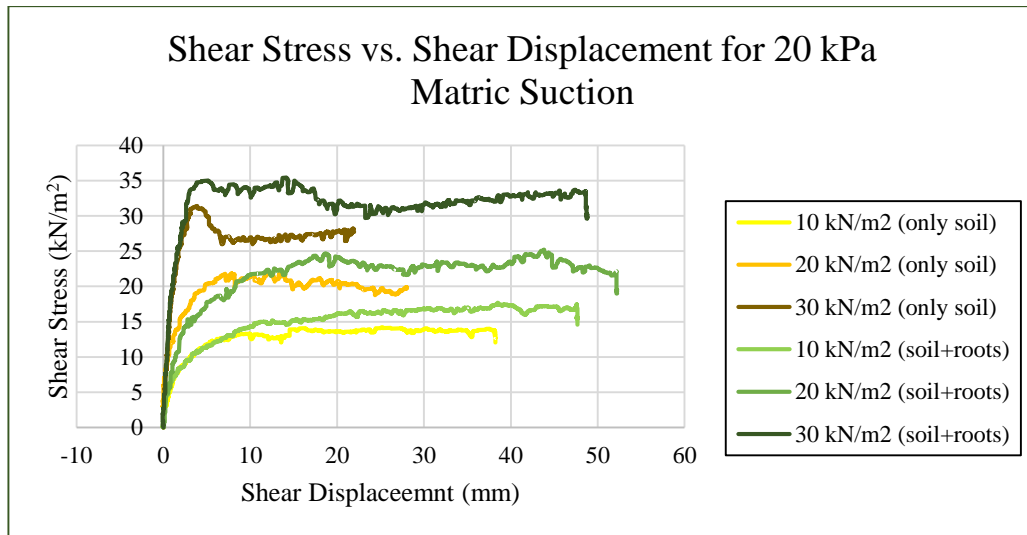


Figure 6.16: Shear Stress vs. Shear Displacement for 20 kPa Matric Suction

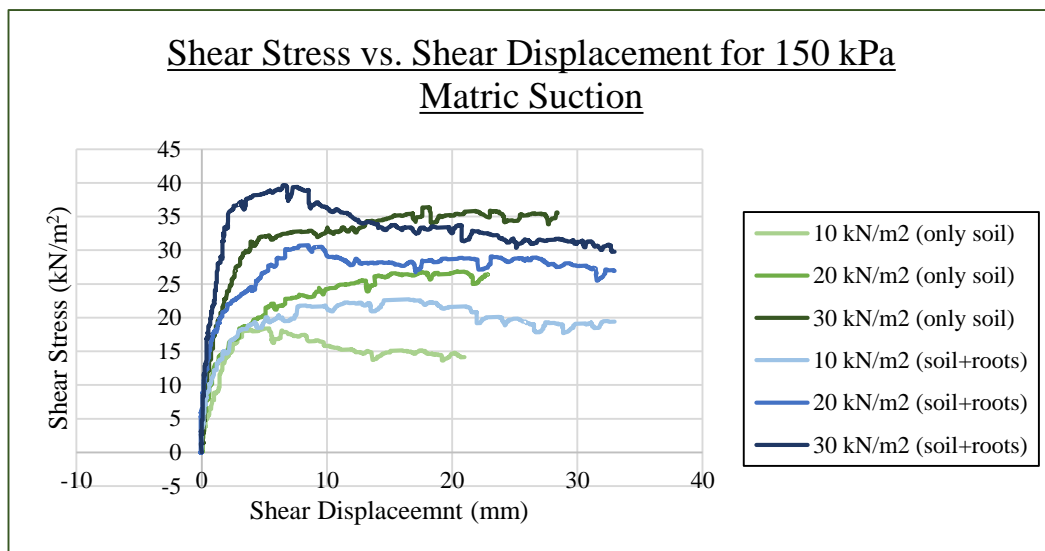


Figure 6.17: Shear Stress vs. Shear Displacement for 150 kPa Matric Suction

According to the above presentation, the shear strength of the root-permeated soil specimens was higher than the unreinforced specimens in each case, which agrees with previous studies carried out by Docker and Hubble (2001).

Then, Table 6.2 shows the summary of the test results and relevant observations of the 24 direct shear tests for four different matric suction values with three different normal loads. For each case, the table represents the normal stress, matric suction/ volumetric moisture content, reinforced peak shear stress, unreinforced peak shear stress, RAR

value at the shear plane, dry biomass of the roots per unit soil volume, total leaf area of the plant and the width of the shear zone.

According to observed values of RAR, dry biomass of roots per unit volume of soil, and total leaf area for each tested plant, the similarity of tree plants was identified again as the visual inspection carried out before direct shear testing. The average values of RAR, dry biomass of roots per unit volume of soil, and total leaf area for each tested plant were $6.22 \times 10^{-3} \%$, 0.575 kg/m^3 and 1195 cm^2 , respectively. After that, a theoretical value of c_r (discussed in section 6.1) was calculated as the difference between the reinforced and unreinforced peak shear stresses under three different vertical stresses for each matric suctions when the other shear strength parameters were referred to in the same condition. The results are presented in Table 6.3.

Table 6.3: Summary of the test results

Sample No	Vertical Stress (kN/m ²)	Matric Suction (kPa)/ Volumetric Water Content	Reinforced τ_{Peak} (kN/m ²)	Unreinforced τ_{Peak} (kN/m ²)	RAR (%) $\times 10^{-3}$	Dry Bio Mass of roots per unit volume the soil (kg/m ³)		Total leaf area (cm ²)	Height of shear zone (mm)
						Upper half	Lower half		
1	10	0/0.44	13.75	11.14	6.49	0.628	0.006	1278	42
2	20		21.74	18.86	5.7	0.448	0.026	1354	45
3	30		30.57	28.39	6.38	0.486	0.02	998	42
4	10	10/0.15	16.11	13.75	6.33	0.536	0.036	1085	35
5	20		24.74	21.5	6.1	0.56	0.044	1315	37
6	30		34.96	31.74	5.48	0.624	0.032	1243	32
7	10	20/0.10	17.66	14.21	6.42	0.41	0.04	1182	25
8	20		25.21	21.85	7.02	0.694	0.026	1243	28
9	30		35.44	31.4	5.12	0.412	0.034	1308	26
10	10	150/0.05	22.75	18.42	5.96	0.578	0.05	1064	17
11	20		30.74	26.89	6.33	0.61	0.028	984	15
12	30		39.63	36.39	7.34	0.512	0.05	1289	15
Average values					6.22	0.542	0.033	1195	

Table 6.4: c_r value calculated as the difference between the reinforced and unreinforced peak shear stresses under three vertical stresses for each matric suctions

Normal Load	10 kN/m ²			20 kN/m ²			30 kN/m ²		
	Matric Suction (kPa)/volumetric water content	Reinforced τ_{Peak} (kN/m ²)	Unreinforced τ_{Peak} (kN/m ²)	Observed c_r (kN/m ²)	Reinforced τ_{Peak} (kN/m ²)	Unreinforced τ_{Peak} (kN/m ²)	Observed c_r (kN/m ²)	Reinforced τ_{Peak} (kN/m ²)	Unreinforced τ_{Peak} (kN/m ²)
0/0.44	13.75	11.14	2.61	21.74	18.86	2.88	30.57	28.39	2.18
10/0.15	16.11	13.75	2.36	24.74	21.5	3.24	34.96	31.74	3.22
20/0.10	17.66	14.21	3.45	25.21	21.85	3.36	35.44	31.4	4.04
150/0.05	22.75	18.42	4.33	30.74	26.89	3.85	39.63	36.39	3.24

Furthermore, the failure envelopes were obtained for each case with and without tree roots as per Figure 6.18, 6.19, 6.20, and 6.21. The results are summarized in Table 6.4 with their accuracy level.

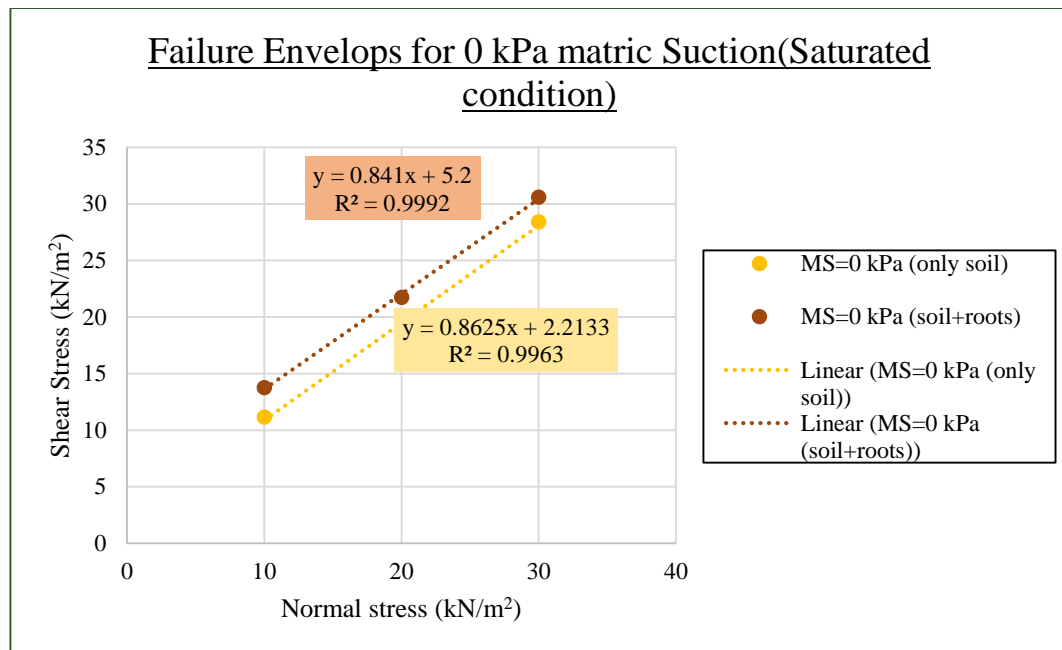


Figure 6.18: Failure Envelops for 0 kPa matric Suction (Saturated condition)

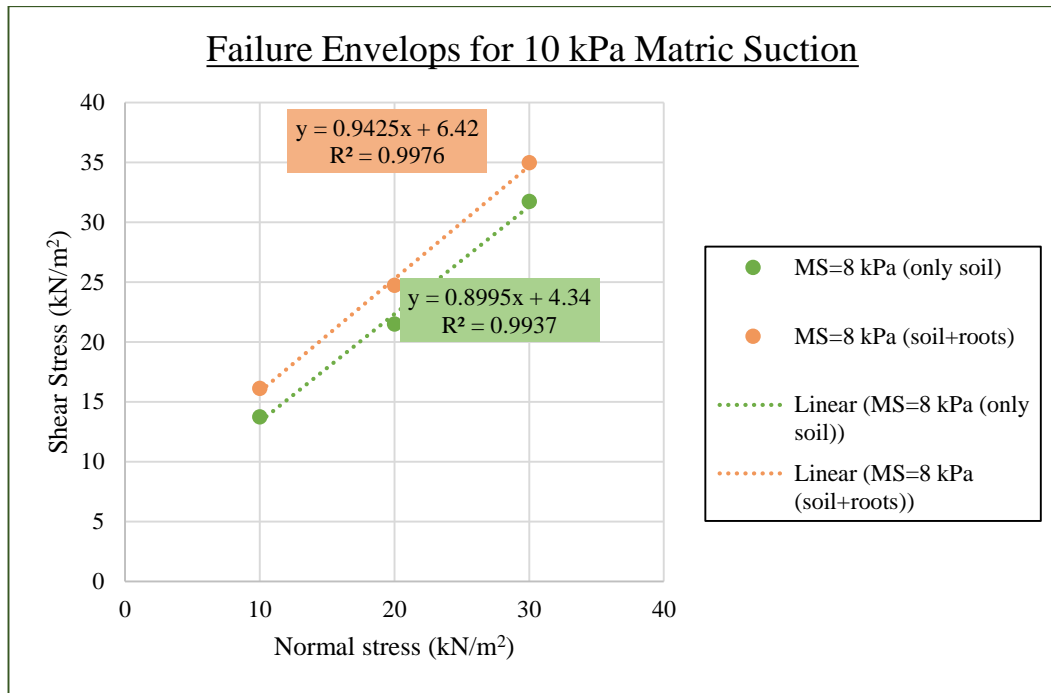


Figure 6.19: Failure Envelops for 10 kPa Matric Suction

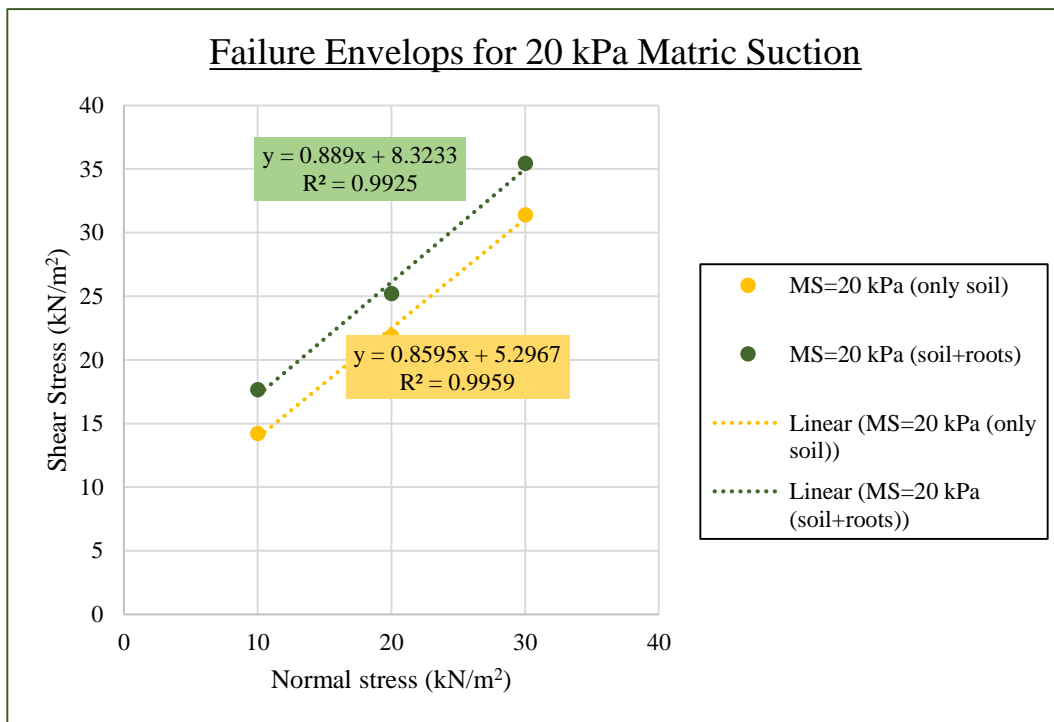


Figure 6.20: Failure Envelops for 20 kPa Matric Suction

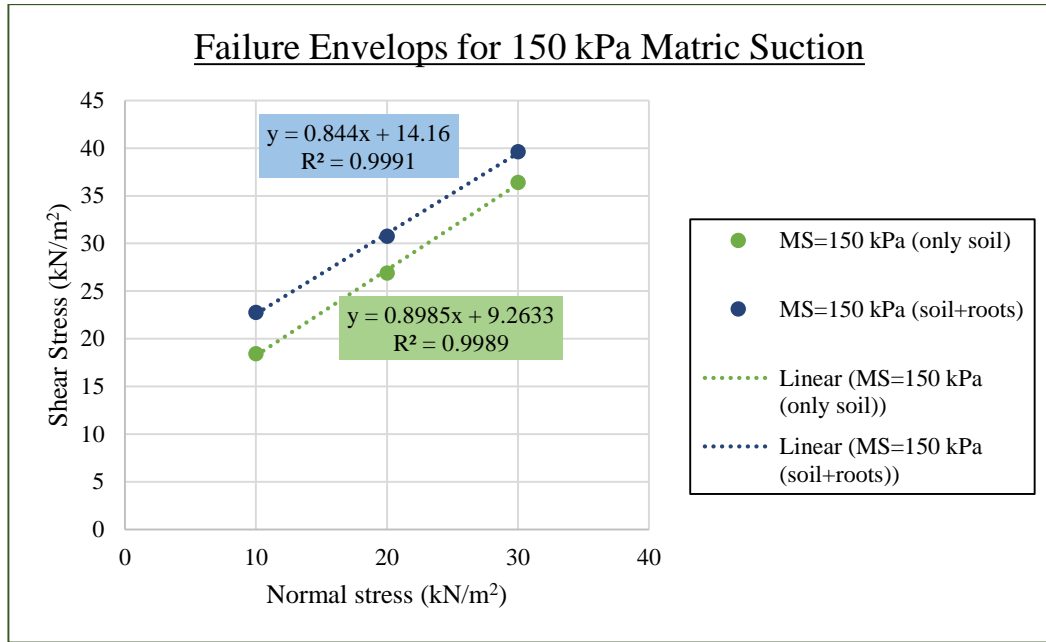


Figure 6.21: Failure Envelops for 150 kPa Matric Suction

Table 6.5: Failure envelopes for each case

Matric Suction (kPa)/volumetric water content	Reinforced failure envelop	Unreinforced failure envelop
0/0.44	$\tau_f = 0.841\sigma_n + 5.2$ $R^2 = 0.9992$	$\tau_f = 0.8625\sigma_n + 2.2133$ $R^2 = 0.9963$
10/0.15	$\tau_f = 0.9425\sigma_n + 6.42$ $R^2 = 0.9976$	$\tau_f = 0.8995\sigma_n + 4.34$ $R^2 = 0.9937$
20/0.10	$\tau_f = 0.889\sigma_n + 8.3233$ $R^2 = 0.9925$	$\tau_f = 0.8595\sigma_n + 5.2967$ $R^2 = 0.9959$
150/0.05	$\tau_f = 0.844\sigma_n + 14.16$ $R^2 = 0.9991$	$\tau_f = 0.8985\sigma_n + 9.2633$ $R^2 = 0.9989$

Then, the difference between the apparent cohesion of reinforced and unreinforced failure envelopes was calculated for each matric suction. That value should theoretically

be equal to the cohesion due to root reinforcement (c_r). The values of observed c_r are present in Table 6.5.

Table 6.6: Calculated c_r values using failure envelopes

Matric Suction (kPa)/volumetric water content	Reinforced failure envelop		Unreinforced failure envelop		$c_r = c_{a,R} - c_{a,UR}$ (kN/m ²)
	$\phi'_{R}(\text{°})$	$c_{a,R}(\text{kN/m}^2)$	$\phi'_{UR}(\text{°})$	$c_{a,UR}(\text{kN/m}^2)$	
0/0.44	40	5.2	41(ϕ')	2.13(c')	2.99
10/0.15	43	6.42	42	4.34	2.08
20/0.10	42	8.32	41	5.30	3.03
150/0.05	40	14.16	42	9.26	4.90

Finally, the summary of the results for observed c_r for each matric suction value by using two different methods is presented in Table 6.6.

Table 6.7: Summary of the observed c_r values following both approaches

Normal Load	10 kN/m ²	20 kN/m ²	30 kN/m ²	$c_r = c_{a,R} - c_{a,UR}$ (kN/m ²)
Matric Suction (kPa)/volumetric water content	Observed c_r (kN/m ²)			
0/0.44	2.61	2.88	2.18	2.99
10/0.15	2.36	3.24	3.22	2.08
20/0.10	3.45	3.36	4.04	3.0266
150/0.05	4.33	3.85	3.24	4.8967

The effective shear strength parameters of the selected soil type can be obtained using the unreinforced direct shear tests carried out under saturated conditions. As per above observations, the effective friction angle and effective cohesion of the selected soil type were 41⁰ and 2.21 kN/m² respectively. The friction angle of each case has varied between the 40⁰ to 43⁰ which is approximately equal to the effective friction angle of the selected soil. According to the kind of literature, the effective friction angle of soil does not change significantly with the improvement of the matric suction and the root reinforcement. That statement confirms with test results of this research again with the observation.

Furthermore, the cohesion due to soil suction (c_s) should be equal in reinforced and unreinforced situations during the same level of matric suction. As the above, the cohesion due to root reinforcement (c_r) can be calculated by two different methods; (01) as the difference between the reinforced and unreinforced peak shear stresses under three different normal stresses for each matric suction; and (02) the difference between the apparent cohesion of reinforced and unreinforced failure envelopes of each matric suction. These observed c_r values which were calculated both ways for all trials should be equal to the difference between the apparent cohesion of reinforced and unreinforced shear strength in saturated samples of 2.99 kN/m². According to the summary in Table 6.7, the c_r values have slightly increased with matric suction in both ways. This observation also confirms the finding of Jotisankasa and Taworn, 2016; Gonzalez-Ollauri and Mickovski, 2017; Yildiz et al., 2018.

Finally, it can be concluded that the cohesion due to root reinforcement of the *Alstonia macrophylla* is slightly increased with the matric suction in the Sri Lankan Silty Sand.

6.7 Summary

The tree roots influence the bioengineering solutions such as slope stabilizations in mechanical (root reinforcement) and hydrological (soil suction) ways. Many studies only considered the mechanical behavior of tree roots, ignoring the implications of transpiration on the pore water pressure. Furthermore, other previous studies were carried out in the field to capture the vegetated-induced suction effect of the tree roots on the strength of the soil. However, previous researchers have tried to model the coupled effect of root reinforcement and soil suction, but these models are very complicated.

Moreover, recent laboratory research has shown that the mechanical interactions between roots and soil, such as root tensile strength and root cohesiveness, are suction-dependent. Therefore, this study investigated the influence of matric suction on root reinforcement of the *Alstonia macrophylla* with selected soil using large-scaled direct shear tests by varying the soil suction.

The effective friction angle and cohesion of the selected soil type were 41° and 2.21 kN/m² respectively with 1500 kg/m³ dry density of the soil. The friction angle of each

case has varied between the 40° to 43° which is approximately equal to the effective friction angle of the selected soil. As the first observation, the effective friction angle of the soil does not change significantly with improvement of the matric suction and the root reinforcement.

Cohesion due to root reinforcement (c_r) of the *Alstonia macrophylla* should theoretically equal to the difference between the apparent cohesion of reinforced and unreinforced shear strength in saturated samples. This value was 2.99 kN/m^2 when RAR, dry biomass of roots per unit volume of soil, and total leaf area of the plant were $6.22 \times 10^{-3} \%$, 0.575 kg/m^3 and 1195 cm^2 respectively. As per the observations, the cohesion due to root reinforcement of the *Alstonia macrophylla* is slightly increased with the matric suction in the Sri Lankan Silty Sand.

Chapter 7

7 CONCLUSION AND RECOMMENDATION

7.1 General Summary

Vegetation aims to stabilize slopes by mechanically strengthening soils through root systems and hydrologically reducing soil water content through transpiration and precipitation interception. Tree roots mechanically and hydrologically increase the strength of the soil as the important component of the vegetation. Previous studies, however, focused on the mechanical and hydraulic impacts of tree roots separately when evaluating the impact of vegetation, which failed to yield reliable results because suction influences on mechanical characteristics of tree roots. Therefore, this study aimed at investigating the influence of suction on the mechanical behavior of the *Alstonia macrophylla* roots in the Sri Lanka Silty Sand. Chapter 1 introduced and described the nature of this study. Chapter 2 was a comprehensive and insightful literature review of previous studies related to this study. The unsaturated behavior of the soil was reviewed in the first half of this chapter by presenting the comparative study between the experimental and analytical methods which were used to develop the SWCC. In the second half of this chapter, the broad discussion was carried out about the employment of tree roots for ground improvement by following the effect of root reinforcement and soil suction. Chapter 3 explained the laboratory experimental procedures used to determine the basic soil properties of the selected soil type. Further, this selected soil was classified as well graded silty sand. Chapter 4 explained the study of the mechanical and hydrological behaviors of the selected plant. The suitability of *Alstonia macrophylla* for the main test procedure could be identified according to the observation of the experiments conducted under this title. Chapter 5 presented the SWCC for the selected soil type which is developed according to the experimental (pressure plate apparatus, moisture and suction sensors, and WP4C) and analytical (prediction models of Arya and Paris (1981), Aubertin et.al (2003), and Wang et al. (2017) procedures. Chapter 6 described the influence of matric suction on root reinforcement by conducting several large scaled direct shear tests.

7.2 Specific Conclusion

7.2.1 Most reliable experimental and analytical procedures which can be used to SWCCs for Sri Lanka Silty Sand.

This study presented the SWCC for Sri Lankan coastal silty sand developed using chilled mirror dew-point technique, WP4C and a comparison between the performance of a few prediction models. The SWCC was also developed experimentally using a pressure plate and suction-moisture sensors in order to validate the findings from the chilled mirror dew-point technique, WP4C. The performance of the prediction models was evaluated by using Arya and Paris (1981), Aubertin et al. (2003), and Wang et al. (2017). According to the verification obtained using the pressure plate and suction-moisture sensor, WP4C can produce results quickly, precisely, and consistently in a wider range of total suction. Therefore, the chilled mirror dew-point technique, WP4C can be recommended as a relatively convenient experimental method to develop the SWCC for sandy soil. However, samples need to be handled carefully to preserve the basic soil characteristics. Prediction models were firstly developed using the values of model parameters proposed by the authors for sandy soil. Aubertin et al. (2003) and Wang et al. (2017) predictions were more accurate than Arya and Paris (1981) model when they were compared with the developed experimental SWCC. In addition, the values of the model parameters of Aubertin et al. (2003) and Wang et al. (2017) models were recalculated such that the deviation between experimentally generated SWCC and model-developed SWCC was became as the minimum. As per the results, the Wang et al. (2017) model is more suited to generate SWCC analytically for this soil type.

7.2.2 Identified components of the increase in the shear strength of root permeated soil, during direct shear testing

Number of 24 successful vegetated and non-vegetated specimens were tested under the four distinct degrees of suction and three different applied stresses in this study to mainly investigated the influence of matric suction on root reinforcement of the *Alstonia macrophylla* with Sri Lankan Silty Sand using large-scale direct shear tests.

For instance, the majority of previous research (such as Jotisankasa and Mairaing, 2014; Rahardjo et al., 2014; Ni et al., 2018) considered that the tensile strength of the roots and any additional shear strength produced by the root cohesion were independent of suction and would remain constant over time. However, the cohesion due to root reinforcement of the *Alstonia macrophylla* is slightly increased with the matric suction in the Sri Lankan Silty Sand as per the observations of this study.

The influence of the matric suction on the root reinforcement can be defined as an increment of the shear strength due to an integrated root-suction system. Therefore, the following three components related to root permeated soil can be expressed as follows,

$\Delta\tau_R$ = increase in shear strength due to the effect of root reinforcement only (in a saturated condition)

$\Delta\tau_C$ = increase in shear strength due to an integrated root- suction system.

$\Delta\tau_S$ = increase in shear strength due to increased soil suction from tree transpiration.

7.3 Recommendations for future works

This study has presented the development of the SWCC using WP4C experimentally for only Sri Lankan coastal silty sand. Therefore, the reliability and applicability of the chilled mirror dew-point technique, WP4C has only been checked with unsaturated Silty Sand; It is therefore suggested that, this experiment should be performed with various soil types.

In addition, the SWCCs were developed according to Arya and Paris (1981), Aubertin et.al (2003), and Wang et al. (2017) for the Sri Lanka Silty Sand. Therefore, the reliability of the prediction models was only checked by using above-mentioned models and soil type; It is suggested that this comparison should be carried out with the different models and soil type.

The large-scale direct shear tests were conducted only considering the above-selected soil type and root reinforcement of *Alstonia macrophylla*. Therefore, the influence of the suction was only captured on the root reinforcement of the *Alstonia macrophylla*; It is therefore suggested that, this experiment can be conducted for various tree species

and soil types. Then, the statement that “there is an influence of the matric suction of the soil on the root reinforcement” can be strongly proved with a significant database.

It is strongly suggested that, the mathematical model with user friendly interface can be proposed to quantify the influence of the matric suction on the root reinforcement by using gathered experimental data in this research.

Chapter 8

8 REFERENCES

- Alves, R. D., Gitirana, G. de F. N., & Vanapalli, S. K. (2020). Evaluation of prediction models applied to the soil-water characteristic curve of ideal materials. *E3S Web of Conferences*, 195, 02024. <https://doi.org/10.1051/e3sconf/202019502024>
- Arya, L. M., & Dierolf, T. S. (1989). Predicting Soil Moisture Characteristics from Particle-Size Distributions: An Improved Method to Calculate Pore Radii from Particle Radii. *Indirect Methods for Estimating the Hydraulic Properties of Unsaturated Soils*, 115.
- Arya, L. M., & Paris, J. F. (1981a). A Physicoempirical Model to Predict the Soil Moisture Characteristic from Particle-Size Distribution and Bulk Density Data. *Soil Science Society of America Journal*, 45(6), 1023–1030. <https://doi.org/10.2136/sssaj1981.03615995004500060004x>
- Arya, L. M., & Paris, J. F. (1981b). A Physicoempirical Model to Predict the Soil Moisture Characteristic from Particle-Size Distribution and Bulk Density Data. *Soil Science Society of America Journal*, 45(6), 1023–1030. <https://doi.org/10.2136/sssaj1981.03615995004500060004x>
- ASTM D6836-02(2008)e2—Standard Test Methods for Determination of the Soil Water Characteristic Curve for Desorption Using a Hanging Column, Pressure Extractor, Chilled Mirror Hygrometer, and/or Centrifuge. (n.d.). Retrieved March 29, 2023, from <https://webstore.ansi.org/standards/astm/astmd6836022008e2>
- Aubertin, M., Mbonimpa, M., Bussi re, B., & Chapuis, R. P. (2003). A model to predict the water retention curve from basic geotechnical properties. *Canadian Geotechnical Journal*, 40(6), 1104–1122. <https://doi.org/10.1139/t03-054>
- Barker, D. H. (2001). Innovative bioengineering technique for rapid slope stability. *Geotechnical Engineering, H. Li., Ed., Swets & Zeitlinger, Lisse*, 697–702.
- Bishop, A. W. (1959). The principle of effective stress. *Teknisk Ukeblad, Norwegian Geotechnical Institute*, 106,39, 859–863.
- B hm, M. (1980). *Methods of Studying Root Systems. Berlin: Springer (1979), pp. 200, DM 69, Cambridge University Press.*
- Croney, D., & Coleman, J. D. (1954). SOIL STRUCTURE IN RELATION TO SOIL SUCTION (pF). *Journal of Soil Science*, 5(1), 75–84. <https://doi.org/10.1111/j.1365-2389.1954.tb02177.x>
- Dobson, M. C., & Moffat, A. J. (1995). A re-evaluation of objections to tree planting on containment landfills. *Waste Management and Research*, 13(6), 579–600.
- Docker, B. B., & Hubble, T. T. C. (2001). Strength and stability of *Casuarina glauca* roots in relation to slope stability. *Proceeding of the 14th Southeast Asian Geotechnical Conference, Lisse*, 745–749.

- Docker, B. B., & Hubble, T. T. C. (2008). Quantify root-reinforcement of river bank soils by four Australian tree species. *Geomorphology*, *100*(3–4), 401–418.
- Docker, B. B., & Hubble, T. T. C. (2009). Modelling the distribution of enhanced soil shear strength beneath riparian trees of south-eastern Australia. *Ecological Engineering*, *35*(2009), 921–924.
- Eab, K. H., Likitlersuang, S., & Takahashi, A. (2015). Laboratory and modelling investigation of root-reinforced system for slope stabilisation. *Soils Found.*, *55*(5), 1270–1281.
- Escario, V., & Juca, J. F. T. (1989). Shear strength and deformation of partly saturated soils. *Proceedings of the Twelfth International Conference on Soil Mechanics and Foundation Engineering, Rio de Janeiro, 1*, 43–46.
- Fahati, B., Indraratna, B., & Khabbaz, M. H. (2007). Soft soil improvement induced by tree root suction: Report online. *Australian Geomechanics Journal*, *42*(4), 13–18.
- Fatahi, B., Khabbaz, H., & Indraratna, B. (2009). Parametric studies on bioengineering effects of tree root-based suction on ground behavior. *Ecological Engineering*, *35*, 1415–1426.
- Feddes, R. A., Bresler, E., & Neuman, S. P. (1974). Field Test of Modified Numerical Model for Water Uptake by Root System. *Water Resources and Research*, *10*(6), 1199–1206.
- Feddes, R. A., Kowalik, K., Kolinshka-Malinka, K., & Zaradny, H. (1976). Simulation of field water uptake by plants using a soil water dependent root extraction function. *Journal of Hydrology*, *31*(1–2), 13–26.
- Fredlund, D. G. (1996). *The scope of unsaturated soil mechanics- An overview*.
- Fredlund, D. G., & Morgenstern, N. R. (1977). Stress state variables for unsaturated soils. *Journal of Geotechnical and Geo-Environmental Engineering*, *103*, 447–466.
- Fredlund, D. G., Rahardjo, H., & Fredlund, M. D. (2012). Soil-Water Characteristic Curves for Unsaturated Soils. In *Unsaturated Soil Mechanics in Engineering Practice* (pp. 184–272). John Wiley & Sons, Ltd. <https://doi.org/10.1002/9781118280492.ch5>
- Fredlund, D. G., & Ranhardjo, H. (1993). *Soil Mechanics for Unsaturated Soils*. Wiley.
- Fredlund, D. G., Ranhardjo, H., & Fredlund, M. D. (2012a). Measurement and Estimation of State Variables. In *Unsaturated Soil Mechanics in Engineering Practice* (pp. 109–183). John Wiley & Sons, Ltd. <https://doi.org/10.1002/9781118280492.ch4>
- Fredlund, D. G., Ranhardjo, H., & Fredlund, M. D. (2012b). Theory to practice of unsaturated soil mechanics. In *Unsaturated Soil Mechanics in Engineering Practice* (pp. 1–28). John Wiley & Sons, Ltd. <https://doi.org/10.1002/9781118280492.ch1>

- Fredlund, D. G., & Xing, A. (1994). Equations for the soil-water characteristic curve. *CANADIAN GEOTECHNICAL JOURNAL*, 31(4), 521–532.
- Fredlund, M. D., Fredlund, D. G., Wilson, G. W., & Sillers, W. S. (1996). Design of a knowledge-based system for unsaturated soil properties. *Proceedings of the Third Canadian Conference on Computing in Civil and Building Engineering, Montreal, QC*, 659–677.
- Gan, J. K.-M., & Fredlund, D. G. (1988). Multistage direct shear testing of unsaturated soils. *Geotechnical Testing Journal, ASTM*, 11(2), 132–138.
- Gardner, W. R. (1960). Dynamic aspects of water availability to plants. *Soil Science*, 89(2), 63–73.
- Gee, G. W., Campbell, M. D., Campbell, G. S., & Campbell, J. H. (1992). Rapid Measurement of Low Soil Water Potentials Using a Water Activity Meter. *Soil Science Society of America Journal*, 56(4), 1068–1070. <https://doi.org/10.2136/sssaj1992.03615995005600040010x>
- Ghestem, M., Sidle, R. C., & Stokes, A. (2011). The influence of plant root systems on subsurface flow: Implications for slope stability. *Bio Science*, 61(11), 869–879.
- Gilmen, E. F. (1980). *An Illustrated Guide to Pruning, Environmental Horticulture Department, IFAS, University of Florida*.
- Gonzalez-Ollauri, A., & Mickovski, S. B. (2017). Plant-soil reinforcement response under different soil hydrological regimes. *Geoderma*, 285, 141–150.
- Green, S. R. (1992). Radiation balance, transpiration and photosynthesis of an isolated tree. *Agricultural and Forest Meteorology*, 64(1993), 201–221.
- Greenway, D. R. (1987). Vegetation and slope stability. *Geotechnical Engineering and Geomorphology*, 187–230.
- Haverkamp, R., & Parlange, J.-Y. (1986). PREDICTING THE WATER-RETENTION CURVE FROM PARTICLE-SIZE DISTRIBUTION: 1. SANDY SOILS WITHOUT ORGANIC MATTER: 1. *Soil Science*, 142(6), 325.
- Hillel, D., Talpaz, H., & Van Keulen, H. (1976). A Macroscopic Sacle model for water uptake by anon uniform root system and of water and salt movement in the soil profile. *Soil Science Society of America Proceedings*, 121, 242–255.
- Indraratna, B., Fahati, B., & Khabbaz, H. (2006). Numerical analysis of matric suction effects of tree roots. *Proceedings of the Institution of Civil Engineers: Geotechnical Engineering*, 159(2), 77–90.
- Iskandar, D. T. (1978). A new species of Barbourula: First record of a discoglossid anuran in Borneo. *Copeia*, 564–566.
- Jones, D. E., & Holtz, W. G. (1973). *Expansive Soils—The Hidden Disaster*. 139–153.
- Jotisankasa, A., Mairaing, W., & Tansamrit, S. (2014). Infiltration and stability of soil slope with vetiver grass subjected to rainfall from numerical modeling. *Proceedings of the 6th International Conference on Unsaturated Soils, UNSAT*

2014, *Unsaturated Soils: Research & Applications Sydney Australia 2-4 July 2014*, 1241–1247.

- Jotisankasa, A., & Taworn, D. (2016). Direct shear testing of clayey sand reinforced with live stake. *Geotechnical Testing Journal*, 39(4), 608–623.
- Kramer, P. J. (1995). *Water relation of plant and soil ;roots and root systems; chapter 5, academic press, London.*
- Leung, A. K., & Ng, C. W. W. (2013). Analyses of groundwater flow and plant evapotranspiration in a vegetated soil slope. *Canadian Geotechnical Journal*, 50(12), 1204–1218.
- Leung, F. T., Yan, W. M., Hau, B. C., & Tham, L. G. (2015). Root systems of native shrubs and trees in Hong Kong and their effects on enhancing slope stability. *Catena*, 125, 102–110.
- Lu, N., & Likos, W. J. (2006). Suction stress characteristic curve for unsaturated soil. *J. Geotech. Geoenviron. Eng.*, 1322, 131–142.
- Lynch, J. (1995). Root architecture and plant productivity. *Plant Physiology*, 109(1), 7.
- Mahannopkul, K., & Jotisankasa, A. (2019). Influences of root concentration and suction on *Chrysopogon zizanioides* reinforcement of soil. *Soils and Foundations*, 59(2), 500–516. <https://doi.org/10.1016/j.sandf.2018.12.014>
- Martin, R. P. (2001). Panelist Report-landscaping and bio-engineering of slopes in Hong Kong. *Geotechnical Engineering, H. Li.,Ed., Swets & Zeitlinger, Lisse*, 661–670.
- Martin, R. P., Li, C. O., & Pryor, M. R. (2001). Bio-engineering and landscape treatment of slopes and retaining walls in Hong Kong,s landslip preventive measures programme. *Geotechnical Engineering, H. Li.,Ed., Swets & Zeitlinger, Lisse*, 863–868.
- Mulyono, A., Subardja, A., Ekasari, I., Lailati, M., Sudiria, R., & Ningrum, W. (2018). *IOP Conf. Series: Earth and Environmental Science*. 118. <https://doi.org/doi:10.1088/1755-1315/118/1/012038>
- Ng, C. W. W., Leung, A. K., Kamchoom, V., & Garg, A. (2014). A novel root system for simulating transpiration induced soil suction in centrifuge. *Geotech. Test. J.*, 35(5). <https://doi.org/10.1520/GTJ20130116>
- Ng, C. W. W., Woon, K. X., Leung, A. K., & Chu, L. M. (2013). Experimental investigation of induced suction distribution in a grass-covered soil. *Ecological Engineering*, 52, 219–223.
- Nimah, M. H., & Hanks, R. J. (1973). Model for estimating soil water, plant and atmospheric inter relations. *Soil Science Society of America*, 37(4), 522–527.
- Nishimura, T., & Fredlund, D. G. (2001). Failure envelope of a desiccated, unsaturated silty soil. *Proceedings of the Fifteenth Internal Conference on Soil Mechanics and Foundation Engineering*, 615–618.

- Noraini, M. T., & Ghani, J. A. (2001). Bioengineering on slopes for landslide stabilization and prevention in Malaysia. *Geotechnical Engineering, H. Li., Ed., Swets & Zeitlinger, Lisse*, 875–879.
- Operstein, V., & Frydman, S. (2000). The influence of vegetation on soil strength. *Proceeding of the Institution of Civil Engineers-Ground Improvement, 4(2)*, 81–89.
- Parker, J. C., Kool, J. B., & van Genuchten, M. Th. (1985). Determining Soil Hydraulic Properties from One-step Outflow Experiments by Parameter Estimation: II. Experimental Studies. *Soil Science Society of America Journal, 49(6)*, 1354–1359. <https://doi.org/10.2136/sssaj1985.03615995004900060005x>
- Pollen-Bankhead, N., & Simon, A. (2010). Hydrologic and hydraulic effects of riparian root networks on streambank stability: Is mechanical rootreinforcement the whole story? *Geomorphology, 116(3)*, 353–362.
- Rahardjo, H., Satyanaga, A., Leong, E. C., & Ng, Y. S. (2014). Performance of an instrumented slope covered with shrubs and deeprooted grass. *Soils Found., 54(3)*, 417–425.
- Sattelmacher, B., Marschner, H., & Kühne, R. (1990). Effects of the temperature of the rooting zone on the growth and development of roots of potato (*Solanum tuberosum*). *Annals of Botany, 65(1)*, 27–36.
- Shao, M., & Horton, R. (1998). Integral Method for Estimating Soil Hydraulic Properties. *Soil Science Society of America Journal, 62(3)*, 585–592. <https://doi.org/10.2136/sssaj1998.03615995006200030005x>
- Terzaghi, K. (1936). The shear strength of saturated soils. *The First International Conference on Soil Mechanics and Foundation Engineering, Cambridge, MA, 1*, 54–56.
- van Genuchten, M. Th. (1980). A Closed-form Equation for Predicting the Hydraulic Conductivity of Unsaturated Soils. *Soil Science Society of America Journal, 44(5)*, 892–898. <https://doi.org/10.2136/sssaj1980.03615995004400050002x>
- Vanapali, S., & Fredlund, D. (2000). Comparison of different procedures to predict unsaturated soil shear strength. *Advances in Unsaturated Geotechnics, 1995–209*.
- Vanapali, S. K., Fredlund, D. G., Pufahl, D. E., & Clifton, A. W. (1996). Model for the prediction of shear strength with respect to soil suction. *CANADIAN GEOTECHNICAL JOURNAL, 33(3)*, 379–392.
- Waldron, L. J., & Dakessian, S. (1981). Soil reinforcement by roots: Calculation of increased soil shear resistance from root properties. *Soil Science, 132*, 427–435.
- Wang, J.-P., Hu, N., François, B., & Lambert, P. (2017). Estimating water retention curves and strength properties of unsaturated sandy soils from basic soil gradation parameters. *Water Resources Research, 53(7)*, 6069–6088. <https://doi.org/10.1002/2017WR020411>

- Whisler, F. D., Klute, A., & Milington, R. J. (1968). Analysis of steady state evapotranspiration from a soil column. *Soil Science Society of America Proceedings*, 32, 167–174.
- Wu, T. H., McKinnell lii, W. P., & Swanston, D. N. (1979). *Strength of tree roots and landslides on Prince of Wales Island, Alaska*. 16(1), 19–33.
- Ziemer, R. R. (1981). The role of vegetation in the stability of forested slopes. *Proc. Int. XVII IUFRO World Congress*, 297–308.

Annexes

ANNEX 1 – BASIC SOIL STUDY

Specific Gravity of the Selected Soil Type

This test was carried out according to the ASTM D854-83 standard by using a density bottle with the soil sample passing through 0.425 mm sieve and pycnometer (Figure 1) with original soil sample. Equation [1] was used to calculate the specific gravity of the soil for both procedures. A correction was utilized to adjust the results at a reference temperature ($T=20^{\circ}\text{C}$) using the equation [2]



Figure 1: Pycnometer

$$G_s = \frac{(M2 - M1)}{(M4 - M1) - (M3 - M2)} \quad [1]$$

Where, M1 – Mass of Bottle, M2 – Mass of Bottle and Soil, M3 – Mass of Bottle, Soil and Water and M4 – Mass of Bottle full of water only

$$G_{s,20} = G_s \times K \quad [2]$$

K is the temperature correction factor

Observations and results of the specific gravity test are represented in the Table 1 and Table 2 respectively.

Table 1: Observation of specific gravity test

Water temperature = 29°C						
Testing Procedure	Soil Specimen No	Bottle No.	Mass of Bottle, M ₁ (g)	Mass of Bottle + Soil, M ₂ (g)	Mass of Bottle + Soil + Water, M ₃ (g)	Mass of Bottle full of water only, M ₄ (g)
Using Density Bottle with soil sample passing 0.425 mm sieve	1	1	29.94	37.31	85.92	81.32
	2	2	27.08	34.57	82.99	78.36
	3	3	29.19	35.81	87.16	82.94
	4	4	27.39	32.58	84.54	81.33
Using Pycnometer	1	1	508.35	559.21	1832.80	1805.50
	2	2	420.28	472.73	1462.00	1431.70

Table 2: Summary of the results of specific gravity test

Testing Procedure	Soil Specimen No	Specific Gravity at 29°C Water temperature	Specific Gravity at 20°C Water temperature
Using Density Bottle with soil sample passing 0.425 mm sieve	1	2.66	2.65
	2	2.62	2.61
	3	2.76	2.75
	4	2.62	2.62
Using Pycnometer	1	2.16	2.15
	2	2.37	2.36

Specific gravity of soil sample was considered as following values,

$$G_s = 2.67$$

$$G_{s,20} = 2.66$$

Particle Size Distribution Analysis

There are two test procedures were conducted to present particle size distribution of the selected soil according to ASTM D422-63 standard and these were as follow,

- ✓ Sieve analysis for particle sizes larger than 0.075 mm in size – wet sieve analysis (Figure 2)
- ✓ Hydrometer analysis for particle sizes smaller than 0.075 mm in size



Figure 2: Wet sieving process

The observations and results of the sieve analysis and hydrometer test are represented in Table 3 and Table 4 respectively.

Table 3: Particle size distribution

Particle Size Distribution - Sieve Analysis						
Client:						
Project:						
B. H. Number:				Depth:		
Total Mass of the Sample:1000g						
Weight of dry soil sample after wet sieving through No. 40 (0.075 mm) = 881.2g						
Sieve Size (mm)	Mass of Sieve (g)	Mass of Sieve + Soil (g)	Mass of soil Retained (g)	% Retained	Cumulative % Retained	% Sieve Analysis
12.700	555.7	555.7	0.0	0.0	0.0	100.0
10.000	1020.0	1020.0	0.0	0.0	0.0	100.0
4.750	890.2	892.8	2.6	0.3	0.3	99.7
3.350	492.6	494.5	1.9	0.2	0.4	99.6
2.360	481.4	484.9	3.5	0.4	0.8	99.2
2.000	542.1	544.9	2.8	0.3	1.1	98.9
1.180	400.5	441.1	40.6	4.1	5.1	94.9
0.600	410.4	627.2	216.8	21.7	26.8	73.2
0.425	457.0	611.9	154.9	15.5	42.3	57.7
0.300	367.2	489.1	121.9	12.2	54.5	45.5
0.150	412.9	672.2	259.3	25.9	80.4	19.6
0.075	404.4	481.3	76.9	7.7	88.1	11.9
pan	364.7	483.5	118.8	11.9	100.0	0.0

Table 4: Hydrometer test

Hydrometer Analysis of Soils														
Project:														
Weight of Sample (g)		50								T °C		29		
Hydrometer Type										Gs		2.67		
Hydrometer No										K		0.01223		
Meniscus Correction Cm		0.5								a		1		
Dispersing Agent Correction Cd		2								Cylinder No:				
Bore Hole No.:					Depth of Sample:					Date:				
Day	Time	Time After Start			Time (min)	Temp. °C	R'H	RH = R'H + Cm	L	(L/T) ^{0.5}	D (mm)	R = RH-Cd	% Finer	Modified
		Hours	Minutes	Seconds										
09 Dec.	11.08 am	0	0	30	0.5	29	10	10.5	14.6	5.40	0.066	8.5	17	8.84
09 Dec.	11.09 am	0	1	0	1	29	8	8.5	14.9	3.86	0.047	6.5	13	6.76
09 Dec.	11.10 am	0	2	0	2	29	7	7.5	15.1	2.75	0.034	5.5	11	5.72
09 Dec.	11.12 am	0	4	0	4	29	7	7.5	15.1	1.94	0.024	5.5	11	5.72
09 Dec.	11.13 am	0	5	0	5	29	7	7.5	15.1	1.74	0.021	5.5	11	5.72
09 Dec.	11.16 am	0	8	0	8	29	7	7.5	15.1	1.37	0.017	5.5	11	5.72
09 Dec.	11.23 am	0	15	0	15	29	7	7.5	15.1	1.00	0.012	5.5	11	5.72
09 Dec.	11.38 am	0	30	0	30	29	7	7.5	15.1	0.71	0.009	5.5	11	5.72
09 Dec.	12.08 am	1	0	0	60	29	7	7.5	15.1	0.50	0.006	5.5	11	5.72
09 Dec.	01.08 pm	2	0	0	120	29	6	6.5	15.25	0.36	0.004	4.5	9	4.68
09 Dec.	03.08 pm	4	10	0	250	29	5	5.5	15.4	0.25	0.003	3.5	7	3.64
10 Dec.	11.08 am	24	0	0	1440	29	5	5.5	15.4	0.10	0.001	3.5	7	3.64

Plasticity Characteristics of Soils

Liquid limit test was planned to conduct using the Casagrande apparatus and penetration method according to ASTM D4318-83. The test was unsuccessful with the Casagrande apparatus due to the difficulty during the sample preparation. Therefore, the liquid limit for the selected soil type was obtained by conducting the penetration test as shown in Figure 3 and the observation of the test is shown in Table 5. However, the liquid limit of soil has been considered as 17.5% as shown in Figure 4. The plastic limit test could not be conducted because of the difficulty that occurred with remolding. According to the visual inspection, this soil type can be categorized as the Sandy soil. Therefore, it was assumed that the soil did not behave in plastic range and the plastic index was considered zero.



Figure 3: Penetration test

Table 5: Observation of penetration test

Can No	Initial Reading		Final Reading		Penetration (mm)	Weight of Can (g)	Weight of Can + Wet Soil (g)	Weight of can + Dry Soil (g)	Moisture Content
	Div.	(mm)	Div.	(mm)					
S1	10	1.0	96	9.6	8.6	10.3	28.36	26.43	0.12
S2	25	2.5	156	15.6	13.1	9.75	34.25	31.07	0.15
S3	20	2.0	174	17.4	15.4	9.34	30.85	27.93	0.16
S4	7	0.7	253	25.3	24.6	9.51	44.45	38.9	0.19

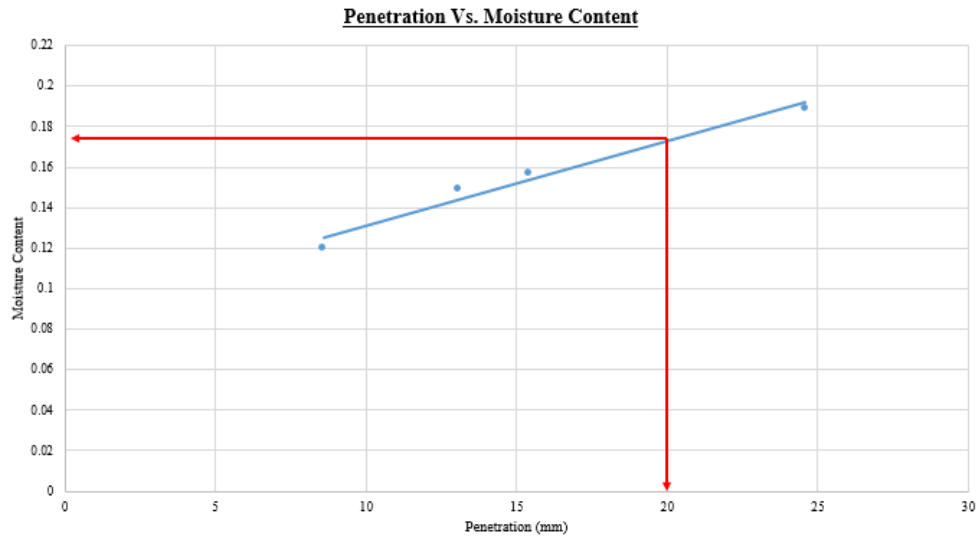


Figure 4: Result of penetration test

Organic Content

This test was conducted according to ASTM D2974-71 and observation are as fallows,

Dry Weight of Porcelain pan = 22.43g

Weight of oven dry soil sample with porcelain pan = 49.67g

Weight of oven dry soil sample = 27.24g

Weight of soil sample dried by furnace with porcelain pan = 49.32g

Weight loss of sample after putting furnace = 0.35g

$$\text{Therefore, Organic Content of soil} = \left(\frac{0.35}{27.24} \right) \times 100 = 1.28\%$$

Proctor Compaction test

According to the proctor compaction test results, maximum dry density of the selected soil type was 1918.88 kg/m³ at 6.77% optimum moisture content. The observed results are included in Table 6.

Table 6: Proctor compaction test

Trial Number	Mass of mould (kg)	Mass of mould + Soil (kg)	Moisture can No	Mass of wet soil + can (g)	Mass of dry soil + can (g)	Mass of can (g)	Avg. moisture content (%)	Bulk density (kg/m³)	Dry density (kg/m³)
1	4.305	6.041	1	48.7	47.8	10.3	2.40	1838.98	1795.88
2	4.305	6.115	2	60.2	58.3	9.6	3.90	1917.37	1845.38
3	4.305	6.183	3	72.2	69.2	9.9	5.06	1989.41	1893.61
4	4.305	6.19	4	86.1	82.4	10.2	5.12	1996.82	1899.48
5	4.305	6.239	5	123.3	116.1	9.7	6.77	2048.73	1918.88
6	4.305	6.25	6	76.1	71.2	9.3	7.92	2060.38	1909.25
7	4.305	6.227	7	38.7	34.8	9.6	15.48	2036.02	1763.15

In-situ Density test

The in-situ density test was followed for the soil barrowed area and the average in-situ density was measured with 1521.94 kgm^{-3} . The test results with the observation are shown in Table 7

Table 7: In-situ density test

Density measurements				Moisture content measurements						
Can Number	Can weight(g)	Can volume (cm ³)	weight of wet soil(g)	Can number	Can weight (g)	weight of wet soil(g)	weight of dry soil(g)	MC	Bulk density (kgm ⁻³)	Dry density (kgm ⁻³)
1	96	100	249.36	1	20.19	41.18	40.73	0.021908	1533.6	1500.721
2	104	100	258.75	2	17.94	45.64	45.1	0.019882	1547.5	1517.332
3	96	100	248.67	3	14.68	35	34.56	0.022133	1526.7	1493.642
4	96	100	251.73	4	14.55	44.37	43.71	0.022634	1557.3	1522.833
5	96	100	256.78	5	17.76	38.45	38.03	0.02072	1607.8	1575.162

ANNEX 2 – EMPIRICAL CORRELATION BETWEEN THE ROOT WATER UPTAKE AND TOTAL LEAF AREA

Table 01: Summary of results

Date	Starting time	Finishing time	Temperature (°C)	Humidity (%)	Height of the tree (cm)	No of leaves	Total area of leaves (cm²)	Avg. rate of transpiration (mm/min)
21/09/2022	13:30	16:00	26-32	75-85	25	5	277	0.354
22/09/2022	13:34	16:00	26-32	75-85	25	6	491	0.610
4/10/2023	13:10	16:00	26-32	75-85	25	7	502	1.901
5/10/2022	13:00	16:00	26-32	75-85	25	8	559	3.140
17/10/2022	13:00	16:00	26-32	75-85	25	9	613	3.766
18/10/2022	6:00	16:00	26-32	75-85	25	10	682	4.123

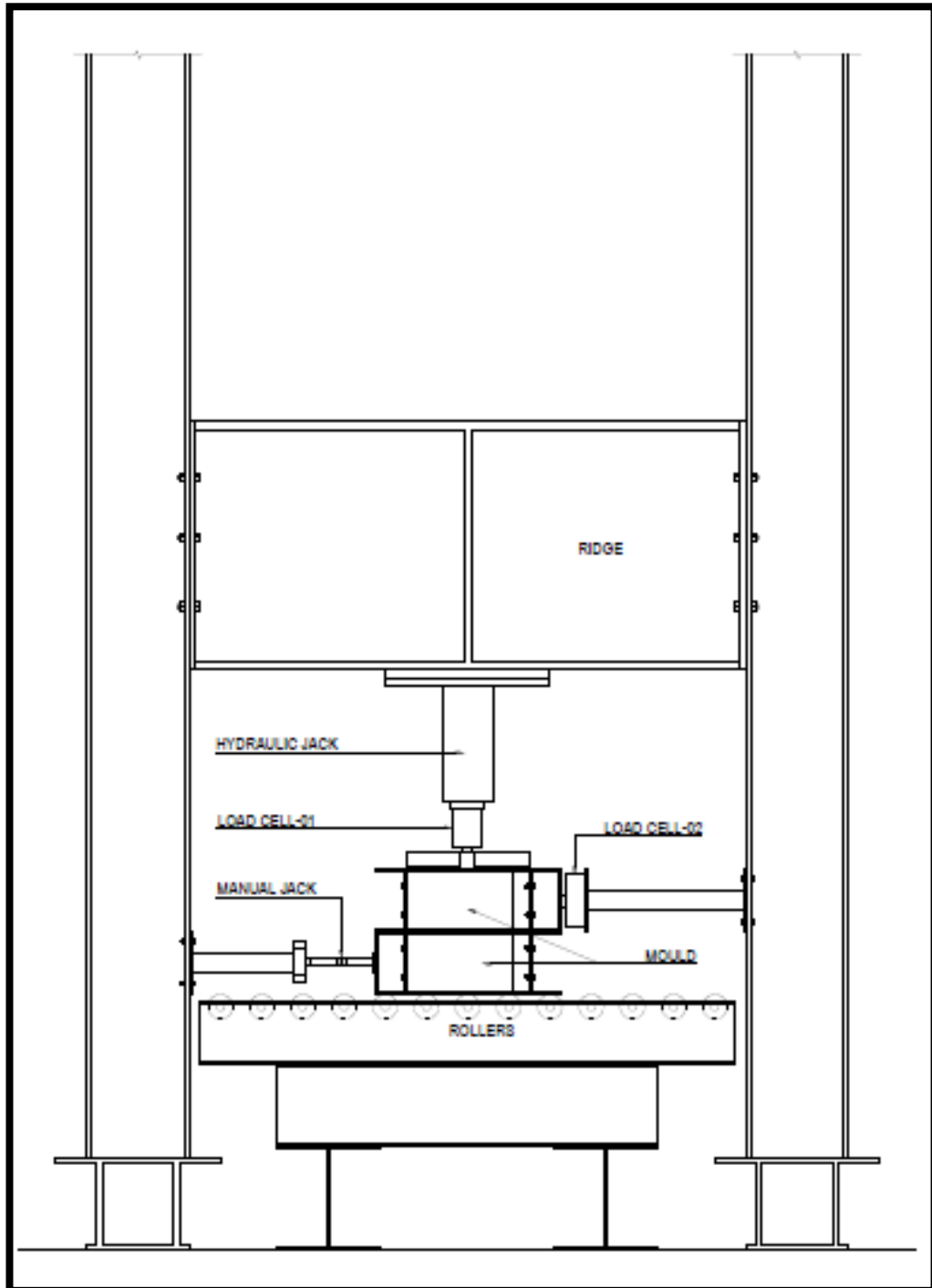
ANNEX 3 – DEVELOPMENT OF SWCC

Table 01: Observations of WP4C instrument

Cup Number	Weight of empty cup (g)	Weight of cup + wet soil (g)	Weight of cup + dry soil (g)	Total Suction (kPa)	Temp. (°C)	Filling volume (mm ³)	Bulk Density (kg/m ³)	Gravimetric moisture content	Dry Density (kg/m ³)	Volumetric moisture content (%)
1	24.79	34.18	32.58	5	31.4	5079.98	1848.43	0.2054	1533.47	31.496
2	24.63	33.96	32.45	10	31.6	5079.98	1836.62	0.1931	1539.38	29.725
3	24.77	33.47	32.48	20	31.9	5079.98	1712.61	0.1284	1517.72	19.488
4	24.49	32.56	32.13	140	31.9	5079.98	1588.59	0.0563	1503.94	8.465
5	24.79	32.75	32.46	270	29.9	5079.98	1566.94	0.0378	1509.85	5.709
6	24.79	32.56	32.31	370	29.9	5079.98	1529.53	0.0332	1480.32	4.921
7	24.79	32.75	32.53	1240	29.9	5079.98	1566.94	0.0284	1523.63	4.331
8	24.72	32.5	32.39	5510	29.9	5079.98	1531.50	0.0143	1509.85	2.165
9	24.52	32.01	31.92	8850	29.9	5079.98	1474.42	0.0122	1456.70	1.772

ANNEX 4 – DEVELOPMENT OF LARGE-SCALE DIRECT SHEAR TESTING SETUP

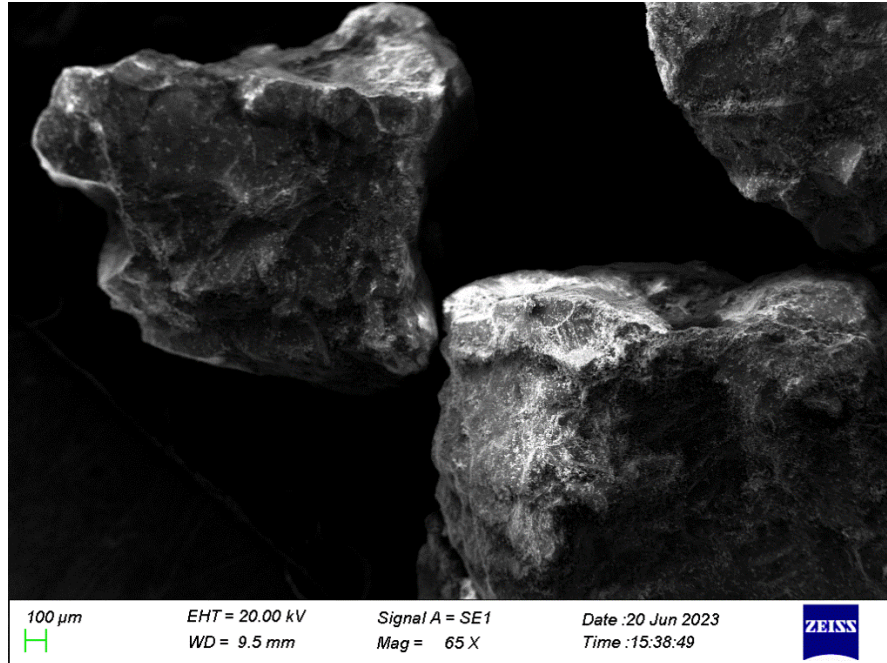
Developed large-scale direct shear testing setup



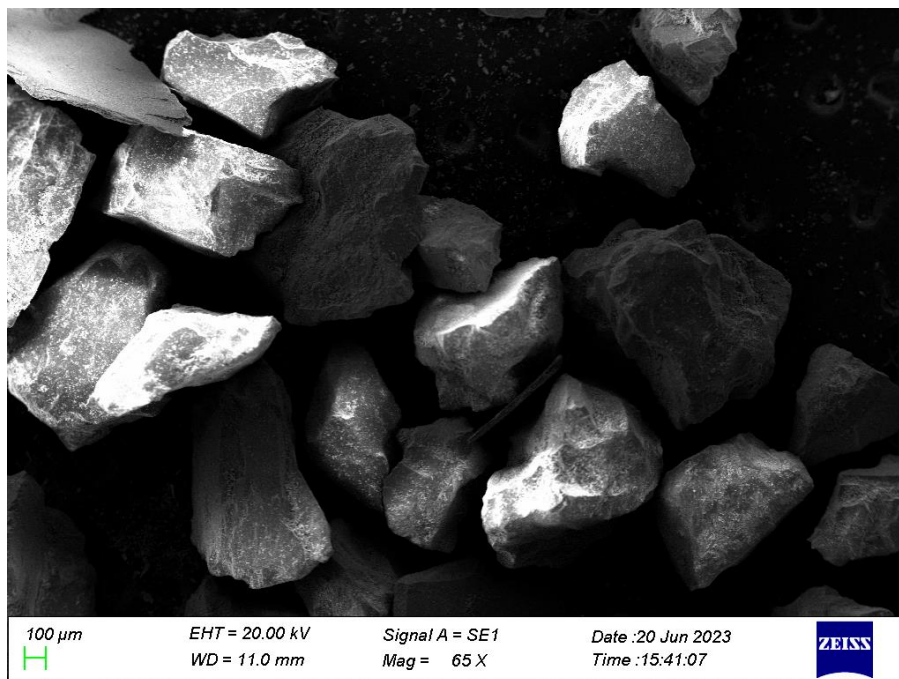
ANNEX 5 – SEM TEST RESULTS

Quarry dusk

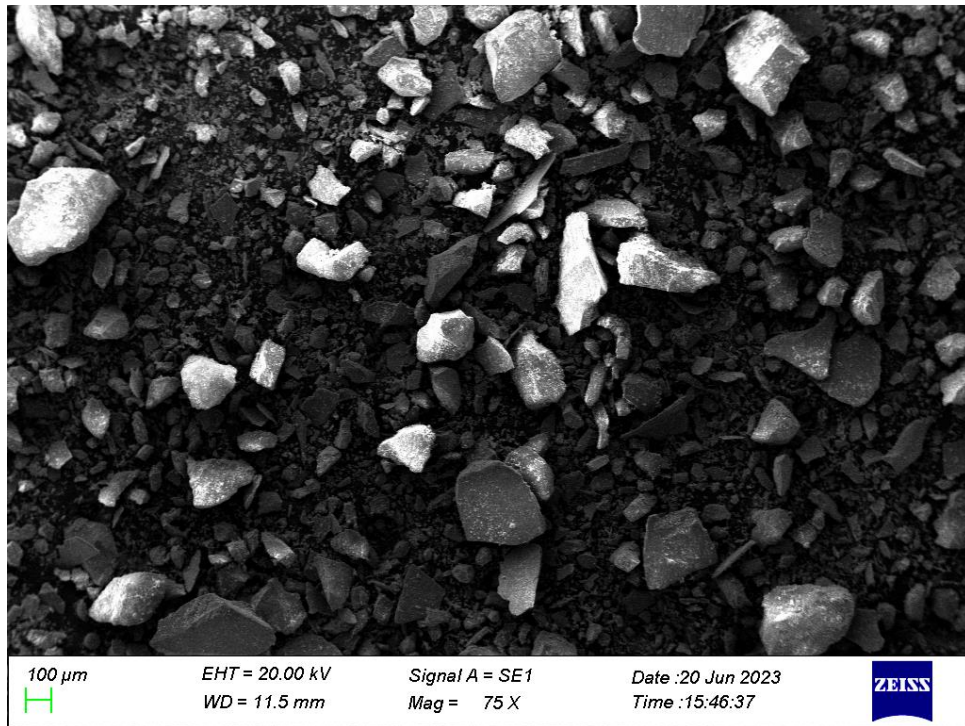
Particle size range – 4.75 – 1.18 mm



Particle size range – 1.18 – 0.425 mm

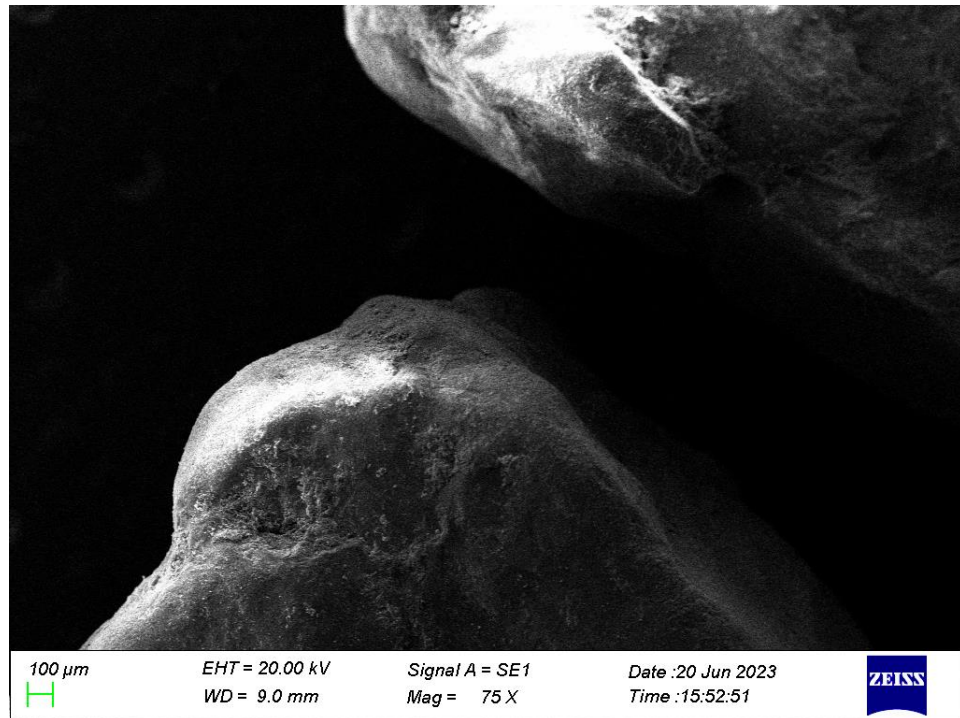


Particle size range – 0.425 – 0.075 mm

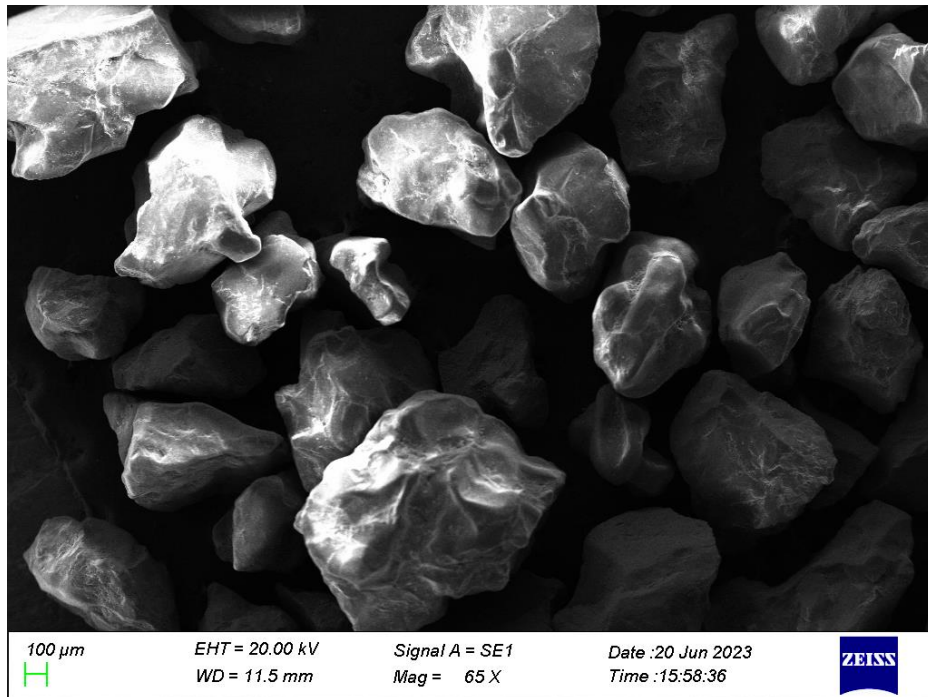


Semi-coastal Silty Sand

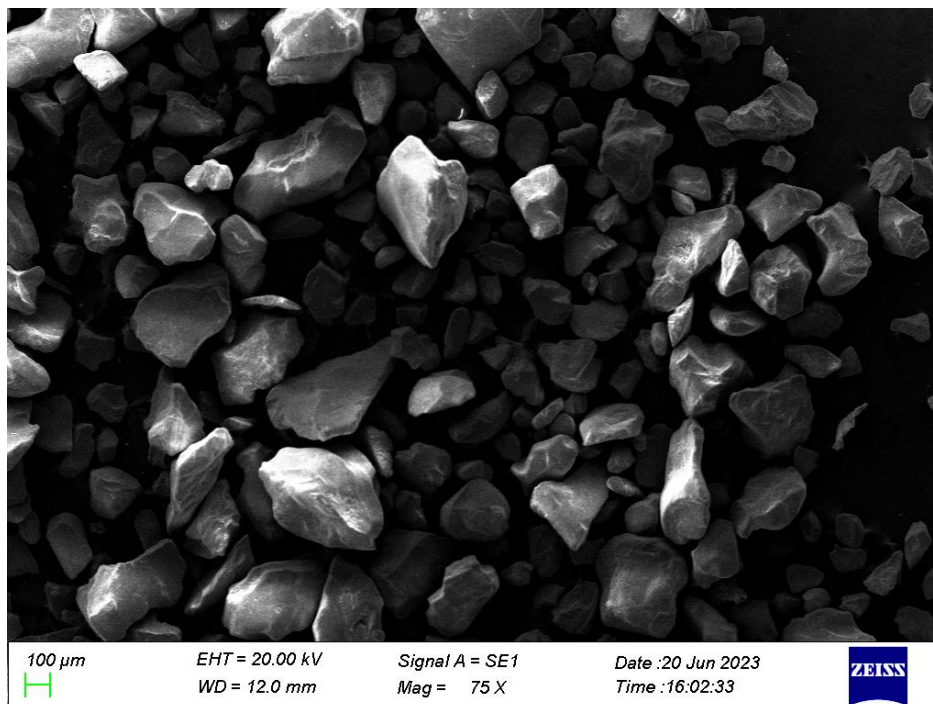
Particle size range – 4.75 – 1.18 mm



Particle size range – 1.18 – 0.425 mm

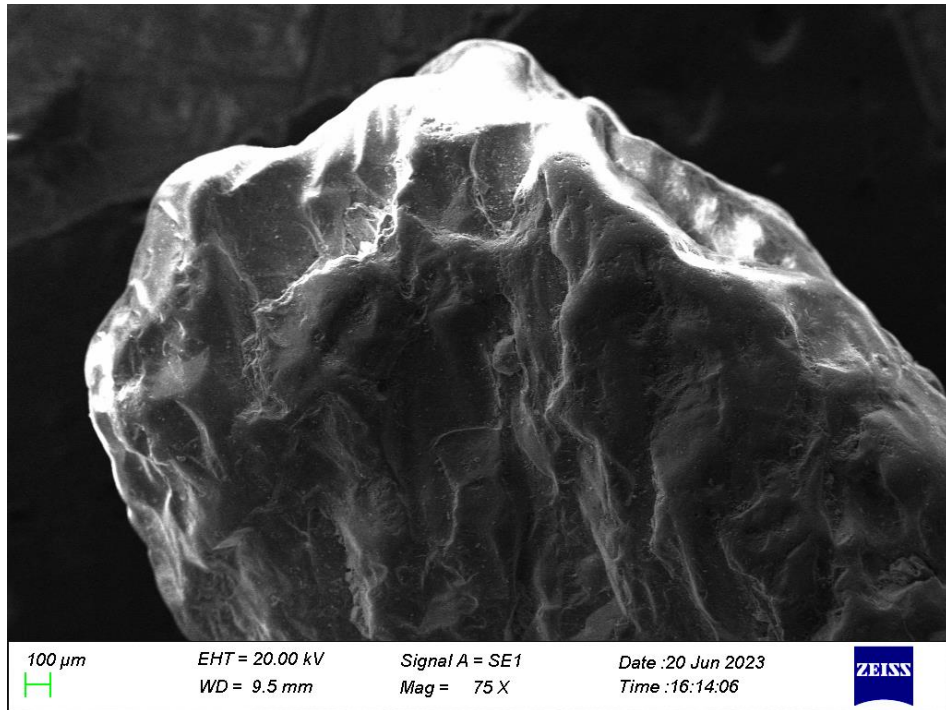


Particle size range – 0.425 – 0.075 mm

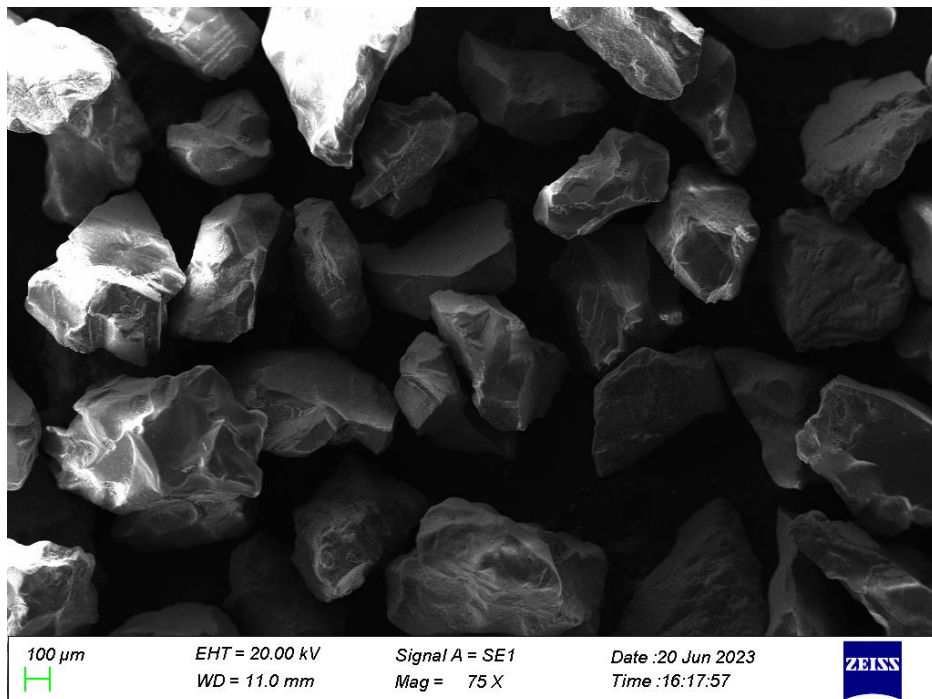


River sand

Particle size range – 4.75 – 1.18 mm



Particle size range – 1.18 – 0.425 mm



Particle size range – 0.425 – 0.075 mm

